

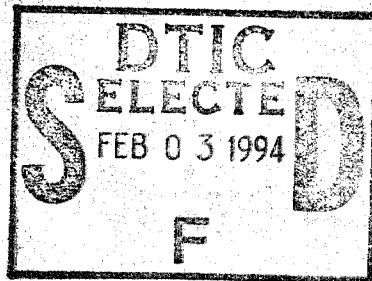
ROBOT ASSISTED MATERIAL HANDLING
FOR SHIRT COLLAR MANUFACTURING
-- TURNING AND PRESSING --
DLA 900-87-0017 Task 0004

FINAL REPORT

VOLUME IV:

Automated Pressing

CENTER FOR ADVANCED MANUFACTURING



This document has been approved
for public release and sale; its
distribution is unlimited.



CLEMSON
UNIVERSITY

College of Engineering
Clemson, South Carolina 29634

DTIC QUALITY INSPECTED 3

ROBOT ASSISTED MATERIAL HANDLING
FOR SHIRT COLLAR MANUFACTURING
-- TURNING AND PRESSING --
DLA 900-87-0017 Task 0004

FINAL REPORT

VOLUME IV:

Automated Pressing

Frank W. Paul
Principal Investigator

and

Kishore Subba-Rao
Research Assistant

Center for Advanced Manufacturing
and
Clemson Apparel Research

Clemson University
Clemson, SC

June 1992

DTIC QUALITY INSPECTED 3

Accession For	
NTIS CRA&I	<input checked="checked" type="checkbox"/>
DTIC TAB	<input type="checkbox"/>
Unannounced	<input type="checkbox"/>
Justification	
By	
Distribution/	
Availability Codes	
Dist	Avail and/or Special
A-1	

19950130 019

SECURITY CLASSIFICATION OF THIS PAGE

REPORT DOCUMENTATION PAGE

1a. REPORT SECURITY CLASSIFICATION Unclassified			1b. RESTRICTIVE MARKINGS		
2a. SECURITY CLASSIFICATION AUTHORITY			3. DISTRIBUTION/AVAILABILITY OF REPORT Unclassified Distribution Unlimited		
2b. DECLASSIFICATION/DOWNGRADING SCHEDULE			4. PERFORMING ORGANIZATION REPORT NUMBER(S)		
5. MONITORING ORGANIZATION REPORT NUMBER(S)			6a. NAME OF PERFORMING ORGANIZATION Clemson University/ Clemson Apparel Research		
6b. OFFICE SYMBOL (If applicable)			7a. NAME OF MONITORING ORGANIZATION Defense Personnel Support Center		
7b. ADDRESS (City, State, and ZIP Code) 500 Lebanon Road Pendleton, SC 29670			7c. ADDRESS (City, State, and ZIP Code) 2800 South 20th street P.O. Box 8419 Philadelphia, PA 19101-8419		
8a. NAME OF FUNDING/SPONSORING ORGANIZATION Defense Logistics Agency			8b. OFFICE SYMBOL (If applicable)		
9. PROCUREMENT INSTRUMENT IDENTIFICATION NUMBER DLA 900-87-D-0017 Delivery Order 0004			10. SOURCE OF FUNDING NUMBERS		
10a. ADDRESS (City, State, and ZIP Code) Room 4B195 Cameron Station Alexandria, VA 22304-6100			PROGRAM ELEMENT NO. 78011S	PROJECT NO.	TASK NO.
					WORK UNIT ACCESSION NO.
11. TITLE (Include Security Classification) Robot Assisted Material Handling for Shirt Collar Manufacturing: Turning and Pressing Vol. IV: Automated Pressing - unclassified					
12. PERSONAL AUTHOR(S) F.W. Paul, Principal Investigator; Kishore Subba-Rao, Research Assistant					
13a. TYPE OF REPORT Final		13b. TIME COVERED FROM n/a TO		14. DATE OF REPORT (Year, Month, Day) 1992 June 23	
				15. PAGE COUNT 118	
16. SUPPLEMENTARY NOTATION					
17. COSATI CODES			18. SUBJECT TERMS (Continue on reverse if necessary and identify by block number)		
FIELD	GROUP	SUB-GROUP			
19. ABSTRACT (Continue on reverse if necessary and identify by block number) This document presents Volume IV of the report of research into the automation of shirt collar manufacturing using robotic methods. Presented is the proof-of-concept device for automation of the pressing operation, wherein both points of a double pointed shirt collar are presented to a pressing machine simultaneously, using appropriate grippers and machine vision systems, to achieve the critical alignment necessary for successful collar manufacture. The results of several trials of the machine are presented, showing the success of the design.					
20. DISTRIBUTION/AVAILABILITY OF ABSTRACT <input checked="" type="checkbox"/> UNCLASSIFIED/UNLIMITED <input type="checkbox"/> SAME AS RPT. <input type="checkbox"/> OTC USERS			21. ABSTRACT SECURITY CLASSIFICATION Unclassified		
22a. NAME OF RESPONSIBLE INDIVIDUAL Frank W. Paul			22b. TELEPHONE (Include Area Code) 803-656-3291		22c. OFFICE SYMBOL

ACKNOWLEDGMENTS

The authors would like to thank all those who were involved with support of this project. Especially, it is appropriate to thank the Defense Logistics Agency, Department of Defense, for support of this work under contract number DLA 900-87-0017 Task 0004. This work was conducted through Clemson Apparel Research, a facility whose purpose is the advancement of apparel manufacturing technology and by the Center for Advanced Manufacturing, Clemson University.

ABSTRACT

Pressing of apparel products and their sub-assemblies is a finishing operation which is critical to the quality of the product or sub-assembly. Material handling and workpiece alignment for pressing are skilled tasks and require a high level of operator training. Automation can improve the consistency of product quality by eliminating the dependence of product quality on operator skill and dexterity. Automation reduces cycle time, increasing production rate.

This thesis presents a study of the visual sensing and control issues for automated pressing of two-dimensional apparel components, using a shirt collar as a case study. An analysis of manipulation primitives for manual shirt collar pressing was done. Procedures were developed for automated collar acquisition and seam alignment by indirect edge alignment. Machine vision was used as a feedback sensor to provide data on location of fabric ply edges. Algorithms were developed for the detection of key fabric ply edge points.

A proof-of-concept machine was designed, built, and experimentally evaluated to validate the developed automation strategy for shirt collars and similar two-dimensional apparel components. The vision sensor could detect fabric edge points with an accuracy of 0.01 inch. Repeated trials proved that automated collar acquisition could be done with a precision of 0.04 inch.

TABLE OF CONTENTS

	Page
TITLE PAGE	i
ABSTRACT	ii
ACKNOWLEDGEMENTS	iii
LIST OF FIGURES	vi
CHAPTER	
I. INTRODUCTION	1
Background	1
Literature Survey	4
Problem Statement and Research Objectives	7
Thesis Organization	8
II. AUTOMATED COLLAR PRESSING	9
Pressing Technology	9
Task Analysis	10
Double-Point Pressing	17
Locating Collar Points	17
Seam Alignment Concepts	18
III. DESIGN AND CONTROL IMPLEMENTATION	40
Creaser Blade Mechanism	40
Vacuum System	44
Linear Drives	48
Vision Sensor	50
IV. ANALYSIS AND EXPERIMENTAL EVALUATION	58
Algorithm for Automated Collar Acquisition and Indirect Seam Alignment	58
Integration with a Robotic Apparel Assembly Workcell	68
Comparison of Pressed Collars	74
Error Analysis	76

Table of Contents(Continued)	Page
V. CONCLUSIONS AND RECOMMENDATIONS	88
Conclusions	88
Recommendations	91
APPENDICES	93
A. Hardware Specifications	94
B. Electrical Wiring Diagrams	99
C. Program Listing	102
REFERENCES	117

LIST OF FIGURES

Figure	Page
1.1 Shirt Collar before and after Turning	3
2.1 Layout and Components of the Lunapress	11
2.2 Shirt Collar Turning on the Lunapress	13
2.3 Shirt Collar Pressing on the Lunapress	15
2.4 2-Piece Creaser Blade Mechanism	19
2.5 Interference between Creaser Blade and Collar	20
2.6 3-Piece Creaser Blade Mechanism	21
2.7 Seam Alignment Error	23
2.8 Mechanism to Simulate Rolling Action of Fingers	24
2.9 Direct Seam Alignment-Conceptual Design	25
2.10 Machine Vision for Direct Sensing	26
2.11 Transmitted Light Sensor	28
2.12 Reflected Light Sensor	30
2.13 Reflected Light Intensity Profile	31
2.14 Indirect Seam Alignment-Double Ply Manipulation	32
2.15 Indirect Seam Alignment-Single Ply Manipulation	34
2.16 Load-Extension Curve for Woven Fabric	36
2.17 Edge Alignment Error	38
3.1 Run Stitch Detail for an Unturned Collar	41
3.2 Bearing Layouts for Creaser Blade Mechanism	43
3.3 Creaser Blade Mechanism Assembly	45
3.4 Methods to Implement Suction Surfaces	47
3.5 Linear Drive Assembly	49
3.6 Collar Loaded on Creaser Blades	51

List of Figures(Continued)

Figure	Page
3.7 Calibration Geometry and Transformations	53
3.8 Control Structure for the Proof-of-Concept Machine	56
3.9 Proof-of-Concept Machine	57
4.1 Flow Chart for Automated Collar Acquisition and Indirect Seam Alignment	59
4.2 Image Processing and Scanning to Locate Edge Points	61
4.3 Procedure for Single-Level Threshold Filtering	63
4.4 Binary Image of Ply Edges and Key Point Locations	64
4.5 Scanning Procedure to Locate an Edge Point	65
4.6 Robotic Apparel Assembly Workcell	69
4.7 Positioning a Turned Collar on the Vacuum Table	71
4.8 Collar Acquisition by Creaser Blades	72
4.9 Automated Edge Alignment	73
4.10 A Visual Comparison of Pressed Collars	75
4.11 Test Profile for Statistical Evaluation of Vision System Performance	77
4.12 Effect of End-Effector Pitch Repeatability on Vision Sensor Performance	79
4.13 Effect of Robot Arm Repeatability on Vision Sensor Precision and Accuracy	82
4.14 Statistical Evaluation of Collar Acquisition Process	84
B.1 Wiring Diagram for the Stepper Motors.....	100
B.2 Wiring Diagram for the Solenoid Valve Card.....	101

CHAPTER I

INTRODUCTION

Background

Pressing of apparel products is either the final operation before product packaging or the finishing operation on one of the sub-assemblies of the product. The apparel industry gives a great deal of importance to this particular manufacturing operation because of two main reasons:

1. Pressing of an apparel component or sub-assembly is an operation which affects the quality, appearance and marketability of the final apparel product.
2. Pressing is a skilled task and product quality depends on operator skill, requiring a high level of operator training.

Apparel products or sub-assemblies can be two-dimensional or three-dimensional. Examples of three-dimensional apparel products include men's and women's suits, trousers and jackets. In the case of three dimensional apparel products, terms such as fabric drape, fall and fit are used to measure product quality. Products such as suits, trousers and jackets are assembled from an array of smaller two-dimensional apparel sub-assemblies. For example, the list of two-dimensional sub-assemblies of a dress shirt include the collar, sleeves, epaulets, pocket and cuffs.

The apparel industry judges the quality of a tailored dress shirt by its collar. The collar is the one that not only plays a key role in deciding the appearance of the shirt,

but is also the most difficult sub-assembly component to manufacture.

A dress shirt collar is comprised of two identical plies, trapezoidal in shape. One of the plies usually has a fused lining to impart stiffness and shape retention capability to the collar. The two plies are overlaid and then "run stitched" along the periphery, with the stitch line offset inward from the ply boundary. This is referred to as an "unturned" collar and is illustrated in Figure 1.1(a). An unturned collar must then be turned inside out to conceal the run stitch. Figure 1.1(b) shows a turned collar. The turned collar is then pressed using a die press to generate a sharp crease along the collar run stitch line. The other effect of the die pressing operation is the extrusion of the collar corners into sharp tips referred to as "points". Both these characteristics; i.e., a sharp crease and sharp collar points are highly desirable and can be considered characteristics of a high quality dress shirt.

Shirt collar turning and pressing are currently carried out on a semi-automatic special purpose machine called the "Lunapress". Turning and pressing on the Lunapress is done one-half collar at a time, which will henceforth be referred to as "single-point turning and pressing". Single-point pressing on the Lunapress suffers from three drawbacks:

1. Quality of the generated crease is directly dependent on operator skill.
2. The central portion of the collar is not pressed.

3. Collar loading and setting time is approximately 15 % of the total cycle time of the Lunapress, which is 40 to 50 seconds per collar and is operator dependent.

Single-point collar pressing produces collars with inconsistent crease quality due to dependence on operator skill and training. Furthermore, the fact that collar loading and setting time takes up 15% of the total cycle time illustrates that material handling slows down the collar turning and pressing cycle.

Automating the collar pressing operation can overcome these pressing limitations. Automation can eliminate dependence of collar crease quality on operator skill and result in consistent quality of collar seams, thereby enhancing the appearance and value of the dress shirt. Automation would also allow for simultaneous pressing of both points thereby significantly reducing the cycle time of the operation. This would enhance productivity and reduce manufacturing costs.

Literature Survey

Attempts to study and automate critical apparel manufacturing operations have been difficult. Research and development work in the area of manipulation of two dimensional apparel components for manufacturing has been on a case by case basis. Current research at the Robotics and Machine Automation Laboratory at Clemson University has concentrated on investigating techniques for automated fabric ply acquisition, pick-and-place, and two dimensional ply

positioning with machine vision assistance. Parker et al. [3] investigated various devices and mechanisms to separate a single fabric ply from a stack. Among the many methods studied were the use of vacuum, adhesives and pins for ply acquisition and destacking. Fabric is a difficult material to handle and manipulate because of its limp nature. Conventional acquisition and gripping techniques developed to handle soft and irregularly shaped objects cannot be applied to fabric.

Torgerson and Paul [4] studied two dimensional fabric ply manipulation of apparel workpieces using machine vision assistance. A solid state camera mounted vertically above the work surface provided kinematic information on how to move the apparel workpieces. Image processing algorithms were used to extract the boundary of the workpieces. These data were used in path planning to compute an open-loop robot trajectory to guide the work pieces under a needle and perform a simulated sewing operation. The apparel workpieces were treated as rigid planar objects and the possibility of buckling or wrinkling of workpieces of thinner woven fabric was not investigated.

Bernadon and Kondoleon [6] developed a prototype flexible apparel assembly workstation to automate the manufacture of sleeves for men's tailored suits. A suction surface was used to hold the workpiece in position. A robot with a custom designed end-effector folded suit sleeves to prepare them for the sewing operation. A vision system provided fabric edge

data which were used to match fabric ply contours by the robotic folder. Edge matching was achieved by aligning the plies at key break points. The system used a microcomputer for real-time control.

Gershon and Porat [7] report on the development of a robotic cell for the automated sewing of contoured seams. A real-time vision system was used for edge tracking and seam width control. A custom designed robot finger with a force sensor was used to monitor and control the tension in the cloth workpiece being sewn. Control algorithms to prevent fabric puckering were developed and implemented. Gershon and Porat have mentioned that extensibility and anisotropic behavior of woven fabric affected the performance of the vision servo system considerably.

Taylor and Koudis [5] have demonstrated the application of robots with specially designed end-effectors to perform complex manipulation of partially assembled apparel workpieces. The particular case investigated was the assembly of the front, rear and gusset panels of men's briefs. The successful accomplishment of a double concealed seam construction by the turning of briefs inside out was demonstrated using a special purpose dexterous end-effector.

The literature review and case studies cited document and illustrate the complexity of the design, sensing and control aspects involved in the manipulation of two dimensional apparel components. The complexity in this area of automation arises from the limp nature of fabric and its anisotropic

behavior. Garment manufacturing and processing tasks involve a considerable degree of dexterity, visual and tactile sensing and hand-eye coordination. Prior to any attempt to automate an apparel manufacturing operation, it is essential to carefully study the motion sequence, sensory capability required and the actuators needed to provide the necessary motion and sensory capabilities for automated operation.

Problem Statement and Research Objectives

The research problem of this thesis can be stated as follows:

Pressing of shirt collars is a skilled task requiring visual and tactile sensing and considerable dexterity. Automation of this task can significantly improve the quality and consistency of processed shirt collars and enhance the value and appearance of dress shirts.

The objectives of this thesis are:

1. to develop an automation strategy to emulate fabric manipulation and visual sensing tasks for automated pressing of two-dimensional apparel components, using shirt collars as a typical example, and
2. to design, build, and experimentally evaluate a proof-of-concept machine to validate the proposed automation strategy.

The first objective deals with the analysis of the motion sequence required for shirt collar pressing. Identification of the design, sensing and control requirements enables the conceptualization of the proof-of-concept machine.

The second objective involves the design and implementation of the concepts developed for automated pressing of shirt collars. Integration of a vision system to provide sensory feedback data on ply edge location will be part of this objective.

Thesis Organization

Chapter II begins with a documentation of the terminology associated with the pressing of shirt collars. A study of manipulation primitives is followed by an analysis of design and visual sensing requirements for automated pressing of shirt collars. Chapter III describes the implementation of the design, sensing and control concepts developed in Chapter II. The design of functional modules of a proof-of-concept machine is presented. The development of control software for an experimental evaluation of the proposed automation strategy is documented in Chapter IV. Finally, conclusions and recommendations are presented in Chapter V. Appendices A, B, and C contain material that detail the thesis work, addressing control hardware, electronic interfaces, and program listings respectively.

CHAPTER II

AUTOMATED COLLAR PRESSING

Pressing Technology

Molding is a process in which heat, moisture, pressure or a combination of these three parameters is used to change the density, form, shape or surface structure of an apparel product or a piece of fabric. Pressing is a type of molding process which varies the fabric's geometric structure or characteristics by applying mechanical pressure to the fabric or apparel workpiece. A combination of heat and pressure is used most often, though the addition of moisture using steam is also employed depending on the fabric type and workpiece dimensions involved. Depending on the manner in which mechanical pressure is applied, pressing processes and equipment can be classified into three major types [11].

1. Buck Pressing

This is a pressing process in which the fabric or product is placed on a fixed surface before pressure is applied with a complementary fixed surface. Each of these fixed surfaces is called a buck.

2. Block Pressing

Blocking is a pressing process in which the fabric or product envelopes a fixed form, called the block, before pressure, heat or moisture is applied to the fabric in order to stabilize the fabric's conformance to the shape and form of the block. This process is mainly used to press two dimensional apparel components such as collars, cuffs and epaulets.

3. Die Pressing

Die pressing is a molding process in which a flat surface is molded into a desired shape by a forgelike process which shapes and distorts the original surface between two complementary interlocking die shapes. This process is mainly used to convert two dimensional workpieces into three dimensional products.

Block pressing is used to press apparel components with parallel or approximately parallel sides such as collars, cuffs and sleeves. In the case of a shirt collar, the block is a stainless steel blade with a profile matching that of the collar run stitch. The turned shirt collar accommodates the blade, otherwise referred to as a creaser blade, in a snug fit, very similar to that of a glove fitting over a hand. In single-point pressing, a separate creaser blade is used for the left and right halves of the collar.

Task Analysis

The Lunapress is an ergonomically designed machine and is an apparel industry standard for single-point turning and pressing of shirt collars. The machine layout and its components are illustrated in Figure 2.1. The Lunapress is designed so that a single operator can carry out turning and pressing of shirt collars while remaining seated. The components which assist in turning are the "turner" and the "clipper". The clipper is a triangular blade which fits into the collar point. The "turner" is a pointed shaft that butts against the clipper, when actuated by a pneumatic cylinder.

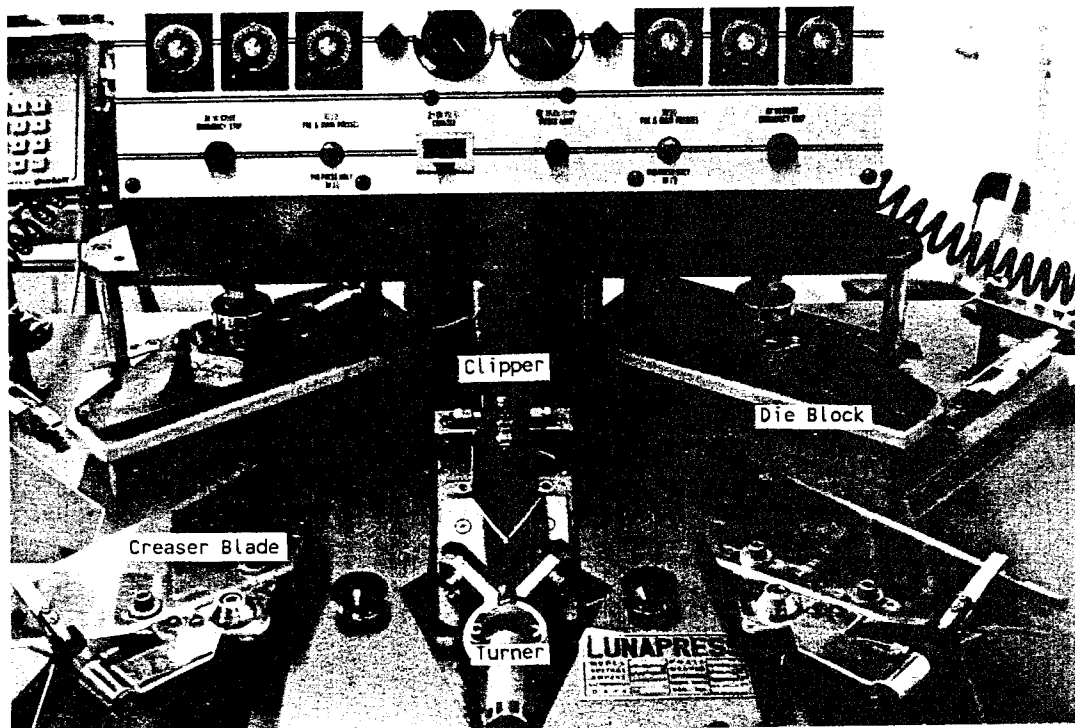


Figure 2.1. Layout and Components of the Lunapress

The components which assist in collar pressing are the creaser blades, clamps, dies and the press. The creaser blades are smooth stainless steel plates with a profile matching the contour of the collar seam. There are two creaser blades, one each for the left and right halves of the collar. The creaser blades are mounted on slideways and are driven by individual air cylinders. They can be moved into the die cavity and later be retracted. The dies are heavy brass blocks which are contoured to complement the creaser blade profile. The die blocks are mounted on a heated base plate. The press plunger is actuated by a heavy duty air cylinder. A ram, attached to the press plunger, applies mechanical pressure on the creaser blade once inserted into the die block.

The single-point turning process begins with the operator picking up a collar from a stack and separating the plies. The opened collar is pulled over the clipper, such that the tip of the triangular clipper blade pushes into the tip of the collar or collar point. Once the clipper is pushed into the collar tip, the turner air cylinder is actuated. The operator now flips the collar inside out by pulling the collar towards him/her. The turner cone is retracted and the collar is released. This procedure is repeated for the other collar point. Collar turning on the Lunapress is done by sequentially turning one point at a time, illustrated in Figure 2.2.

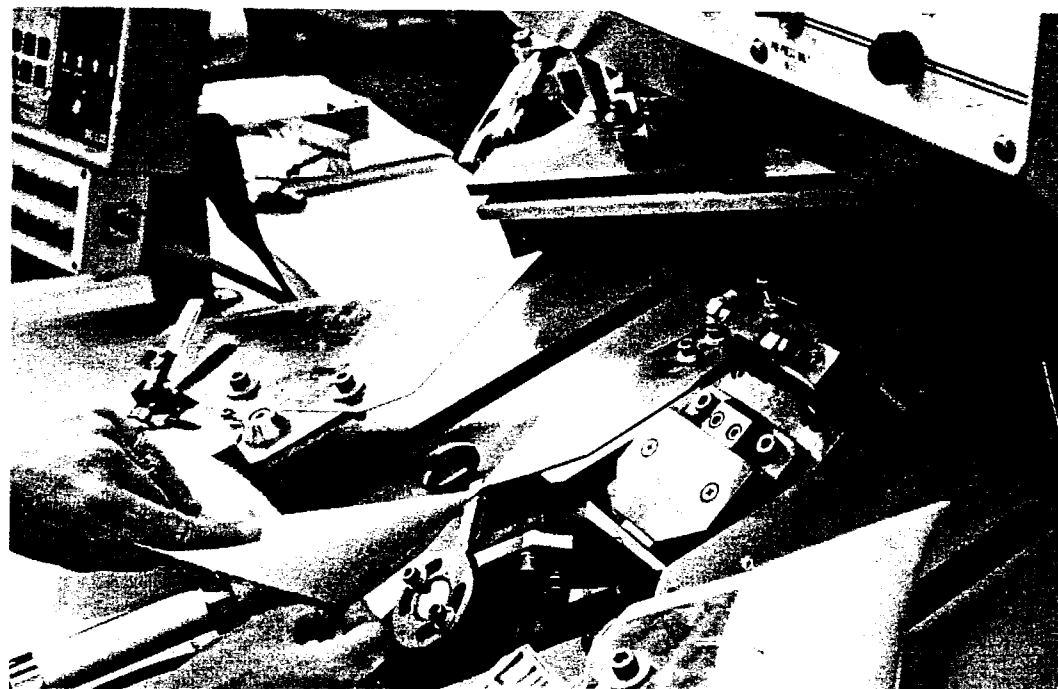
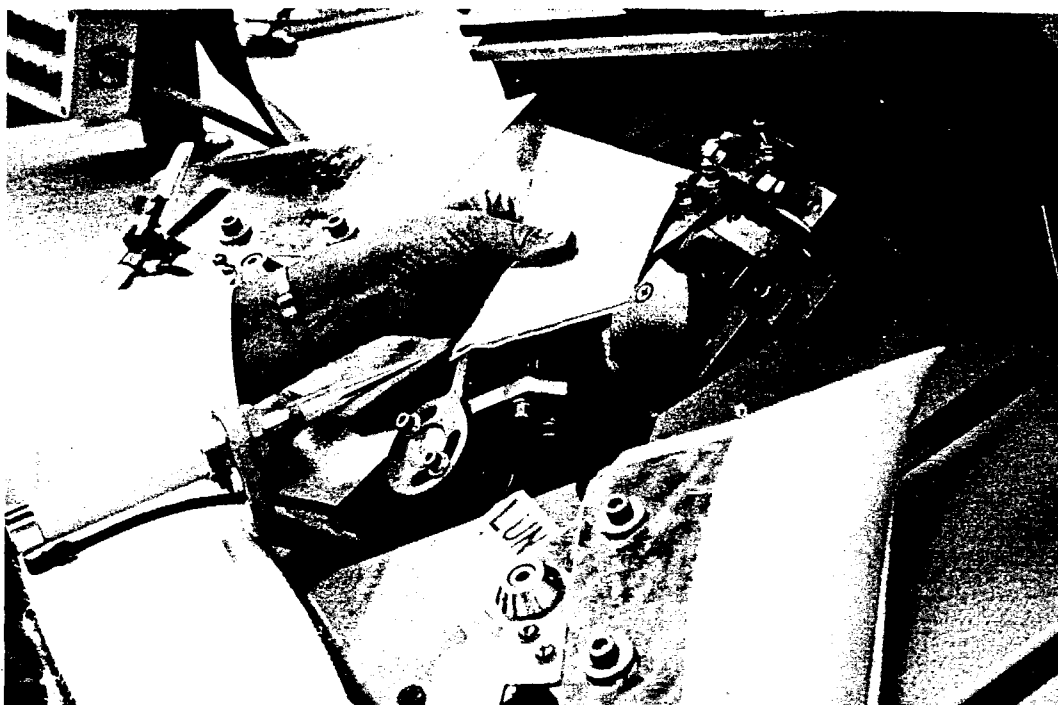


Figure 2.2. Shirt Collar Turning on the Lunapress

The turned collar is further processed by sequential pressing of the collar points. The pressing sequence begins with the operator taking the turned collar off the clipper and opening the collar by separating the plies. The opened collar is placed over one of the creaser blades. The collar is pulled taut over the blade such that the blade tip pushes into the collar point. The next operation is the alignment of the collar seam against the edge of the creaser blade. This is a very critical operation because an error in seam alignment results in distortion of the generated crease. It is essential that the crease be as close to the edge of the creaser blade and be visible from only one side of the collar after it has been pressed. A collar with its seam visible from both sides has a negative effect on the appearance of the collar and hence the dress shirt. Seam alignment is done by rolling the seam between fingers along the run stitch until it is aligned against the edge of the creaser blade, illustrated in Figure 2.3. The collar, once aligned and set on the creaser blade is clamped in place by pneumatic clamps. The operator ensures that all wrinkles are smoothed out before actuating the clamps. Wrinkles are creased by the pressing operation resulting in a defective collar.

The turned collar, aligned, set and clamped onto the creaser blade is moved into the die block for the pressing operation. The press ram is lowered into the heated die block and pressure is applied on the collar. The pressure is applied momentarily, allowing the collar to be creased along

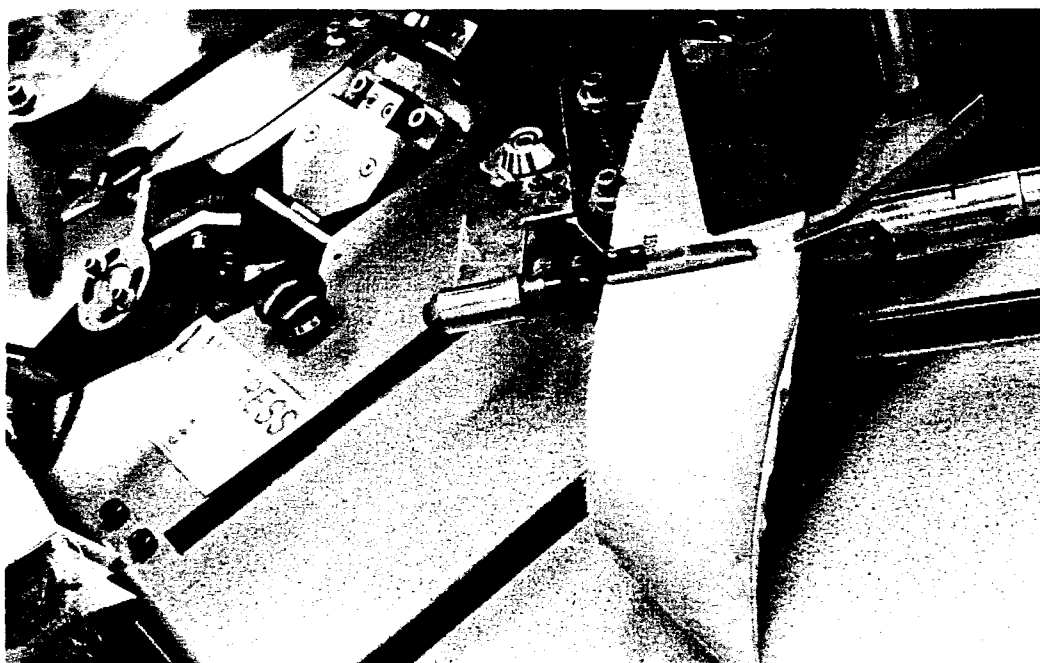
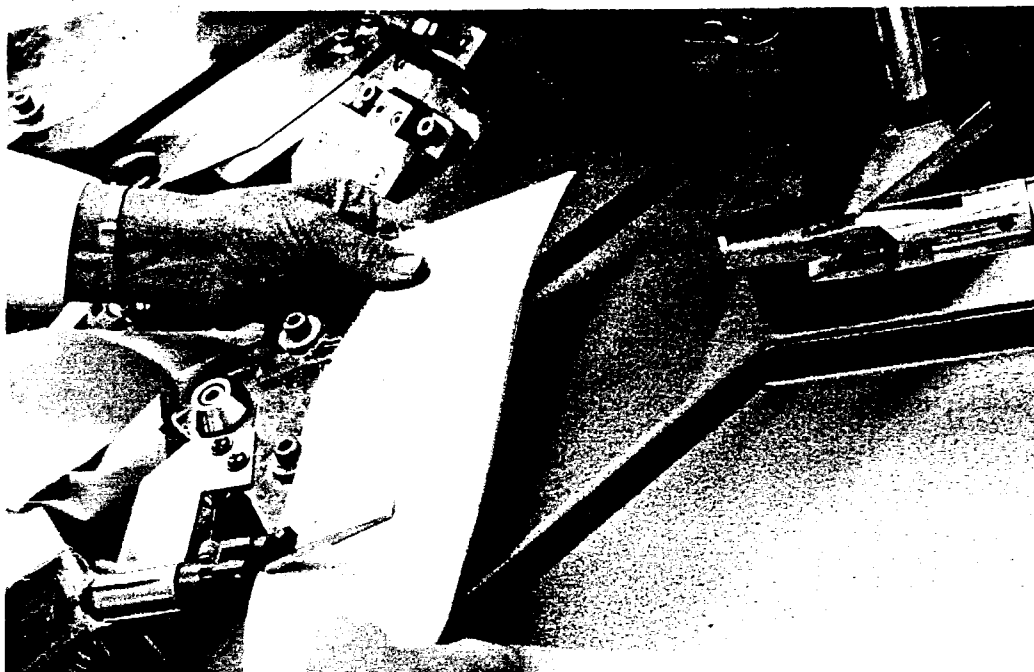


Figure 2.3. Shirt Collar Pressing on the Lunapress

the seam. The creased collar is pinched by a set of pins which protrude from the ram and the base plate of the die blocks. The pressure on the ram is lowered, allowing the creaser blade to retract. The collar stays in place in the die block because of the pinching action of the protruding pins. The ram is lowered for the final press. The press plunger is retracted following the completion of the pressing cycle and the pressed collar is ejected from the die block by an air burst from a nozzle. The entire procedure is repeated for the other half of the collar to complete processing of the shirt collar.

Analysis of single-point pressing of shirt collars on the Lunapress shows that the key tasks to be considered to automate shirt collar pressing are

1. location of collar points by the creaser blade, and
2. alignment of the collar seam against the creaser blade edge.

The accuracy with which the creaser blade locates the collar point directly affects the quality of the collar point produced after pressing. Any error in point location results in improper extrusion in the die blocks. Seam alignment is an equally critical task. Seam alignment error results in a curved seam, which is not acceptable. A large alignment error may cause the seam to "roll over" to both sides of the collar during pressing, which is also unacceptable by apparel industry quality standards.

Double-Point Pressing

Automation of an apparel manipulation task is difficult when repeated location, acquisition, and release of the payload or workpiece is required, because of the limp nature of fabric and its tendency to collapse and buckle. Gopalswamy[10] has commented on the problems encountered during the design of a robot end-effector to handle and manipulate shirt collars. End-effector design was greatly simplified by minimizing the number of workpiece release and acquisition cycles for the task concerned.

Single-point pressing of shirt collars is a task which requires release of the workpiece after it is loaded and set on one of the creaser blades. It has to be relocated and transported to the second creaser blade to press the other half of the collar. The design and sensing requirements for automated pressing can be considerably simplified if workpiece location and acquisition is done only once. The concept of "double-point" pressing evolves from the idea that the complete collar can be processed in a single pressing operation if the turned collar is transferred to a set of creaser blades in a single loading operation.

Locating Collar Points

The loading of a turned collar onto a single creaser blade with a contour matching that of the collar run stitch is not possible. The reasons are the trapezoidal shape of the collar plies and the acute included angle between the collar sides, which place the collar opening on the smaller side.

Figure 2.4 illustrates the use of a pair of moving creaser blades. The expanding blades are moved into the collar and are then moved outward to locate the collar points. The angle of approach of the blades in this configuration results in interference between the collar seam and blade tip, illustrated in Figure 2.5. The line of approach has to be between L_1 and L_2 , to avoid interference between the creaser blade and surrounding fabric towards the end of its stroke.

The two blade concept with a line of approach between L_1 and L_2 would be successful in accurately locating the collar points. However, it is also necessary that the top surfaces of the blades be flush. This ensures that the collar is not creased at the interface of the blades. The top surface of the left and right creaser blades can be made flush with that of the central blade by inserting a third blade between the left and right blades. The conceptual design for the three piece creaser blade mechanism is illustrated in Figure 2.6.

Seam Alignment Concepts

The collar seam is aligned with the creaser blade edge by rolling the fabric between the operator's fingers to correct the local setting of the collar edge. Local correction of seam position is followed by local clamping of the collar plies to maintain alignment. Following seam alignment along the entire length of the collar, the pneumatic clamps are actuated to hold the aligned collar in place before it is inserted into the pressing dies. Manual seam alignment, for single-point pressing on the Lunapress, is done locally, zone

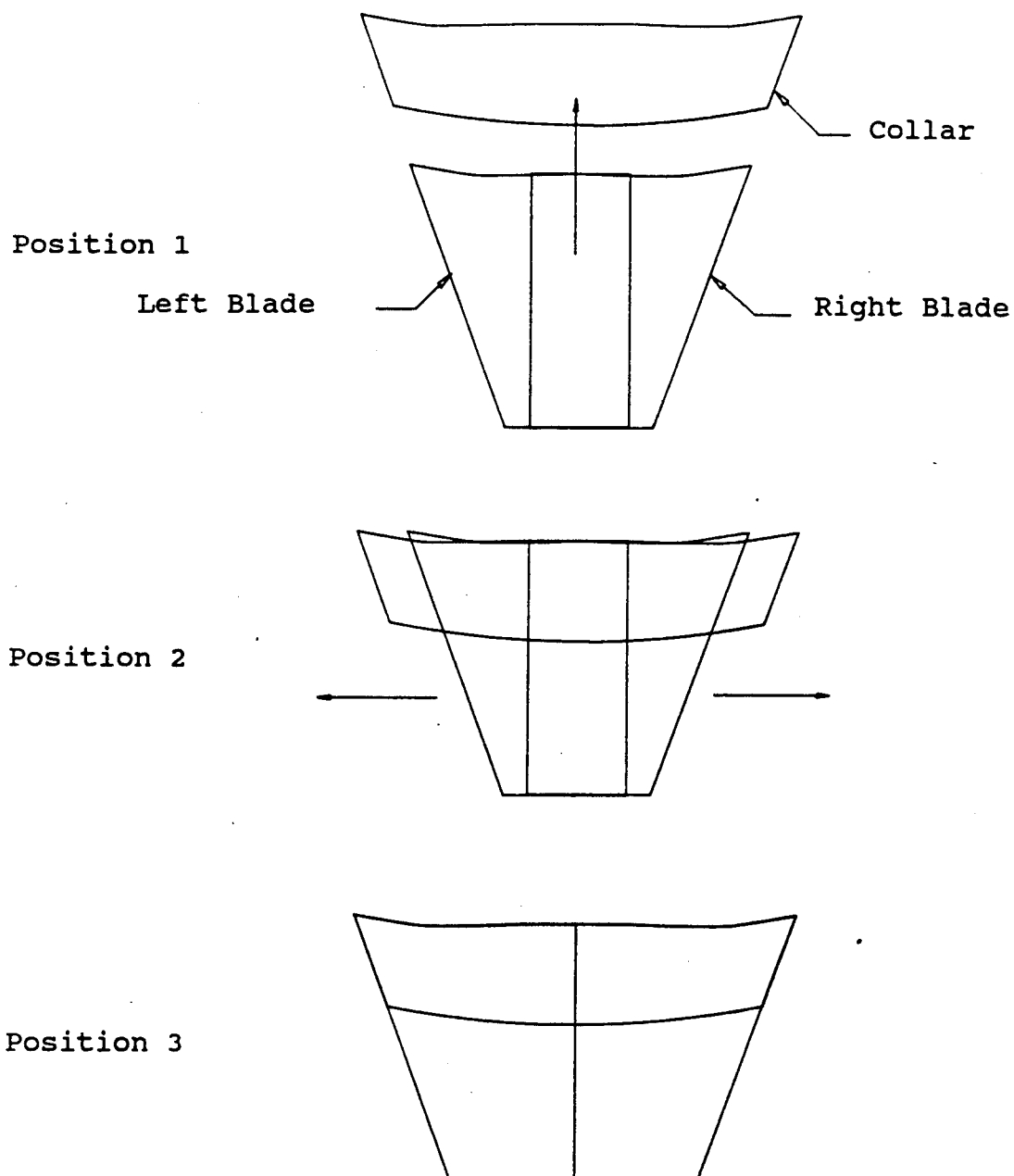
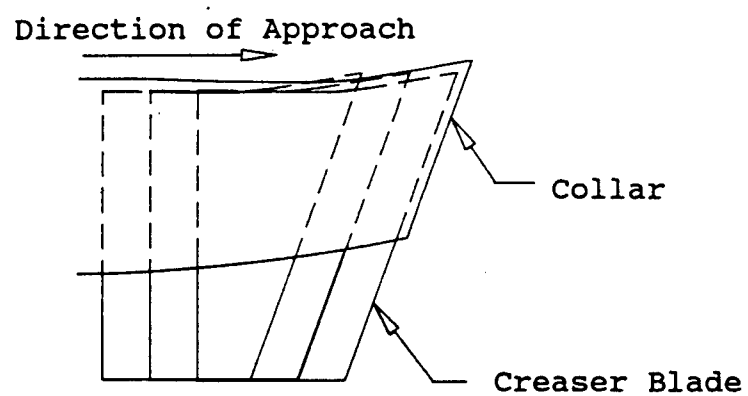
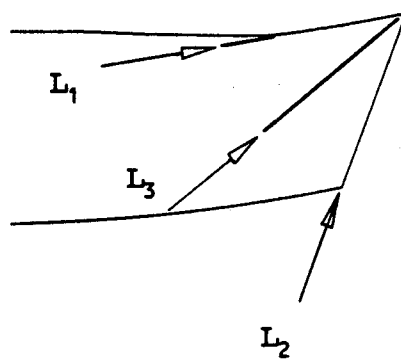


Figure 2.4. 2-Piece Creaser Blade Mechanism



(a)



(b)

Figure 2.5. Interference between Creaser Blade and Collar

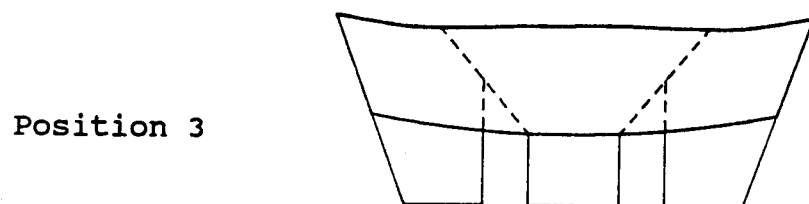
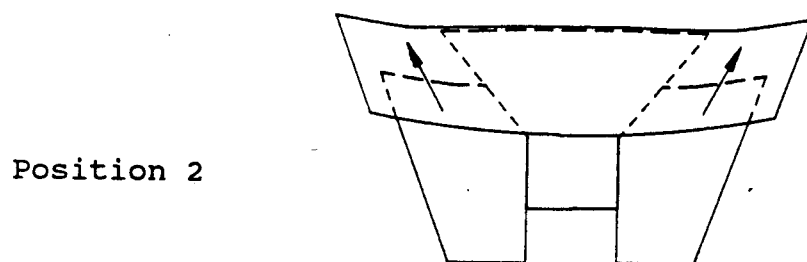
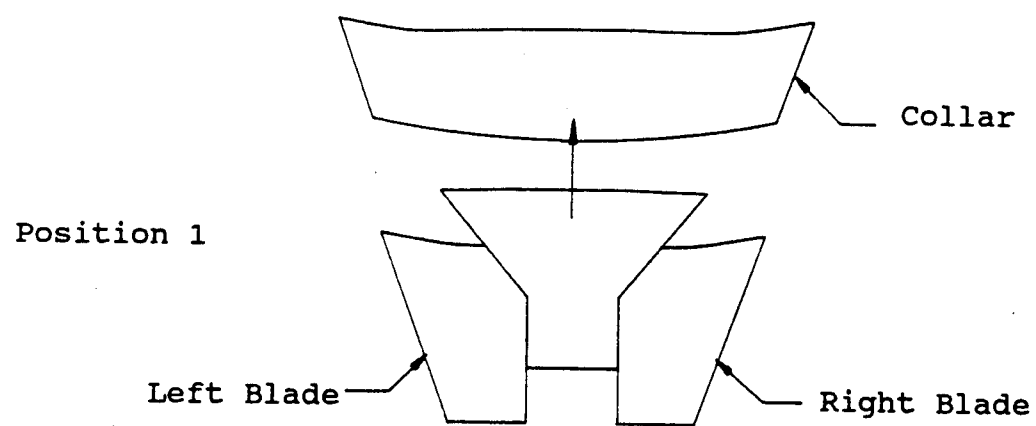


Figure 2.6. 3-Piece Creaser Blade Mechanism

by zone. During the entire course of this operation, there is extensive hand-eye coordination, with the eye acting as the feedback sensor and the hand acting as the actuator or correcting device. Seam position error feedback is a combination of tactile and visual sensing. The operator uses a sense of touch and takes advantage of the difference in the stiffness of the upper and lower ply, to determine where the seam crosses the creaser blade edge while rolling the fabric between his or her fingers.

Seam position sensing and control can be done by direct or indirect methods. Direct seam alignment involves sensing the position of the seam at the front or closed end of the collar, as illustrated in Figure 2.7(a). The seam alignment error may be positive, as shown in Figure 2.7(b) or negative, as shown in Figure 2.7(c). Implementation of the rolling action of the operator's fingers requires a two degree of freedom clamp, illustrated in Figure 2.8. The two degree of freedom clamp would have to be moved laterally along the collar seam, locally adjusting the position of the seam through a sense-adjust-index cycle. A conceptual design for such a device is illustrated in Figure 2.9.

Machine vision is a non-contact sensor which can be used to provide feedback on the position of the seam. In order to detect the seam, a high contrast must exist or be created between the seam and background fabric. Figure 2.10 illustrates two possible camera configurations which can be used to detect the location of the collar seam.

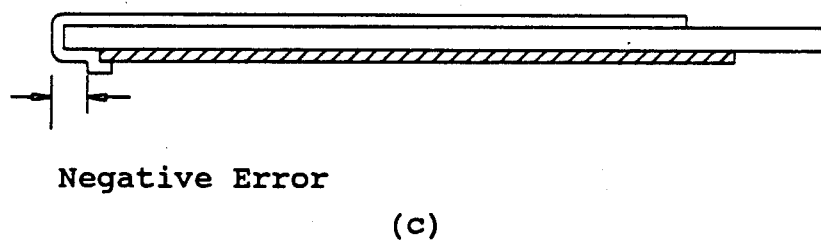
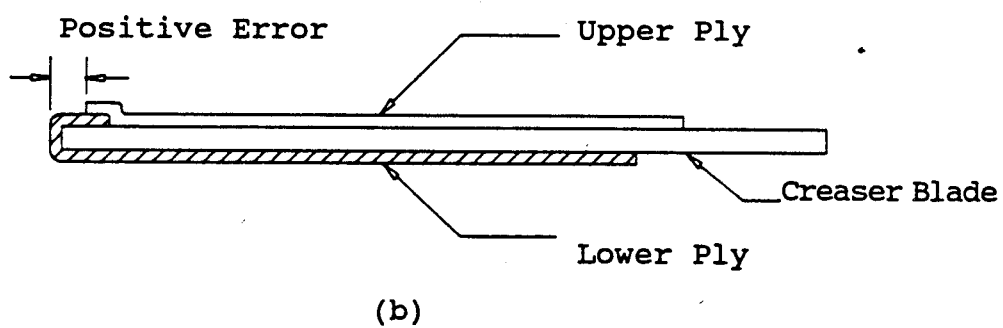
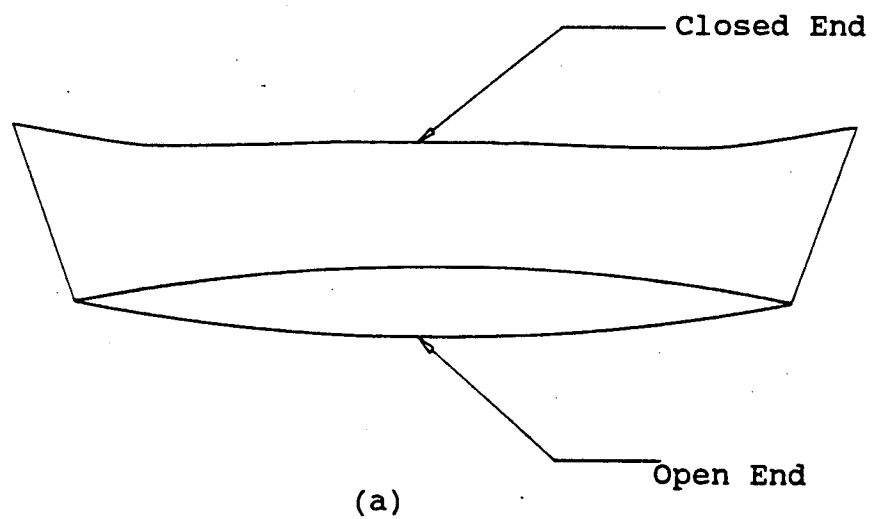


Figure 2.7. Seam Alignment Error

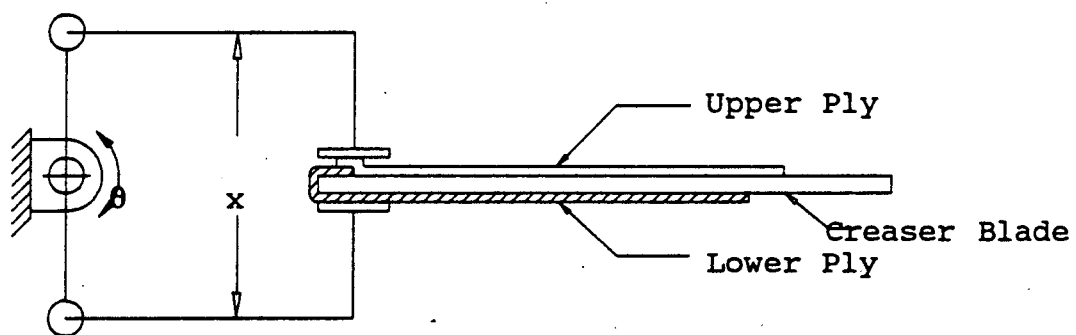


Figure 2.8. Mechanism to Simulate Rolling Action of Fingers

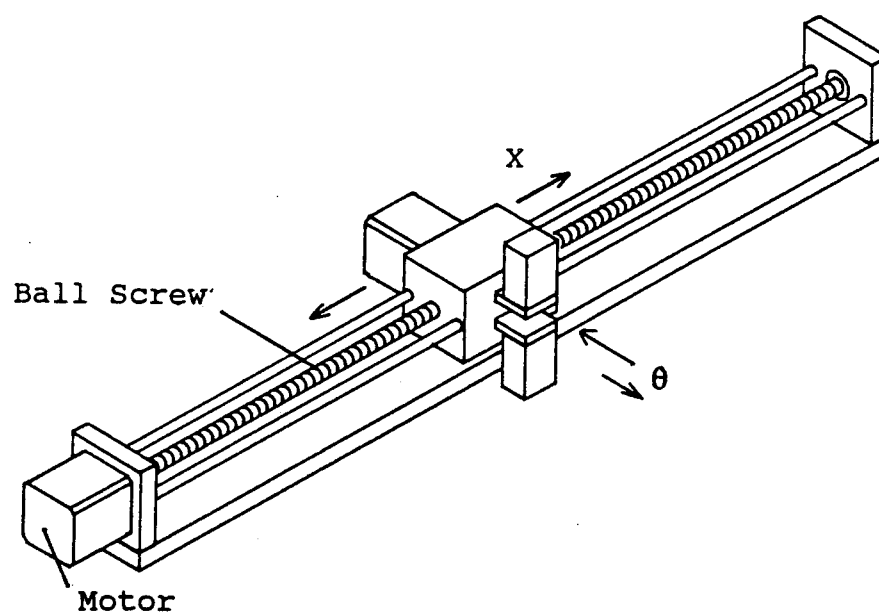


Figure 2.9. Direct Seam Alignment - Conceptual Design

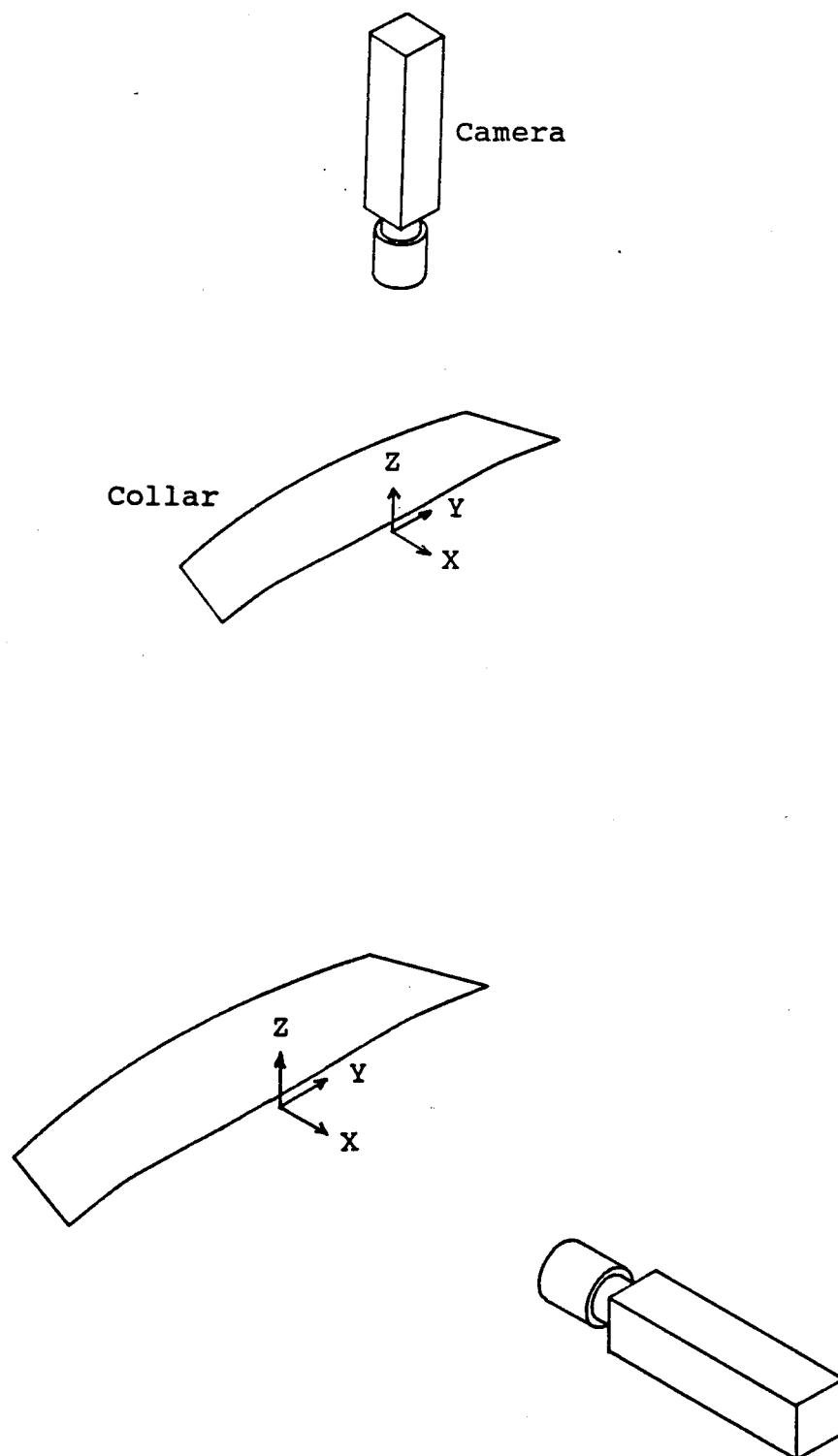


Figure 2.10. Machine Vision for Direct Sensing

Enhancement of the contrast between the seam and the background fabric can be achieved by taking advantage of the fact that there are two layers of fabric under the seam and only one layer of fabric adjacent to the seam junction. Knit and woven fabrics are porous and have a high light transmittance when held taut. The difference in intensities of transmitted light between a double layer and single layer can be used to identify the location of the seam. This principle is illustrated in Figure 2.11, which shows the location of the light source, the single and double layer zones of fabric and the transmitted light received by the receiver, which could be a solid state CCD camera.

A transmitted light seam location system could be implemented using a diffused light source between the fabric and supporting surface. The light source could be placed under the supporting surface if it is transparent. In the case of shirt collar pressing, the creaser blades have to be made of stainless steel, and would therefore be opaque. Since the collar plies are stretched taut after insertion of the creaser blades into the collar, there is no space to accommodate a light source between the fabric and stainless steel creaser blade. After an analysis of other means to implement a transmitted light sensing system, it was concluded that with the given design constraints for double-point collar pressing, a transmitted light sensor was not a viable option.

Reflected light sensors can also be used to detect the location of seams. Detection of a seam by sensing the light

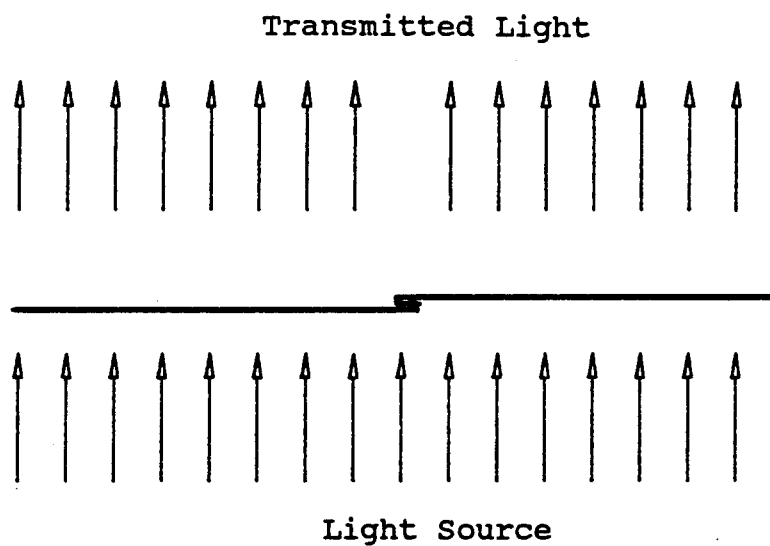
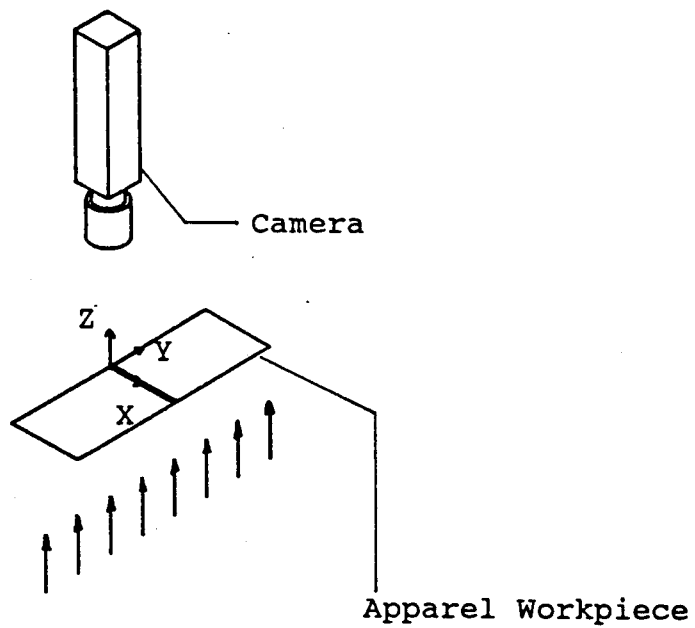


Figure 2.11. Transmitted Light Sensor

reflected from the fabric surface is possible only if a sufficiently high contrast exists between the seam and surrounding fabric. Using the configuration illustrated in Figure 2.12, the change in reflected light intensity along the Y direction in the neighborhood of the seam was measured by scanning pixel values in the Y direction. A diffused fluorescent light source was used. The reflected light intensity profile is shown in Figure 2.13(a). The reflected light intensity shows no sharp drop across the collar seam. In order to be able to locate the position of the seam by sensing reflected light in the neighborhood of the seam, the light intensity should show a sharp change at the seam, as shown in Figure 2.13(b).

Direct seam alignment is difficult to implement because of the problems in sensing or locating the position of points on the seam by direct means. However, the option to apply indirect sensing and control strategies is still open. The free edges of the upper and lower plies of the turned collar which form the opening of the collar pocket are clearly visible and can be located by using a non-contact sensor such as an overhead solid state camera. Figure 2.14(a) illustrates an apparel workpiece comprised of two rectangular pieces of fabric sewn together along a straight line. Figure 2.14(b) illustrates a folding operation of this apparel workpiece over a straight edged creaser blade. If the workpiece lengths L_1 and L_2 are equal, then the free edges of the plies can be used as a reference for seam alignment. By manipulating the fabric

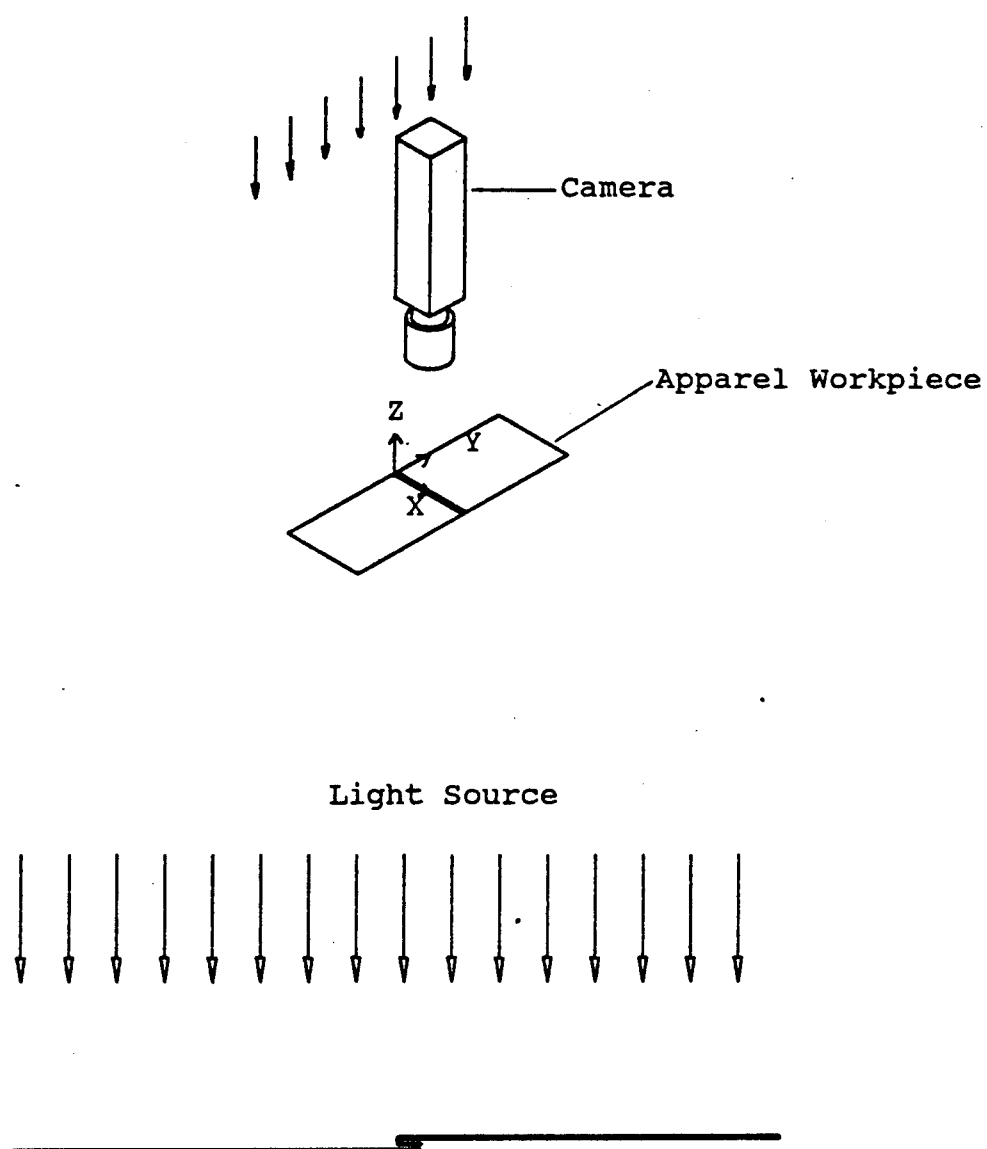
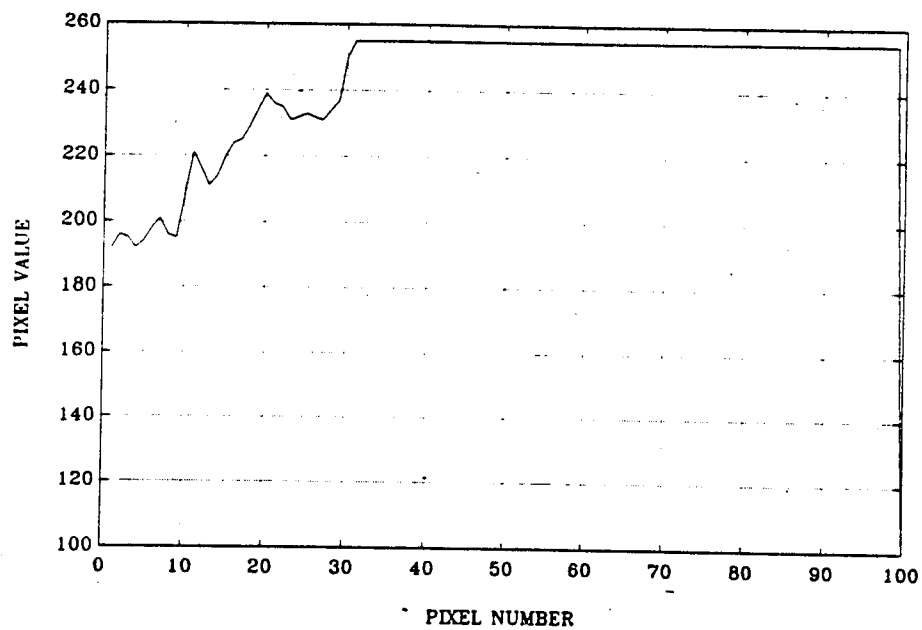
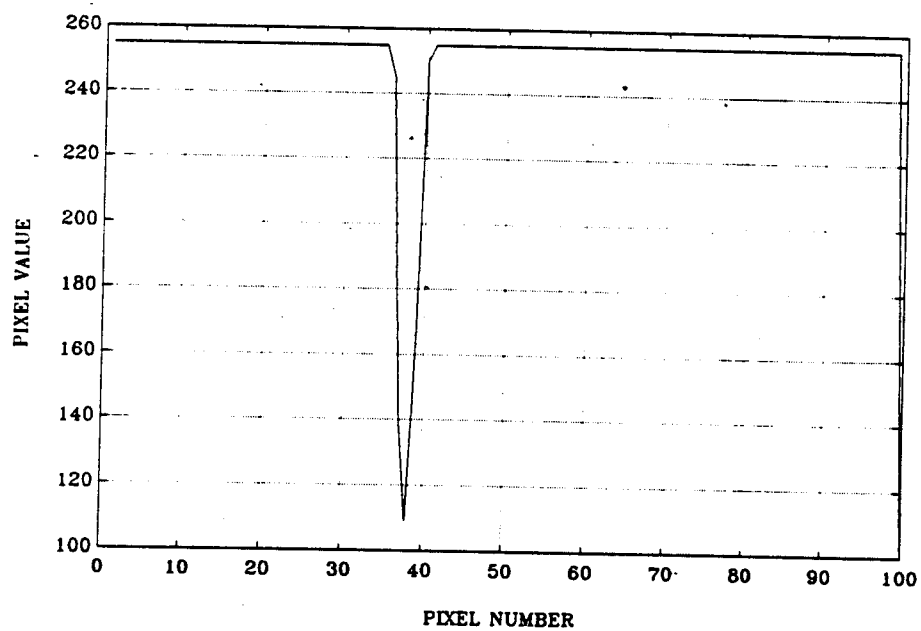


Figure 2.12. Reflected Light Sensor

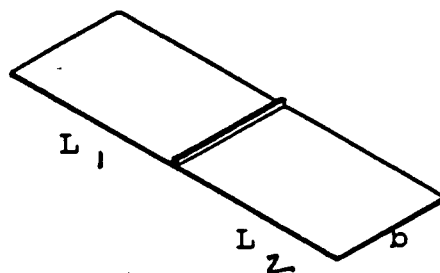


(a)



(b)

Figure 2.13. Reflected Light Intensity Profile



Apparel Workpiece

(a)

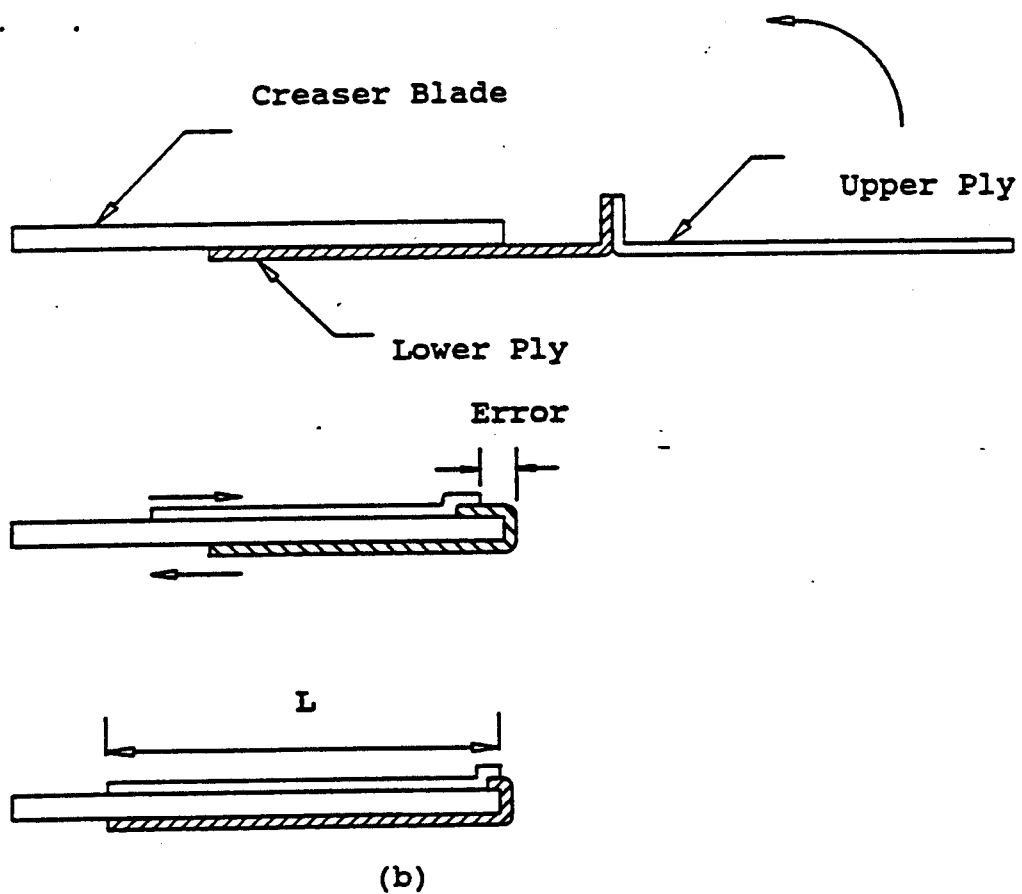
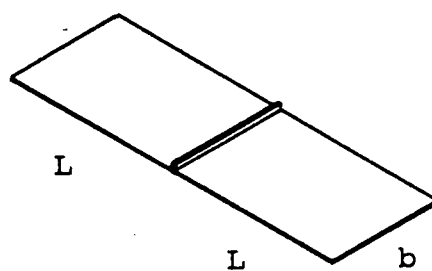


Figure 2.14. Indirect Seam Alignment - Double Ply Manipulation

plies and matching the free edges of the upper and lower plies, the alignment of the seam against the creaser blade edge can be done indirectly. A suitable offset may be provided to compensate for the thickness of the fabric and the creaser blade.

In the case of the dress shirt collar, the upper and lower plies are identical in shape. Before the plies are sewn together, the rear edges of the plies are aligned by the operator. Applying the principle of indirect sensing and control for automated seam alignment, it is possible to predict the position of points on the seam by monitoring the location of points on the free edge of the upper and lower plies of the turned collar. Extending this principle, if one of the plies is clamped and forced to remain stationary, then the seam alignment task by indirect sensing is equivalent to a task of folding an apparel workpiece over a creaser blade. The number of degrees of freedom required is also reduced to two. The operation sequence for indirect seam alignment by manipulating the upper ply alone is illustrated in Figure 2.15.

Seam alignment by a folding operation can be done by holding the lower ply stationary with respect to the creaser blade and pulling back the upper ply to match the free edges of both plies. This will enable the seam alignment task to be carried out by manipulating the upper ply alone. In order to ensure that the lower ply does not move due to fabric creaser blade contact during creaser blade insertion, it has to be



Apparel Workpiece

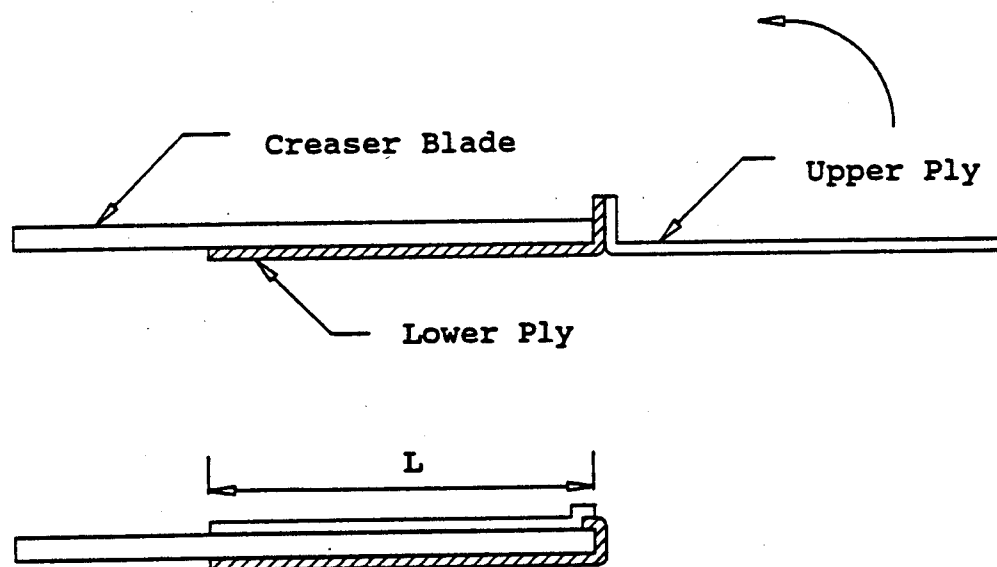
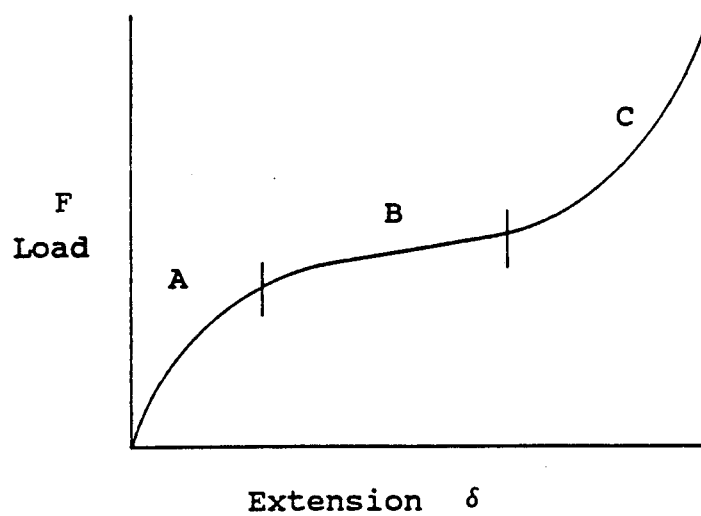


Figure 2.15. Indirect Seam Alignment - Single Ply Manipulation

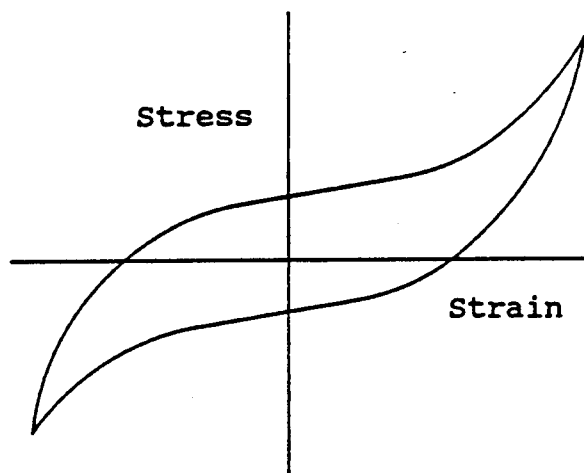
held firmly against lateral forces. Vacuum has been used in many situations requiring apparel workpiece fixturing. Bernadon and Kondoleon [6] have successfully applied vacuum to hold the lower ply of men's suit sleeves stationary on a work surface while a robot equipped with a special cloth picking end-effector folded the sleeve to prepare the sleeve for sewing. When vacuum is used to hold multiple-ply apparel workpieces stationary against lateral forces, the plies must be separated and held apart by external means, to avoid suction forces being applied on the upper ply of the workpiece.

Seam alignment by indirect edge matching involves folding the apparel workpiece over a creaser blade edge. For apparel components made from thick or heavy fabric, such as canvas or denim, the workpieces behave as semi-rigid planar objects. The seam could be modelled as a hinge connecting the two workpieces. However, collars for dress shirts are made of thin woven fabric, whose behavior differs considerably from that of fabrics such as denim or canvas.

A typical load extension curve for fabric stiffness of woven fabric under tensile load is shown in Figure 2.16(a). Phase A of the extension process is the friction zone where inter-fiber frictional forces are overcome. Phase B is the decrimping phase, which involves removal of slack in the weave due to tensile loading. The load extension characteristics of fibers vary depending on the fiber involved. The load extension behavior of woven fabric closely approximates the



(a) Tensile Load



(b) Shear Load

Figure 2.16. Load - Extension Curve for Woven Fabric
(Source : Hearle et al. [12], Structural Mechanics of Fibers, Yarns, and Fabrics)

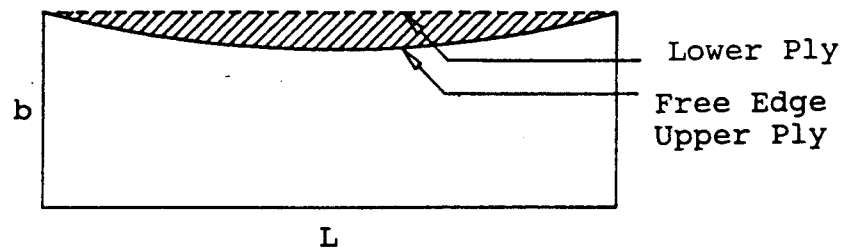
load - extension behavior of its constituent fibers. The beginning of zone C marks the end of the linear portion of the curve and represents yarn extension.

A typical load extension curve for fabric stiffness of woven fabric under an in-plane shear load is shown in Figure 2.16(b). The behavior of woven fabric is very different under a shearing load when compared to that under tensile load. The shear modulus of woven cloth is a few orders of magnitude lower than the tensile modulus. The curve also indicates a distinct hysteresis loop.

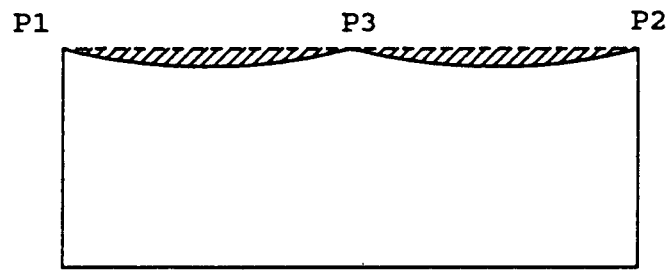
Figure 2.17 illustrates the folding of a rectangular apparel workpiece consisting of two identical plies stitched along a straight line, with an offset from the ply edge. The workpiece is spread out on a suction surface to hold it in position. A creaser blade with a straight edge is placed with its edge exactly overlaid on the stitch line. The upper ply is lifted and folded over the creaser blade edge. The upper ply is pulled back completely such that corresponding end points on both upper and lower ply are matched.

The free edge of the upper ply is distorted into a curve due to a combination of tensile and shear loads generated by the bending of the rib. The edge alignment error is indicated by the shaded area in Figure 2.17. Increasing the number of "control" points, i.e., matching edge points on the upper and lower plies, can progressively decrease edge alignment error.

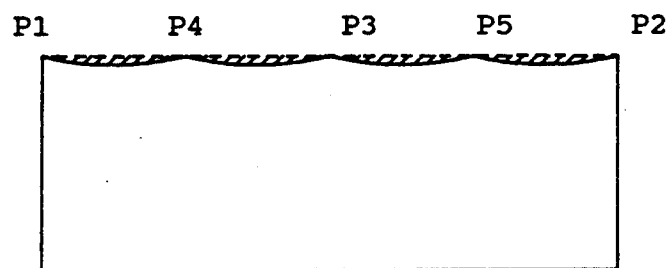
The accuracy of edge matching has a direct effect on the crease generated after pressing. The greater the number of



(a)



(b)



(c)

Figure 2.17. Edge Alignment Error

points aligned on the free edges of the upper and lower plies, the lesser the edge alignment error and the sharper the crease generated after pressing. Minimizing the edge alignment error optimizes the quality of the crease.

Thus, it is possible to hold the bottom ply stationary with respect to the creaser blade and manipulate only the upper ply, for indirect seam alignment. This method requires the use of a two degree of freedom linear drive to control the position of each edge point on the upper ply to be matched to its counterpart on the lower ply. An ideal solution would be to use an infinite number of control points, reducing the edge alignment error to zero. However, due to cost and space constraints, only a finite number of actuators can be accommodated. For this research, a set of three actuators were selected to independently control the position of three control points on the edge of the upper ply.

Chapter III describes the detailed design of the components and functional modules of the proof-of-concept machine. It also describes the control hardware used and the implementation of a vision sensor to provide feedback data for automated indirect edge matching. Chapter IV discusses the development of control algorithms and software used for an experimental evaluation of the design, sensing and control concepts developed in this chapter.

CHAPTER III

DESIGN AND CONTROL IMPLEMENTATION

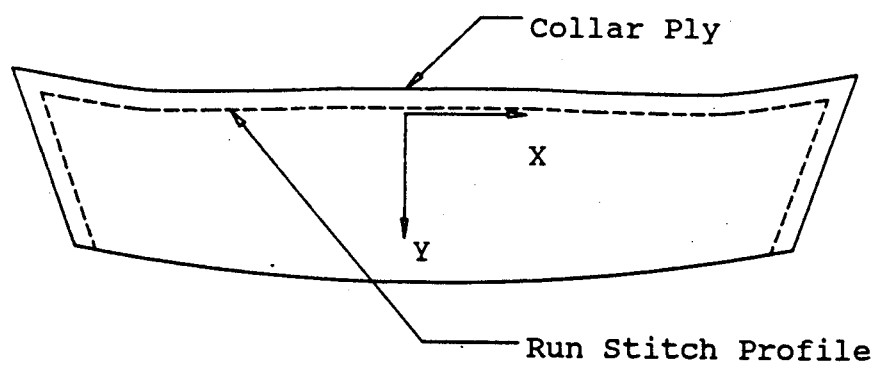
The design, sensing and control concepts discussed and evaluated in Chapter II were implemented on a proof-of-concept machine. The proof-of-concept machine was comprised of four main modules, namely:

1. the creaser blade mechanism,
2. the vacuum system,
3. a set of three linear drives, and
4. the vision sensor.

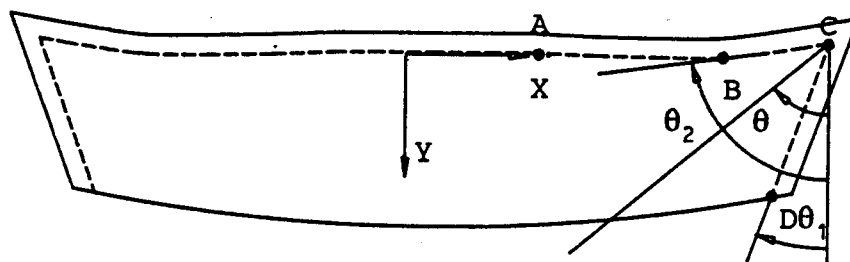
This chapter discusses the design and development of each of the four modules.

Creaser Blade Mechanism

The problem of interference between the moving creaser blades and the collar fabric due to the incorrect selection of the approach angle was introduced and discussed in Chapter II. It is necessary to understand the profile of the run stitch before collar turning takes place in order to determine a suitable angle of approach so as to avoid creaser blade fabric interference. The run stitch profile of an unturned collar is detailed in Figure 3.1(a). The run stitch profile is a series of short straight line segments. From Figure 3.1(b) shows that the run stitch profile starts with a slope of zero at the center of the collar. The slope becomes negative at A and monotonically decreases until the profile reaches point B. At



(a)



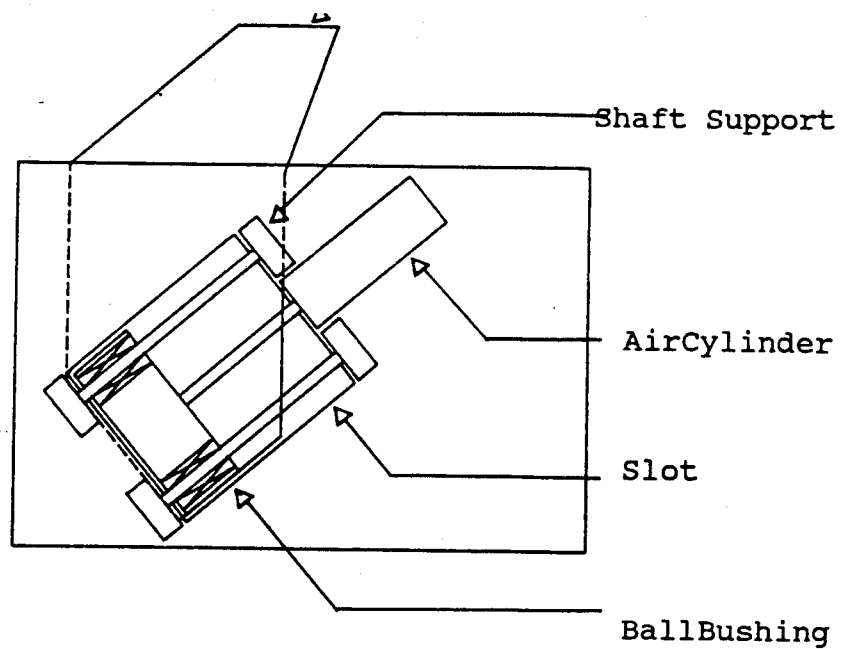
(b)

Figure 3.1. Run Stitch Detail for an Unturned Collar

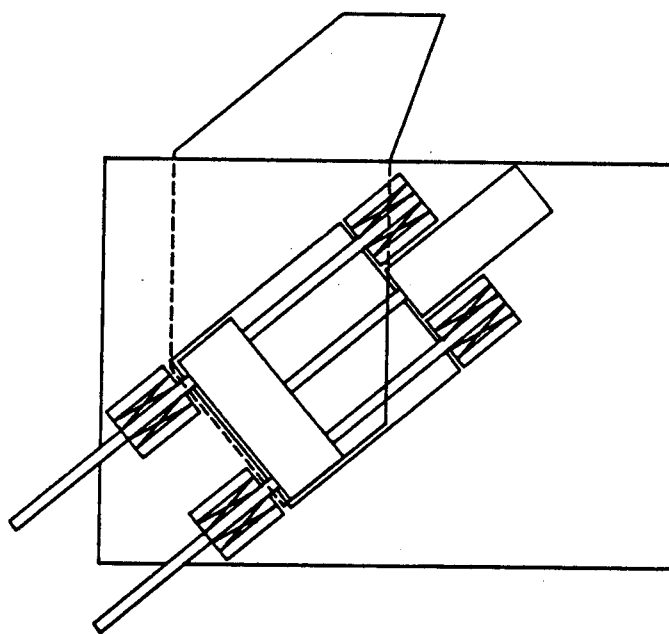
B, there is a sharp increase in the slope of the profile of the run stitch.

A template will fit snugly into the collar tip, if the angle of approach θ is between θ_1 and θ_2 . The value of θ chosen was 50° , so as to set the line of action of the creaser blade along the bisector of the angle BCD. Since the turned collar is not an exact two-dimensional entity, there is a distinct possibility of creaser blade fabric contact before the blade tip locks into the collar point. For an approach angle of 50° , the creaser blade applies a force along the bisector BCD, thereby providing a self-release mechanism to prevent jamming.

Two layouts considered for bearing arrangements and actuator placement are illustrated in Figure 3.2. In Figure 3.2(a), the layout shows a slideway supported on two fixed guide rails, with four anti-friction bearing points to provide support and to prevent cocking. The slideway is driven by a two-way pneumatic cylinder. The slideway, guide rails, rail supports, and pneumatic cylinder are mounted on a base plate. The slideway block moves in a rectangular slot cut into the base plate. The creaser blade is coupled to the sliding block under the base plate. The layout shown in Figure 3.2(b) differs slightly from Figure 3.2(a). The slideway is coupled to the guide rails. Four anti-friction bearing support points are provided. These bearings are fixed and do not move. The pneumatic cylinder, coupled to the slideway, drives the creaser blade. The basic difference between the two layouts



(a)



(b)

Figure 3.2. Bearing Layouts for Creaser Blade Mechanism

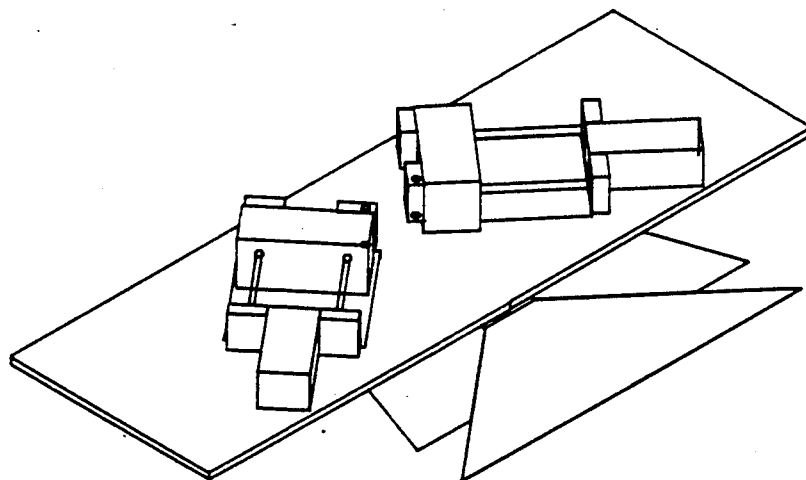
is in the bearing arrangement. The layout in Figure 3.2(a) provides fixed guide rails while the layout in Figure 3.2(b) uses moving guide rails, which protrude into the collar loading zone. The space directly above the free edge of the upper ply of the collar has to be free to accommodate edge alignment devices. Due to this reason, the configuration shown in Figure 3.2(a) was adopted and implemented.

The pneumatic cylinders selected to drive the creaser blade were of the double acting type, with port mounted needle valves to control the air flow rates. Self-aligning ball-bushings were used as anti-friction linear bearings. A three dimensional view of the creaser blade mechanism assembly is shown in Figure 3.3.

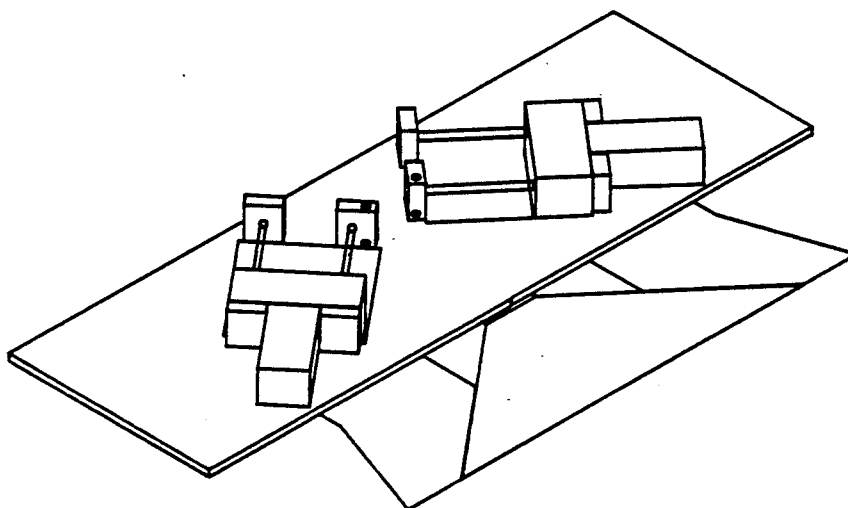
Vacuum System

The creaser blade mechanism was designed to acquire a turned collar in a single loading operation. The turned collar has to be positioned on a flat surface in order to execute the loading operation successfully. In addition to this, the collar needs to be held in place against lateral forces which will come into play towards the end of the creaser blade insertion stroke.

Vacuum has been successfully employed as a fabric fixturing mechanism in previous apparel automation research projects, such as the robotic sleeve folder developed at Draper Laboratories [6]. Vacuum is also used in buck presses to remove wrinkles from apparel workpieces before the pressing operation.



(a)

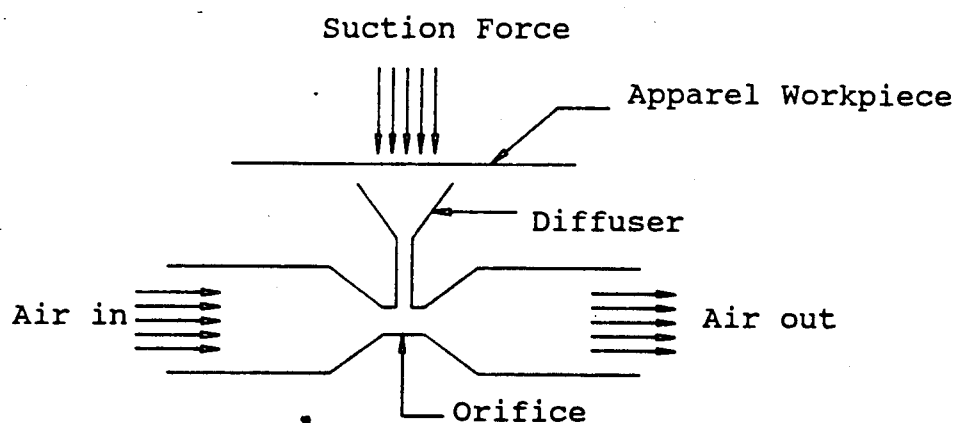


(b)

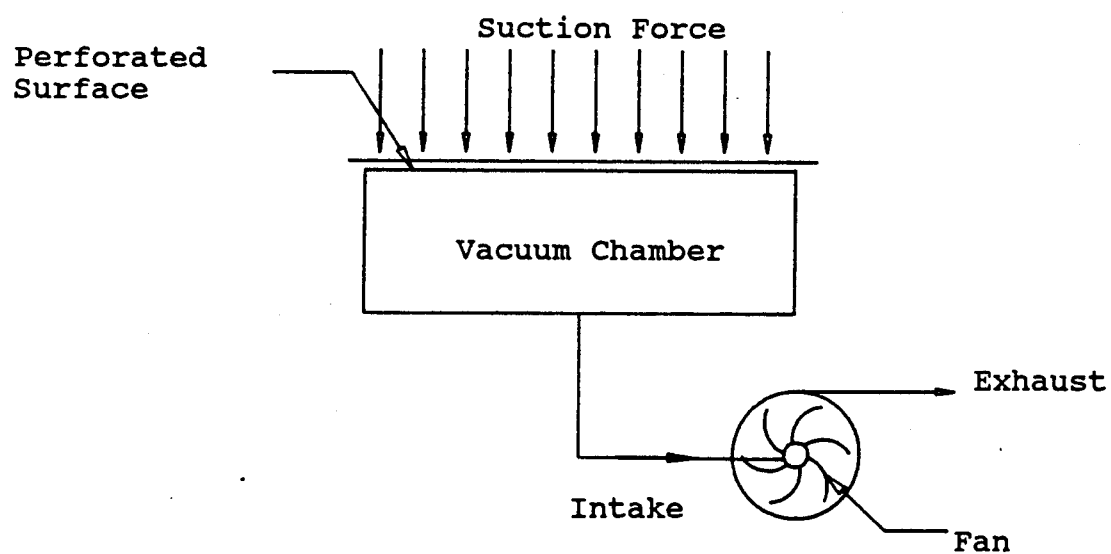
Figure 3.3. Creaser Blade Mechanism Assembly

Two methods to generate suction were investigated. The first method utilized the venturi effect. Suction can be generated by air flow through an orifice, creating a pressure drop at the neck of the orifice. When the neck of the orifice is opened to atmospheric pressure through a diffuser, the mouth of the diffuser acts as a suction pad. A schematic of such a device is illustrated in Figure 3.4(a). A suction surface or vacuum table could be designed by configuring a number of venturi based units in a rectangular array.

The second method investigated was the use of a vacuum system coupled to an evacuation chamber with a perforated plate acting as a suction surface. Figure 3.4(b) illustrates the operation of such a device. The vacuum system is typically a motor driving a fan with an axial intake and a peripheral exhaust. The intake is connected to the evacuation chamber and the exhaust is opened to atmosphere. When the fan is turned on, air from the evacuation chamber is exhausted, creating a pressure drop inside the chamber and a vacuum at the holes of the perforated surface plate. Venturi based suction devices are not capable of generating suction forces large enough to hold a porous apparel workpiece stationary against lateral forces. Fan driven vacuum systems on the other hand, can generate large suction forces because of their large volumetric discharge rates at high speeds. Due to this reason, a suction system utilizing a centrifugal fan was designed and implemented.



(a)



(b)

Figure 3.4. Methods to Implement Suction Surfaces

The suction force generated was controlled because excessive suction would result in the fabric being sucked into the perforations, causing small "dents" in the fabric surface. An intake bypass valve was installed for the control of suction force.

Linear Drives

The pneumatically driven creaser blade mechanism, along with a vacuum suction surface, enables the automatic loading of a turned collar onto the blades in a single operation. The indirect seam alignment operation by edge matching requires a two degree of freedom position controlled clamp. One degree of freedom is needed to activate the clamp which will grip the fabric. The second degree of freedom is needed to pull the clamped fabric ply to match corresponding edge points on the upper and lower plies.

Figure 3.5 is an isometric assembly view of the two degree of freedom linear drive unit. The design utilizes a ball screw and nut arrangement to convert the rotary motion of the drive motor to a linear displacement. A slideway coupled to the ball nut, was used to drive the clamping cylinder, through a pair of guide shafts. The slideway motion was supported with four-point bearing support using anti-friction ball-bushings. A friction pad, mounted at the end of the clamping cylinder, was used to grip the fabric. The clamping cylinder was fitted with anti-torque guide rods, to prevent the friction pads from rotating. The force applied on the friction pads was 10 pounds with a supply pressure of 80 psi,

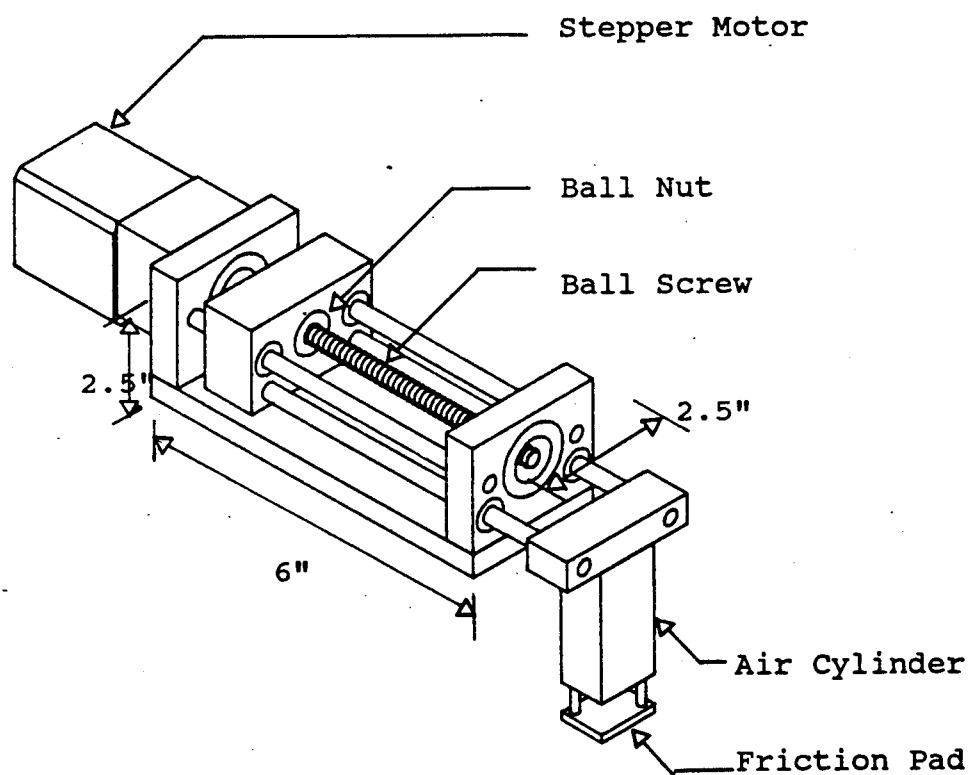


Figure 3.5. Linear Drive Assembly

which was sufficient to prevent slipping between the fabric and the pad.

The ball screw was driven by a 2-phase permanent magnet stepping motor. The motor was interfaced to a matched driver. The stepper drivers were controlled from a motion control card installed in the System Supervisor(SS), which was a microcomputer used for motion control and digital I/O. The ball screw and nut reduction provided a linear stepped resolution of 6.25×10^{-4} inches per step in full step mode and 3.125×10^{-4} inches per step in half step mode. The drive was designed for a working stroke of 6", and was operated at a slew velocity of 5000 steps per second or 3.125 inches per second. The motor generated a pullout torque of 20 oz.in. at a stepping speed of 5000 steps per second, which produced a pulling force in excess of 10 pounds at the friction pads gripping the fabric ply edge. Three identical drives were built and mounted on a plate placed above the base plate of the creaser blade mechanism. The creaser blade mechanism with the three linear drives mounted above is illustrated in Figure 3.6.

Vision Sensor

The vision sensor, which was used to provide feedback data on the location of the edges of the upper and lower plies, was comprised of a CCD camera connected to an image acquisition and processing board installed in the backplane of a second microcomputer, which served as the Vision Controller (VC). An array processor board was installed to speed up

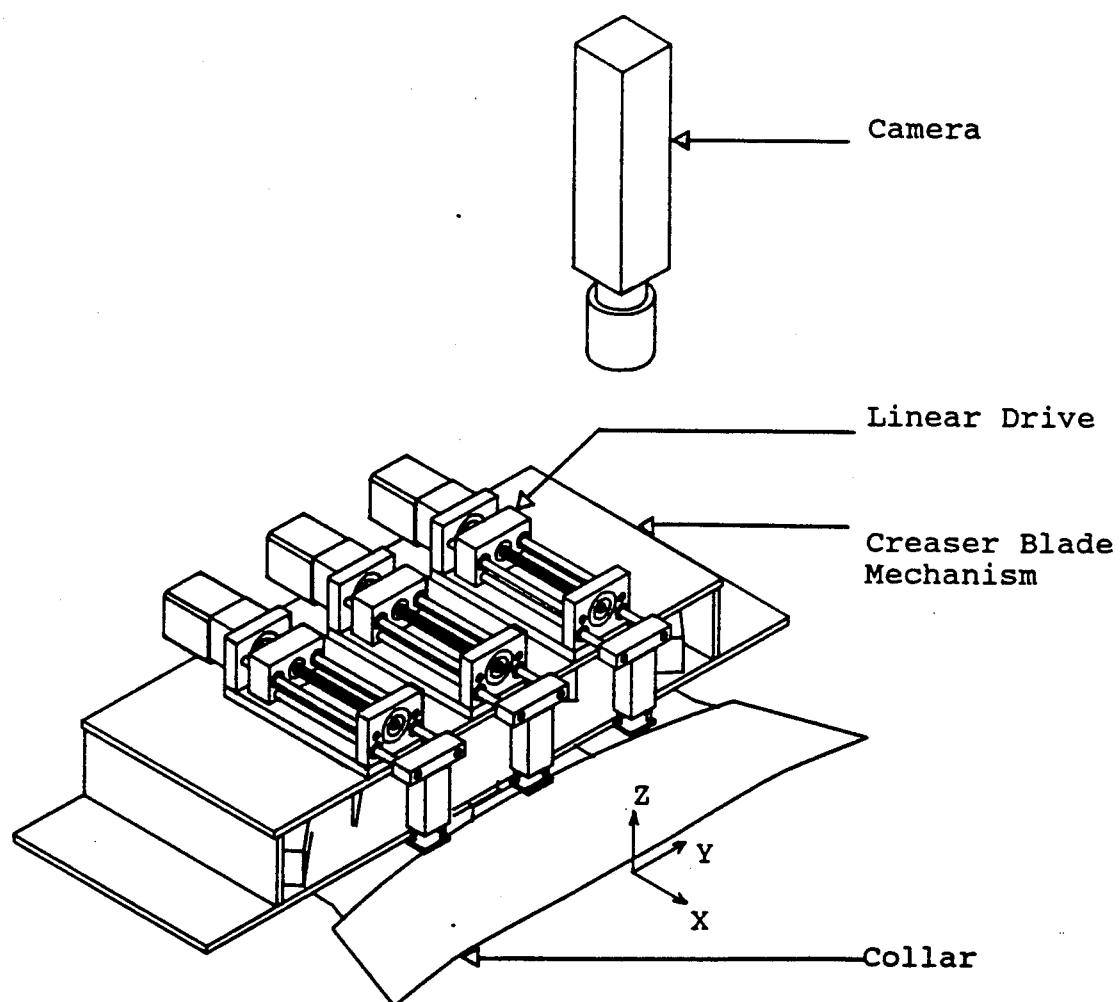


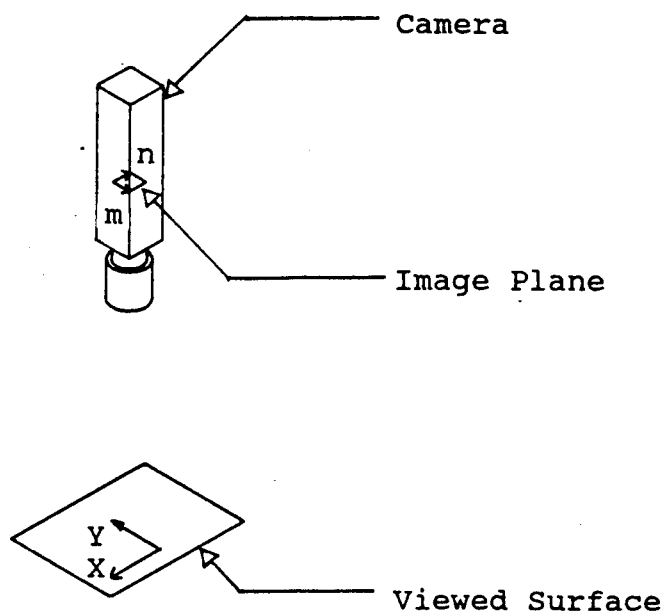
Figure 3.6. Collar Loaded on Creaser Blades

computation during image processing tasks. The camera was mounted with its optical axis vertical, with the focal plane of the lens maintained parallel to the viewed surface. Figure 3.6 shows the camera location and its field of view. Uniform light from overhead fluorescent sources ensured the elimination of shadows on the surface.

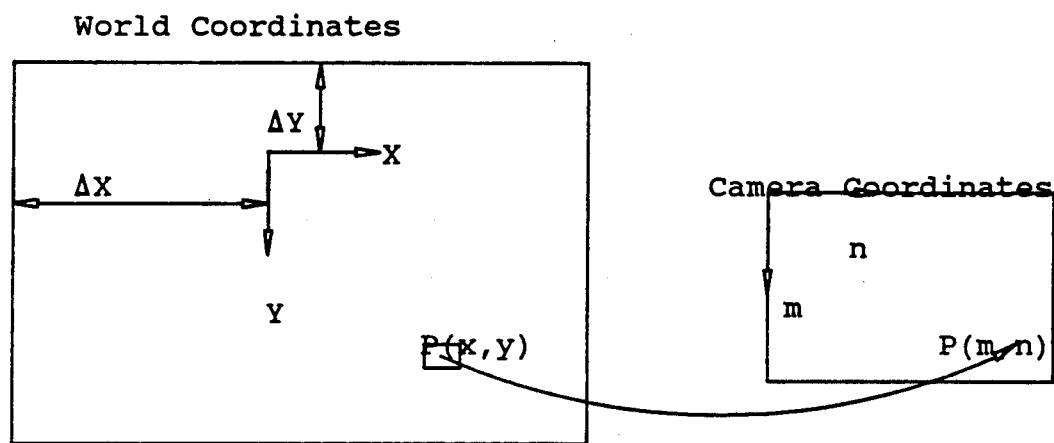
The image plane of the solid state camera was a pixel array composed of 512 rows and 512 columns, covering a rectangular area of 6.6 X 8.8 square millimeters. A standard aspect ratio of 4:3 was used. The camera was interfaced with a high-speed frame acquisition and storage board, installed in a backplane slot of the Vision Controller.

The image acquisition and storage system was capable of storing sixteen 512 X 512 pixel gray scale images in 16 on-board frame buffers. The board also had the capability to perform various operations on the frame buffers such as thresholding, filtering, histograms etc. An 8-bit pixel code provided 256 digital pixel intensity values. The intensity of each of the 512 X 512 pixels in a frame buffer could be read in or altered using a row and column address.

The exact geometric relationship between the viewed surface and the camera imaging plane was determined to calibrate the vision system. Figure 3.7 illustrates the imaging geometry of the camera and the relationship between the view plane and the imaging plane. It can be seen that the rectangular field of view is obtained by projecting the pixel array boundary onto the viewed surface. If the pixel array



(a)



(b)

Figure 3.7. Calibration Geometry and Transformations

had an infinite resolution i.e., an infinite pixel density, then there would be a one to one mapping between a point on the view plane and a corresponding point on the imaging plane. However, since the pixel density is finite, each pixel samples the light from not a single point but a rectangular area on the view plane. This results in the system having a finite spatial resolution.

Calibration of the vision system was carried out at a fixed distance between the camera and viewed surface. The image plane axes m and n were squared with the base frame axes X and Y by suitably rotating the camera. The pixel densities in the X and Y directions were determined by placing a calibration grid on the viewed surface. The calibration grid was a rectangular grid with black horizontal and vertical lines drawn on a white sheet of paper with an interline spacing of one inch. An image of the grid was acquired and stored. This gray-scale image was converted to a binary image using a direct thresholding procedure, to yield an image with binary pixel values. The binary image was scanned in the m and n directions and the number of pixels between consecutive horizontal and vertical lines was counted and averaged for each direction to give $grid_x$ and $grid_y$, the vision system's resolution in pixels per inch in the X and Y directions respectively. With reference to Figure 3.7, the transformations from the view plane to image plane are

$$n = \text{INT}[(X + \Delta x).grid_x], \quad (3.1a)$$

$$m = \text{INT}[(Y + \Delta y).grid_y], \quad (3.1b)$$

where

INT() = a function which returns the integer value of its argument by truncation,

m = pixel row address of a point P on the viewed surface (pixels),

n = pixel column address of a point P on the viewed surface (pixels),

(X,Y) = world coordinates of the point P (inches),

Δx = offset between the m and Y axes (inches),

Δy = offset between the n and X axes (inches).

The transformations from image plane to view plane are

$$X = (n/\text{grid_x}) - \Delta x, \quad (3.2a)$$

$$Y = (m/\text{grid_y}) - \Delta y. \quad (3.2b)$$

Figure 3.8 is a schematic of the control system used to run the proof-of-concept machine and the vision system. The two computers, the Vision Controller(VC) and the System Supervisor(SS) were linked using a RS 232 serial link. All the air cylinders were controlled from a set of solenoid valves, which were interfaced to a digital I/O control module installed in the SS. Inductive proximity sensors were used to sense home positions of the linear drives and were interfaced to the digital I/O control module. Figure 3.9 shows the fully assembled proof-of-concept machine.

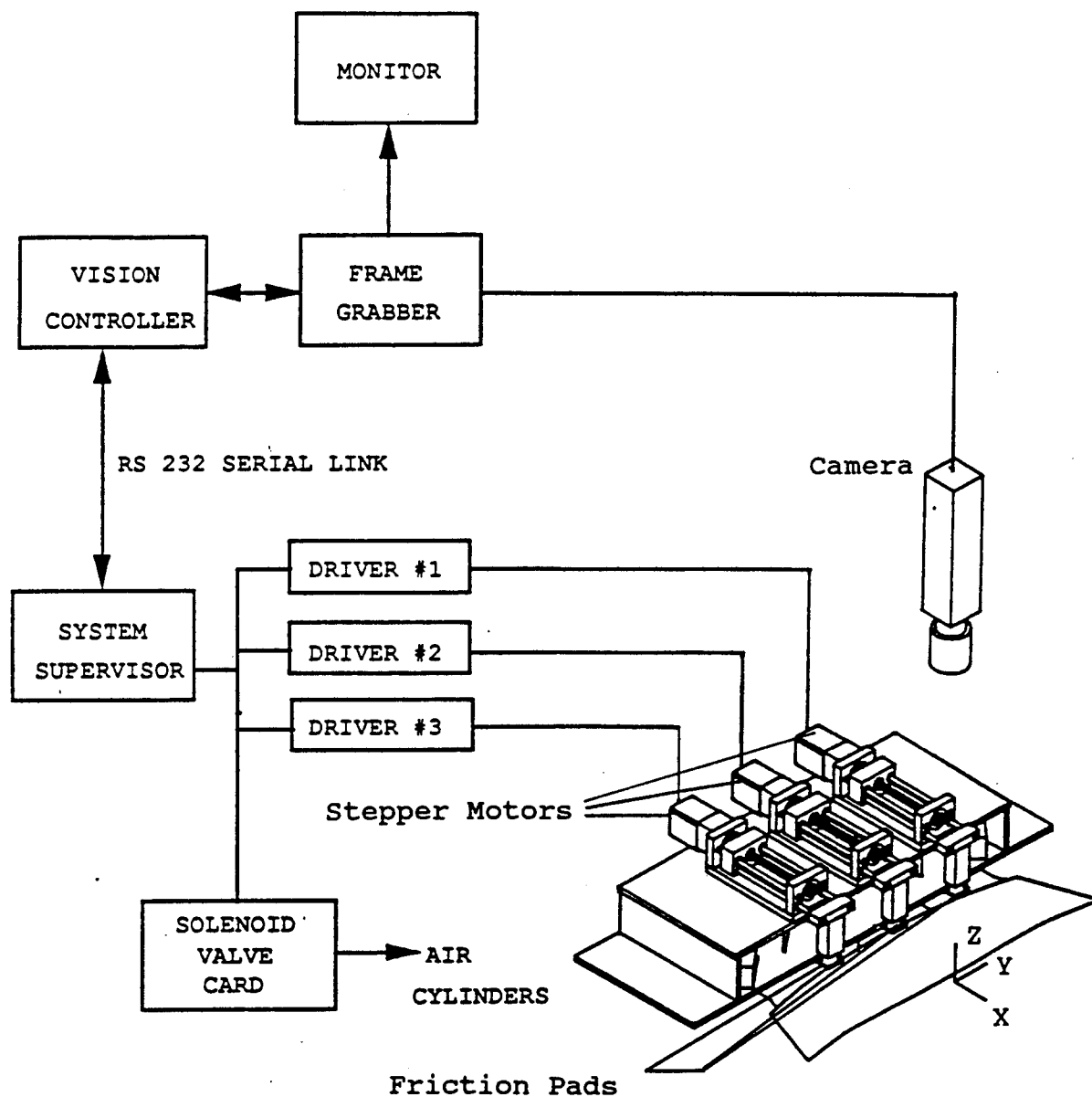


Figure 3.8. Control Structure for the Proof-of-Concept Machine

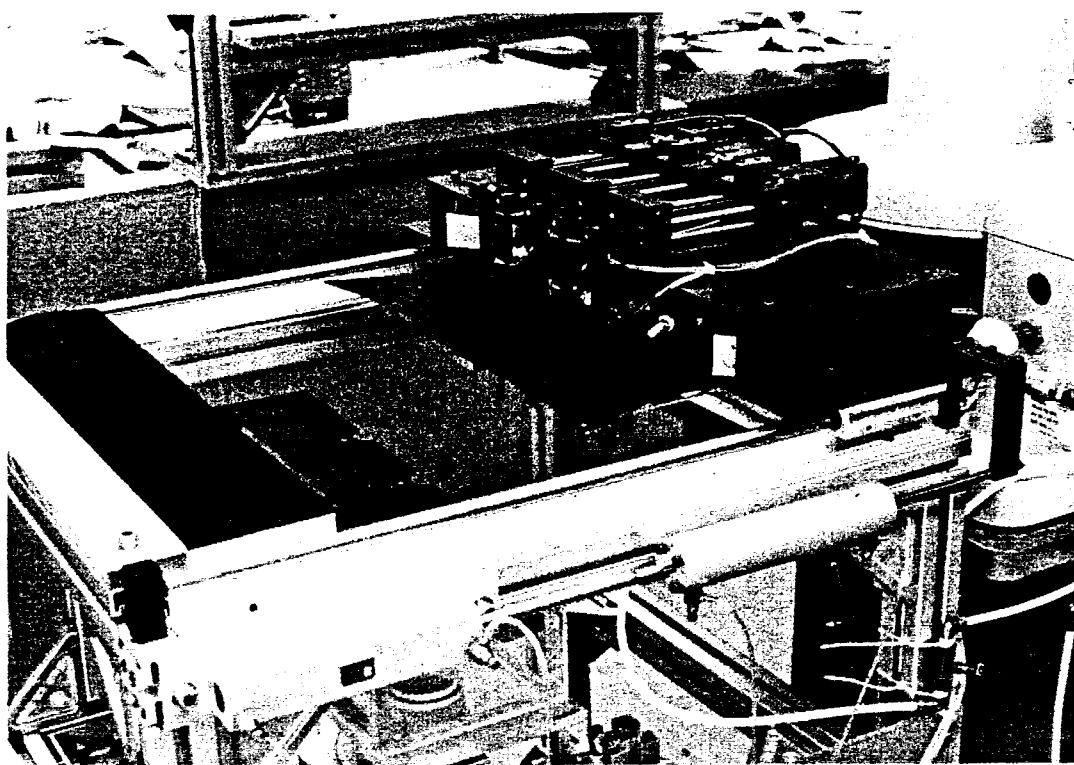


Figure 3.9. Proof-of-Concept Machine

CHAPTER IV

ANALYSIS AND EXPERIMENTAL EVALUATION

Chapter III discussed and documented the design of a proof-of-concept machine, which was built to implement the design and control concepts that were developed in Chapter II. An algorithm was developed to evaluate the validity of the concepts related to automated collar acquisition and automated indirect seam alignment. This algorithm was coded in the C language as programs written to run the proof-of-concept machine. An error analysis was also carried out to evaluate the vision system's accuracy and precision.

Algorithm for Automated Collar Acquisition and Indirect Seam Alignment

Figure 4.1 is a flow chart which shows the various steps of a sequence to carry out automated collar acquisition and automated indirect seam alignment. The proof-of-concept machine is first initialized. This involves initializing the motion control and image processing boards installed in the System Supervisor and the Vision Controller respectively. The three linear stepper drives are initialized, using inductive proximity sensors to determine home position. The other initialization tasks are retracting the clamps and creaser blades.

The machine first acquires a turned collar using the creaser blade mechanism. The vacuum table is raised to its

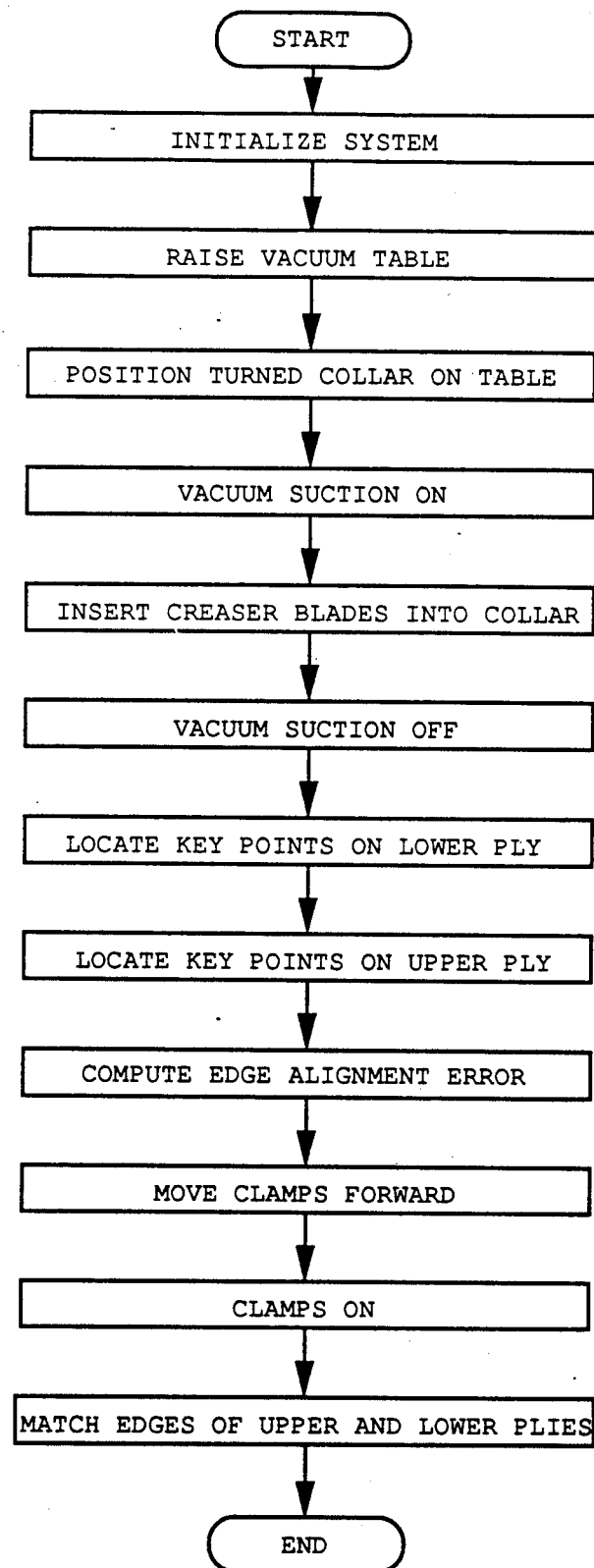


Figure 4.1. Flow Chart for Automated Collar Acquisition and Indirect Seam Alignment

elevated position. A turned collar is positioned on the surface of the vacuum table, with the lower ply i.e., the ply with the fused stiffener, in contact with the suction surface. The upper and lower plies are held apart and the vacuum is activated. At this point, the turned collar is positioned and fixtured on the vacuum suction surface.

The acquisition of the collar by the creaser blade mechanism is done in two stages. The entire creaser blade assembly is moved into the open collar. The air cylinders driving the left and right creaser blades are activated, thereby driving the expanding blades into the collar points and completing collar transfer from the suction surface to the creaser blade mechanism. Following collar acquisition by the creaser blade mechanism, the vacuum is switched off. The System Supervisor now transfers control to the Vision Controller using the RS 232 serial communication link between the two computers.

The Vision Controller first initializes the image acquisition board and waits for a signal from the System Supervisor to start image acquisition and processing operations. The operations of the Vision Controller are listed in a flow chart in Figure 4.2. On receiving a signal from the System Supervisor, the Vision Controller acquires an image of the free edges of the upper and lower plies and stores it in one of the 16 on-board frame buffers. The creaser blades were painted flat black, to provide a high contrast between the collar fabric and background surface. The gray-scale image is

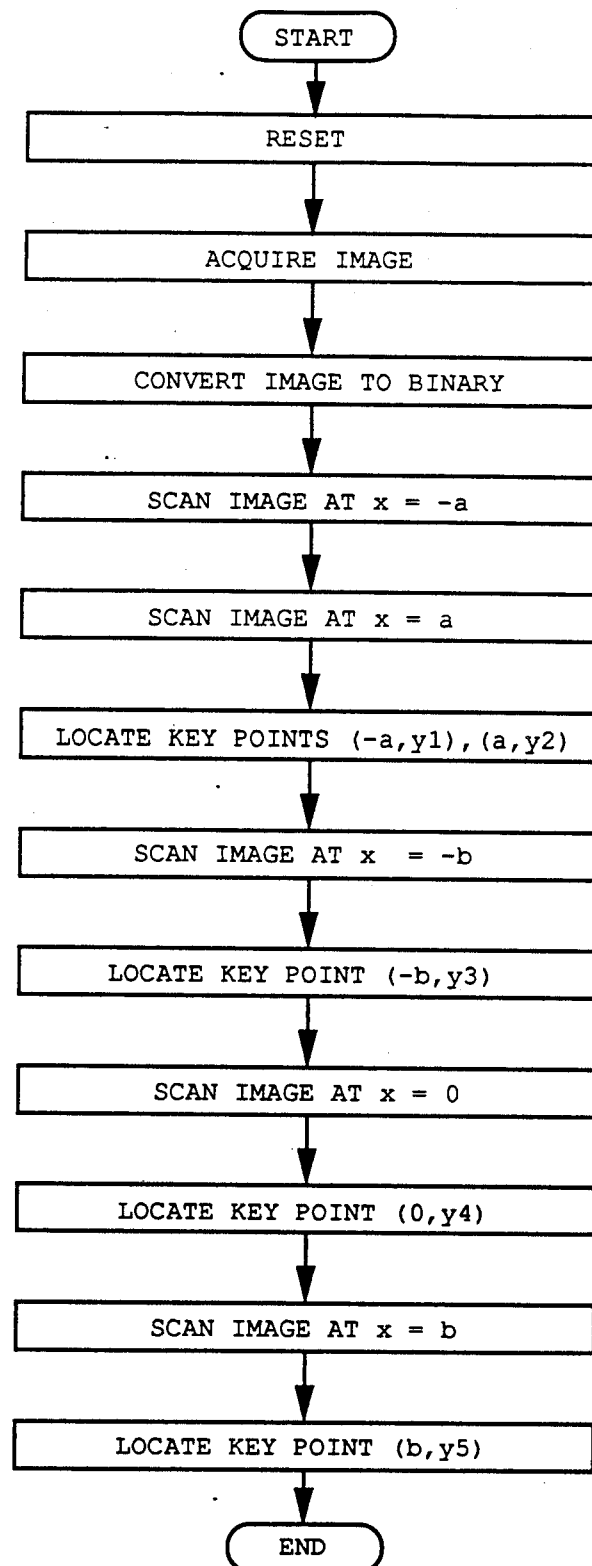


Figure 4.2. Image Processing and Scanning to Locate Edge Points

subjected to a single value threshold filter, which converts all pixels above the threshold to white with an assigned value of 255. All pixels belonging to the dark background are converted to black with an assigned value of 0. The threshold filtering on a frame buffer of 512 X 512 pixels is shown in Figure 4.3. The resulting image is a binary image with all pixels having intensity values of either 0 or 255. The binary image obtained after filtering is shown in Figure 4.4(a).

When the creaser blades are fully extended into the collar, the lower ply remains hidden from camera view because the steel creaser blades separate the two plies. The camera can see only the upper ply and its free edge. However, the lower ply free edge is visible to the camera in two zones, where there is a gap between the central blade and the left and right blades. The scan lines at $x = a$ and $x = -a$ pass over the gaps in the blades and hence detect a pair of edge points which lie on the free edge of the lower ply. For the shirt collar size being researched, the value of a was 3 inches. Since all pixels belonging to the fabric plies, upper or lower, are assigned a "1", pixels on the lower ply are also assigned a "1" as are pixels on the upper ply.

The binary image is scanned in two stages. The first stage, done by scanning the image at $x = -a$ and $x = +a$, locates a pair of edge points on the free edge of the lower ply. The scanning procedure to locate an edge point is shown in Figure 4.5. The procedure is based on comparison of pixel values of adjacent pixels in pairs along a scan line. An edge

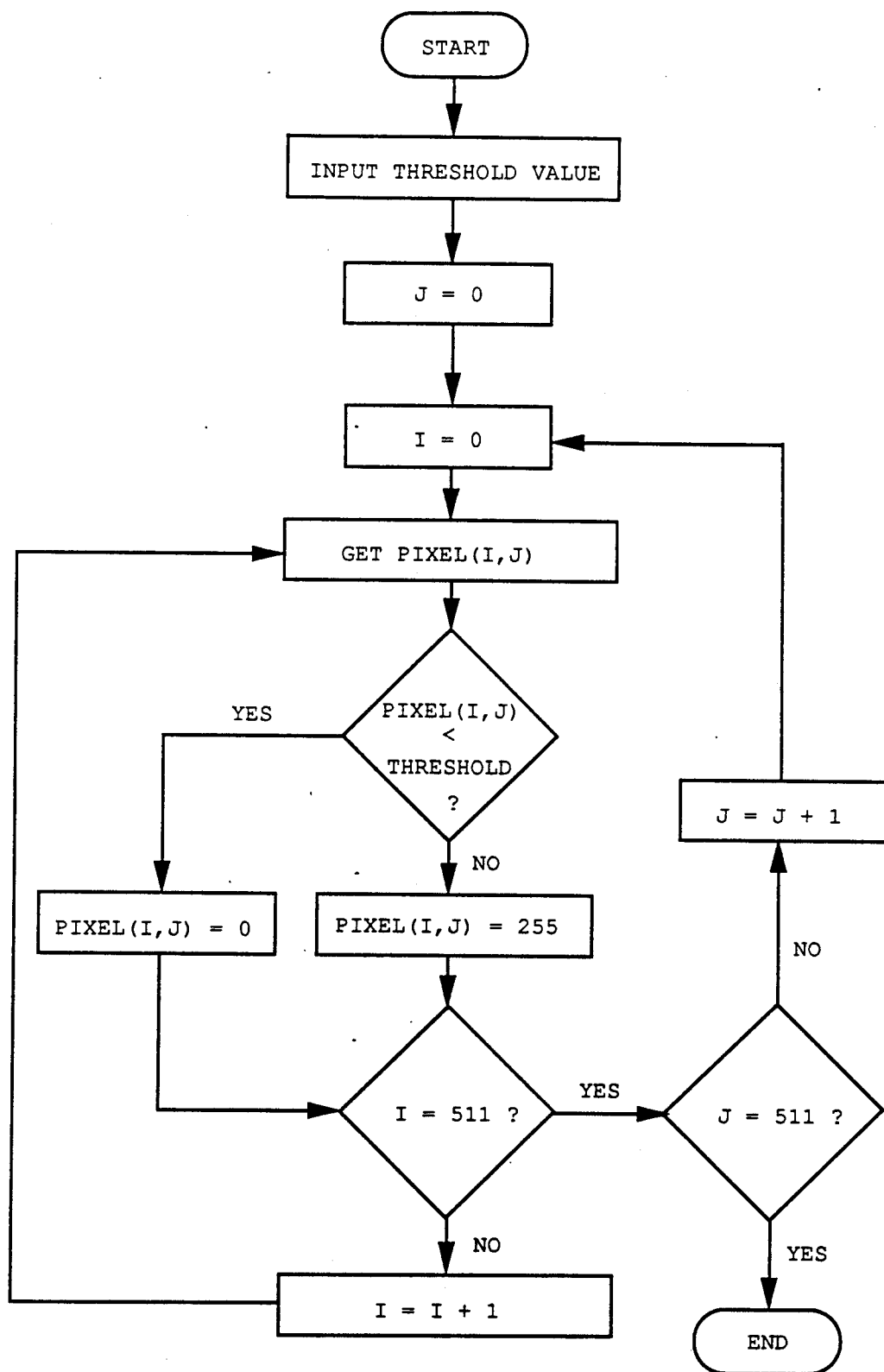
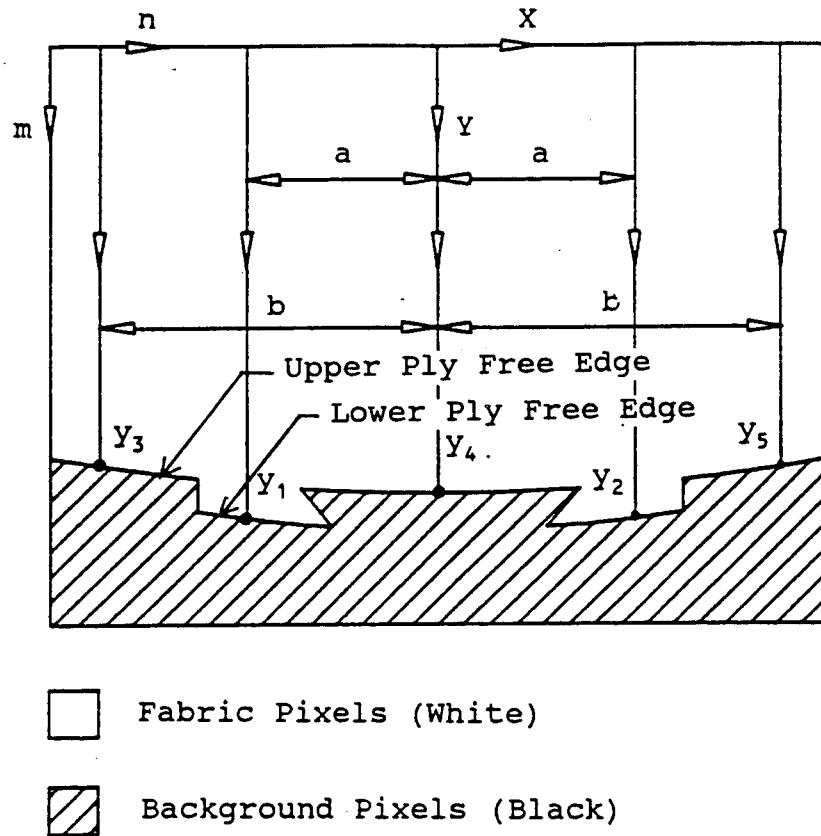
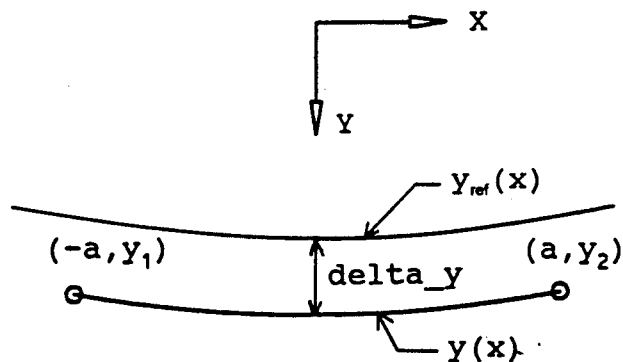


Figure 4.3. Procedure for Single-Level Threshold Filtering



(a) Binary Image



(b) Locating the Lower Ply Edge from Key Points

Figure 4.4. Binary Image of Ply Edges and Key Point Locations

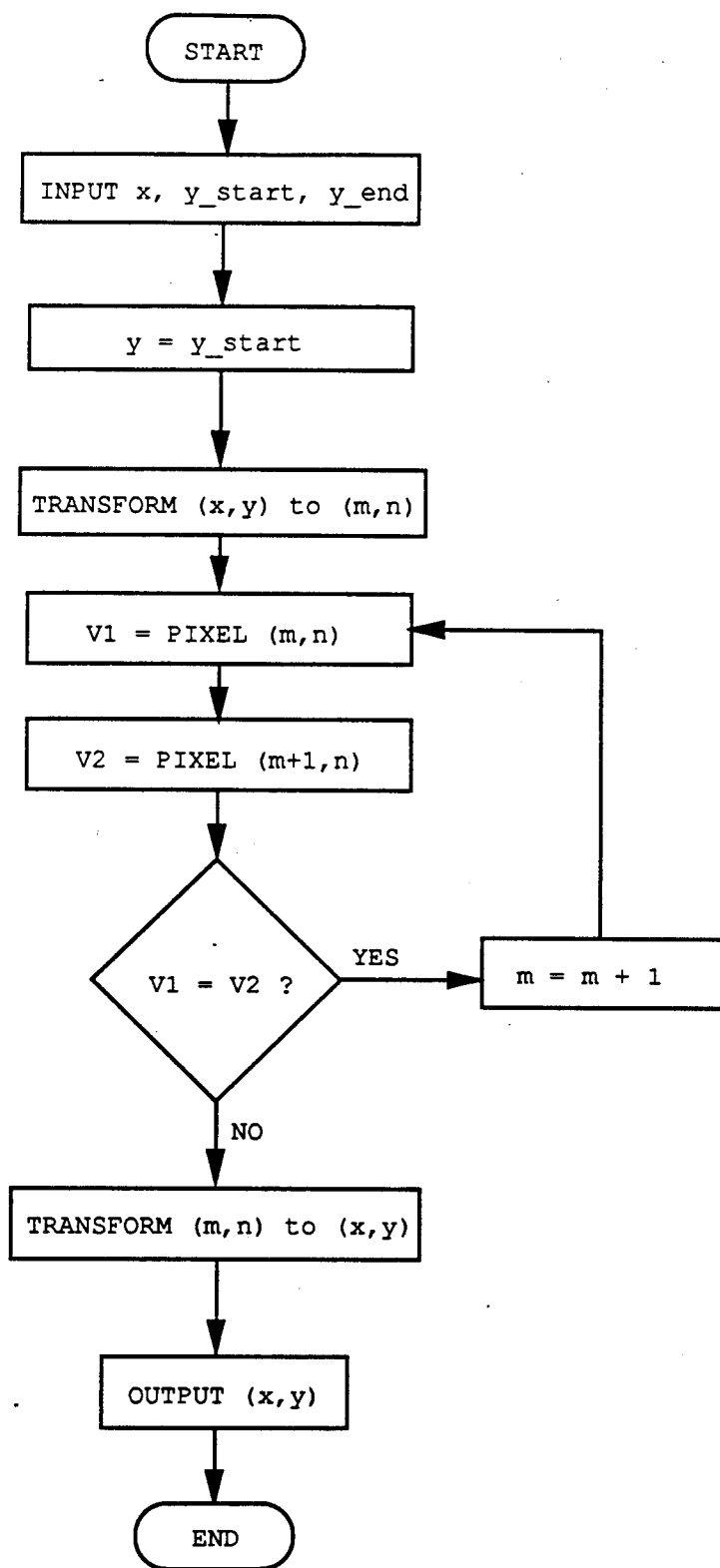


Figure 4.5. Scanning Procedure to Locate an Edge Point

point is detected when adjacent pixels are found to have different values. The transformation from camera to world coordinates and its inverse are given by Equations 3.1 and 3.2.

Variations in collar run stitch dimensions and limitations in the repeatability of collar acquisition by the expanding creaser blades caused the location the free edge of the collar to vary from collar to collar. The equation of the lower ply free edge had to be determined for every collar after acquisition by the creaser blades. Since the lower ply free edge was visible to the camera only at two zones, the detection of the complete profile of the lower ply free edge after creaser blade insertion was not possible. Repeated trials with collar acquisition by the creaser blade mechanism showed that only the shift of the lower ply free edge in the Y direction was significant, and the shift in the X direction and collar skewing could be neglected. Prior to implementing this algorithm, the equation of the free edge of the lower ply for was determined, for the case of the creaser blade profile resting exactly over the collar run stitch. This equation was modified by adding a suitable Y offset for each collar loaded on the creaser blades.

The creaser blades were extended and an unturned collar was placed on top of the blades with the collar points coinciding with the creaser blade tips. Since the upper and lower ply free edges were pre-aligned before the run stitch operation, only a single profile was visible to the camera.

The vision sensor scanned the image along 11 scan lines to determine the coordinates of 11 points on the free edge of the lower ply. The equation of the lower ply free edge was determined by fitting a second degree polynomial through the set of 11 points, using the method of least squared error. The equation of the curve of the lower ply free edge was

$$y_w(x) = 4.20 - 0.02 \cdot x^2. \quad (4.1)$$

Equation 4.1 represents points on the lower ply free edge if the creaser blade edge rests exactly on the run stitch, which would be the case of perfect collar loading. However, due to the Y shift in the lower ply free edge, shown in Figure 4.4(b), this equation does not actually represent the location of the lower ply free edge, and has to be modified to account for the Y shift for each collar loaded on the creaser blades. The modified equation of the free edge of the lower ply is given by

$$y(x) = y_w(x) + \text{delta}_y \quad (4.2)$$

where delta_y is an offset to compensate for the Y shift and is given by

$$\text{delta}_y = (y_1 + y_2)/2.0 - [y_w(-a) + y_w(a)]/2.0. \quad (4.3)$$

The second stage of image scanning involves scanning along $x = -b$, $x = 0$ and $x = b$, which are the lines of action of the friction pads of the three linear drives. The pads grip the upper ply free edge as the drives pull it back to match it to the lower ply free edge. For the collar size being researched, the three drives were spaced 3.5 inches apart. This spacing was not optimal and was arbitrary.

Scanning along $x = -b$, $x = 0$, and $x = +b$ locates a set of three points, $(-b, y_3)$, $(0, y_4)$, and (b, y_5) , on the free edge of the upper ply. The two stage scanning procedure yields a set of five key edge points.

The edge alignment error is given by

$$y(-b) - y_3 \quad \text{at } x = -b, \quad (4.4a)$$

$$y(0) - y_4 \quad \text{at } x = 0, \quad (4.4b)$$

$$y(+b) - y_5 \quad \text{at } x = +b. \quad (4.4c)$$

The alignment error at three key points is passed from the Vision Controller to the System Supervisor using the RS-232 serial link between the machines. Stepper motor commands are then generated to move the centers of the friction pads over the points $(-b, y_3)$, $(0, y_4)$, and $(+b, y_5)$ of the upper ply. The air cylinders driving the upper and lower ply clamps are activated, causing the collar to be pinched between the upper and lower clamps. The upper ply clamps are pulled back by the linear drives to correct the edge alignment error.

The algorithm identified in the flow charts of Figures 4.1, 4.2, 4.3, and 4.5 was coded in Microsoft C. A program listing for the main program as well as the relevant sub-program files is included in Appendix C.

Integration with a Robotic Apparel Assembly Workcell (AAW)

The proof-of-concept pressing machine was integrated into a robotic apparel assembly workcell and used as a double-point collar pressing station. The workcell, illustrated in Figure 4.6, was comprised of five modules.

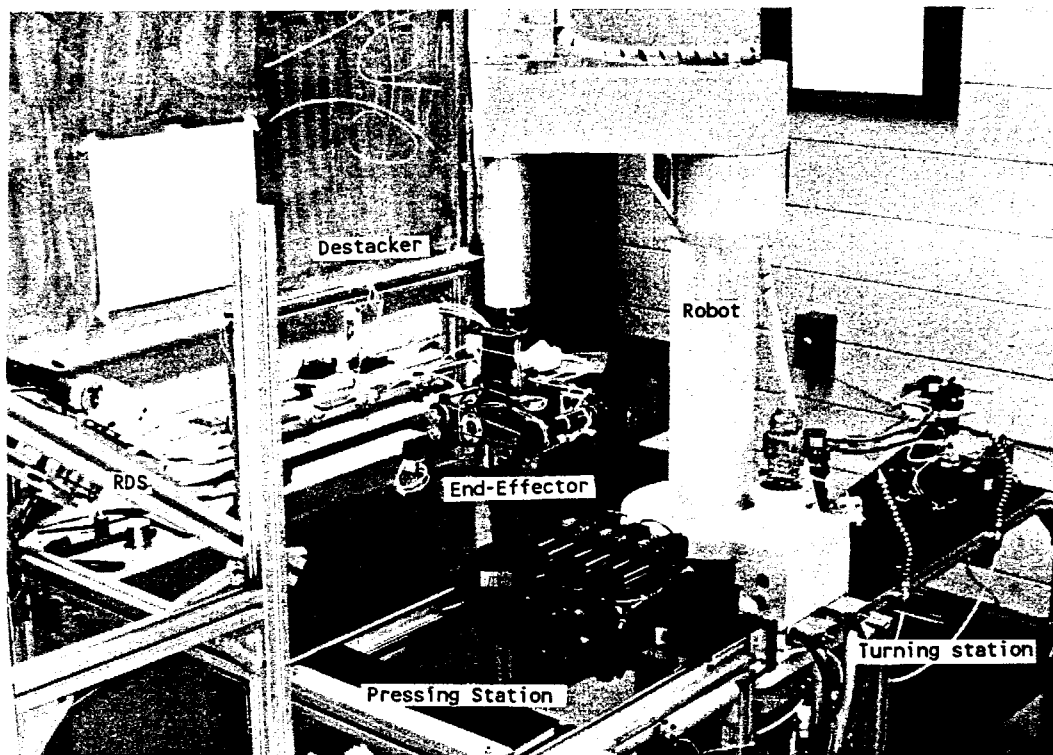
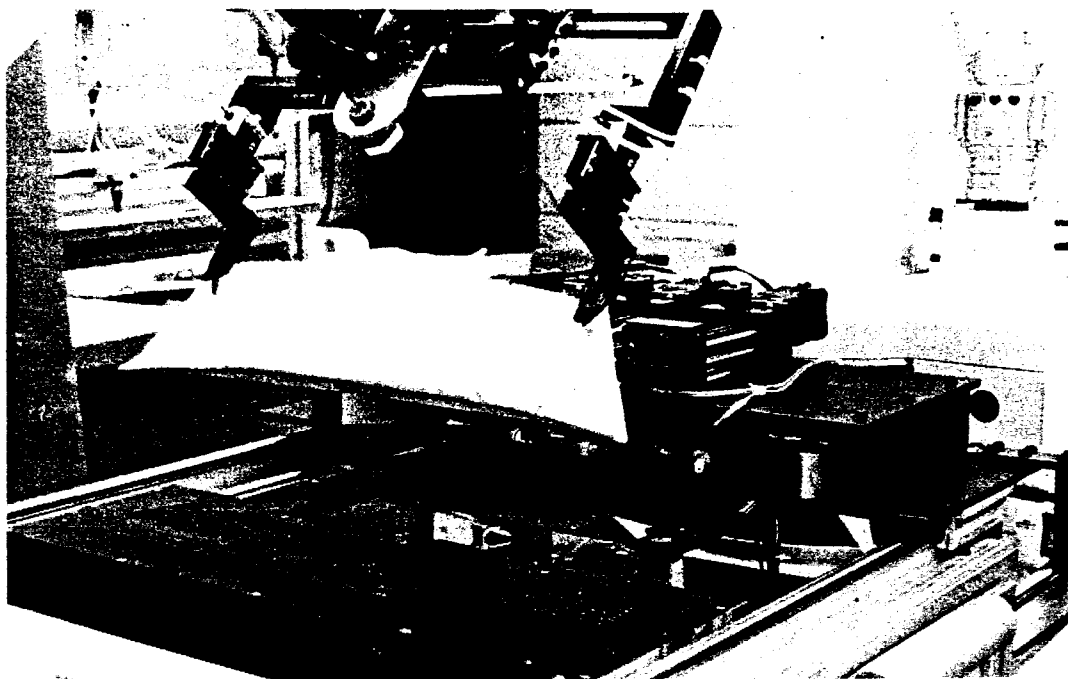


Figure 4.6. Robotic Apparel Assembly Workcell (AAW)

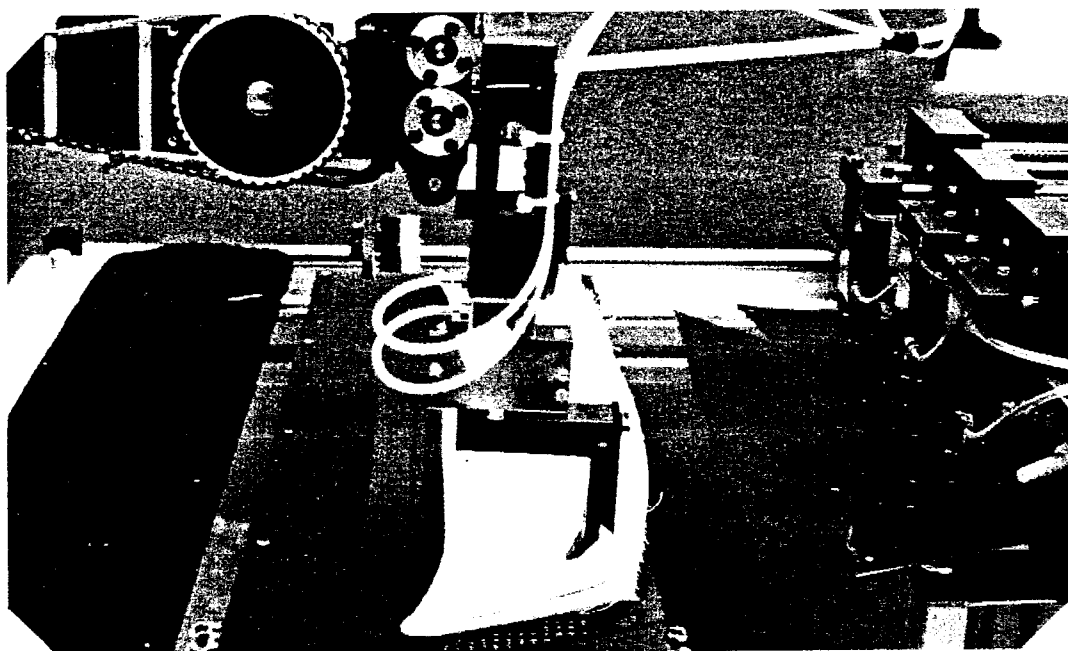
1. a proof-of-concept double-point turning machine,
2. a proof-of-concept double-point pressing machine,
3. a laser Range Data Scanner (RDS),
4. a 4-DOF SCARA robot equipped with an apparel handling end-effector, and
5. a collar de-stacker.

The robotic workcell was capable of producing a turned and pressed collar at the end of a cycle. The cycle begins with the destacker picking up a collar from the stack and separating the plies. The robot with a special apparel handling end-effector acquires the collar from the destacker and transports it to the turning station. The turning station acquires the collar from the end-effector and turns the collar using a double-point turning procedure. The turned collar is picked up by the end-effector and transported over to the pressing station, where it is scanned by the Range Data Scanner (RDS), to determine the three-dimensional location of the collar points. Using this information, a robot trajectory is computed to accurately position the collar on the vacuum suction surface, for transfer to the double-point pressing station. The pressing station then acquires the collar from the end-effector and executes the automated edge alignment procedure outlined in the flow charts of Figures 4.1, 4.2 and 4.3 and 4.5. The operations of the proof-of-concept pressing station are sequentially illustrated in Figures 4.7, 4.8 and 4.9.

The average cycle time for collar acquisition, image processing, and edge alignment was 20 seconds per collar. The

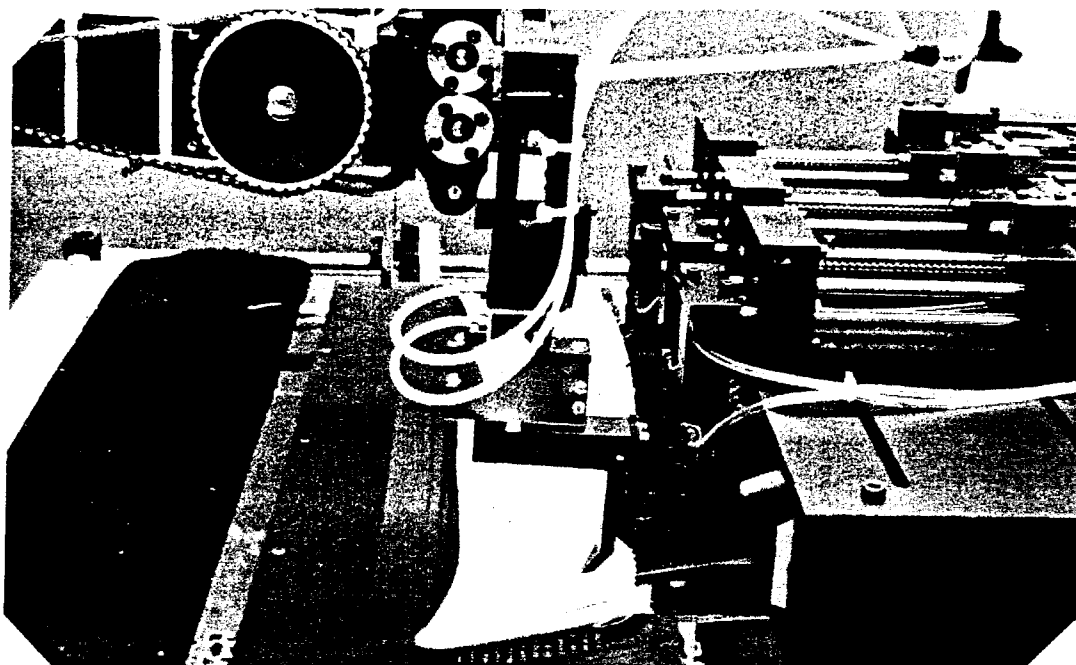


(a)

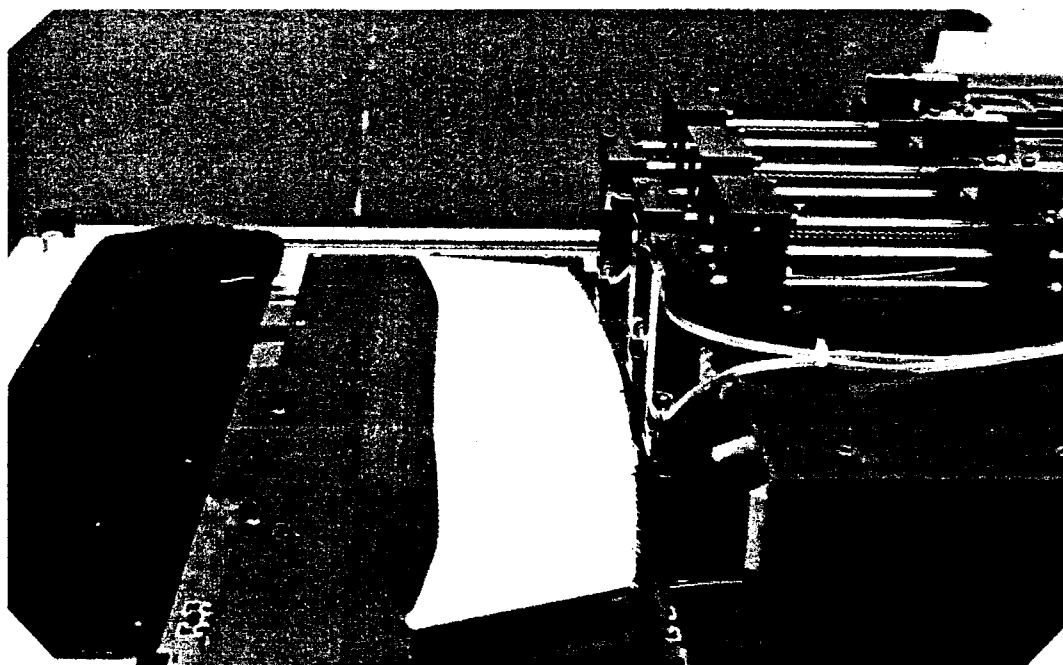


(b)

Figure 4.7. Positioning a Turned Collar on the Vacuum Table

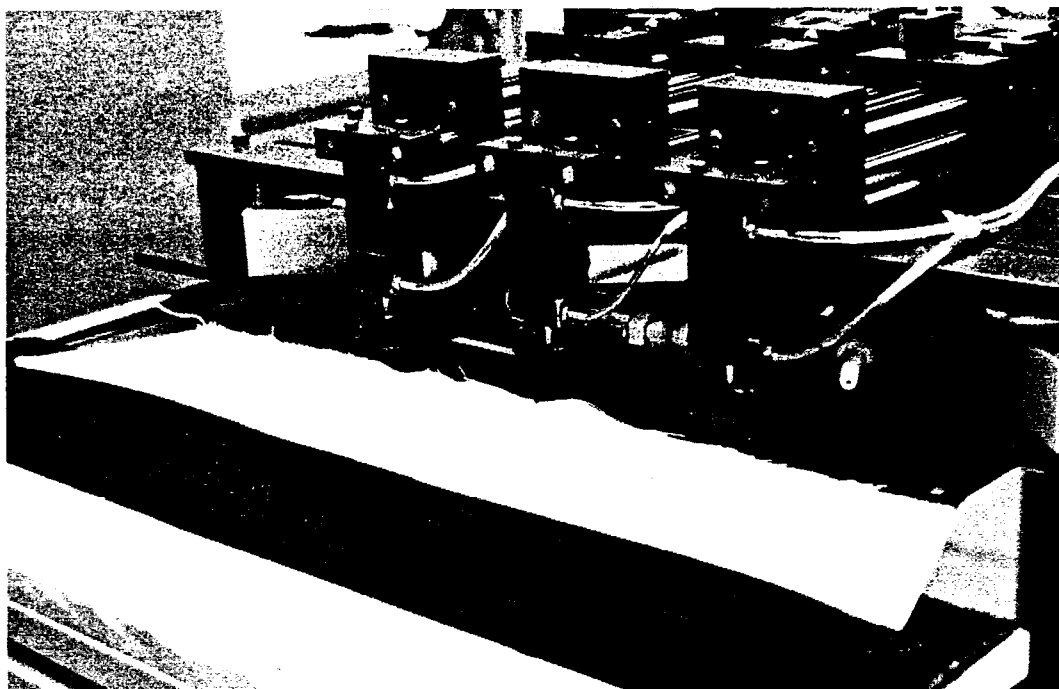


(a)

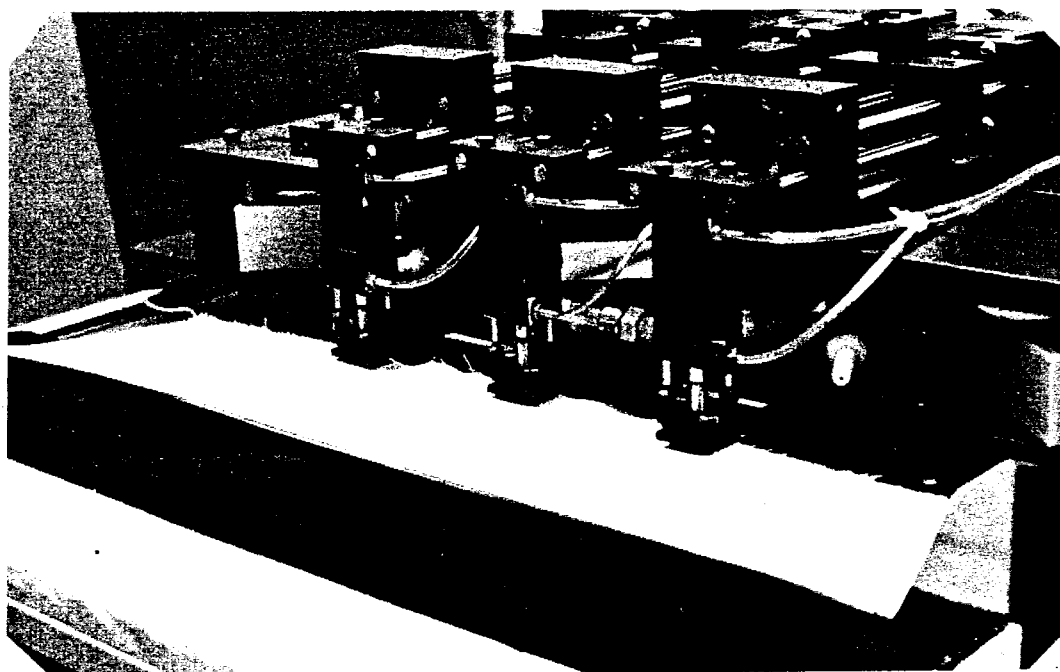


(b)

Figure 4.8. Collar Acquisition by Creaser Blades



(a)



(b)

Figure 4.9. Automated Edge Alignment

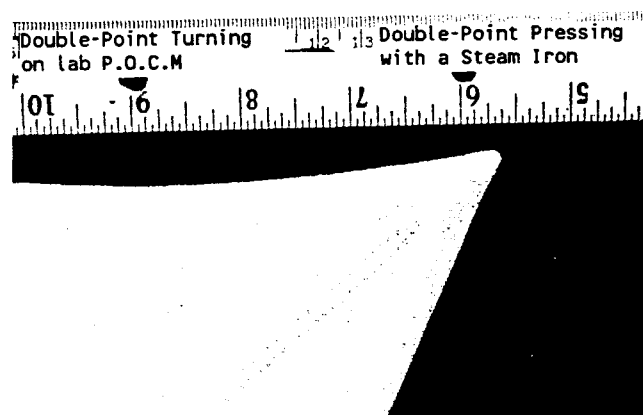
time required to carry out collar pressing in a die press has to be included, to estimate the total pressing cycle time.

The programs developed for demonstrating the feasibility of automated collar acquisition and indirect seam alignment were modified for integration with the main control program of the AAW. The operation of the AAW through a complete collar processing cycle was recorded on video tape. A second video tape showing detailed operation of the pressing station alone was also prepared. This thesis research was further documented by taking close-up pictures and slides of all the individual modules of the proof-of-concept pressing station for further reference.

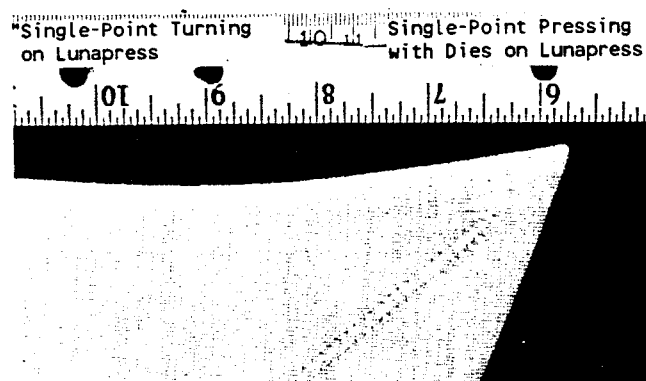
Comparison of Pressed Collars

A visual comparison was made between a collar pressed using the proof-of-concept machine and one pressed manually on the Lunapress. The collar on the proof-of-concept machine was pressed with a hand-held steam iron, whereas the one off the Lunapress was pressed in a heated die. A die press was not added to the proof-of-concept machine because of constraints of time.

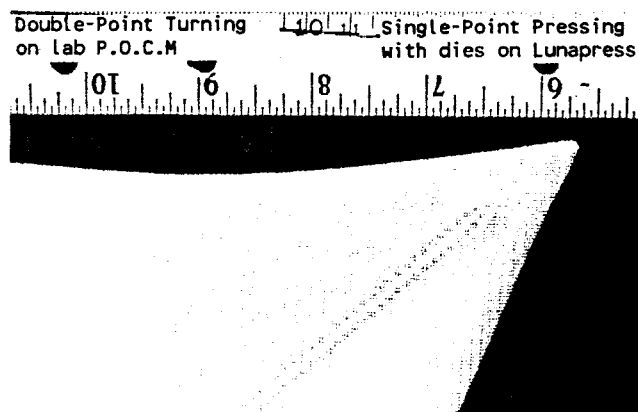
Figures 4.10(a) and (b) are visual comparisons between the two collars. The comparison shows that the accuracy of seam alignment in both cases is comparable. The collar points produced by pressing a collar using a hand-held steam iron are not as sharp as those produced by the Lunapress. Collar points pressed in a heated die undergo an extrusion, which results in sharp points. Collar points pressed with a hand-



(a)



(b)



(c)

Figure 4.10. A Visual Comparison of Pressed Collars

held steam iron tend to flatten, resulting in slightly rounded points.

Error Analysis

An error analysis was performed to evaluate vision sensor performance and repeatability of the creaser blade mechanism with respect to collar acquisition.

Vision System Performance Evaluation

The camera used as the vision sensor was a mobile unit, which was mounted on a robot end-effector. Prior to image acquisition and processing operations, the camera was moved into a predetermined location by the robot, and the end-effector was pitched 90 degrees to bring the camera into viewing position. Two factors which affected the precision of the vision system were robot arm repeatability and end-effector pitch repeatability. Experiments were conducted to determine the effect of each of the two factors on vision sensor precision.

Error analysis experiments were conducted using a black semi-circle with a 3 inch radius, drawn on a white sheet of paper, as a test profile. This profile was placed on the creaser blade mechanism with its center coinciding with the origin of the world coordinate frame XOY, and its diameter aligned with the X axis, as shown in Figure 4.11. The true world coordinates of all points on the semi-circle were defined by

$$x^2 + y^2 = 9. \quad (4.5)$$

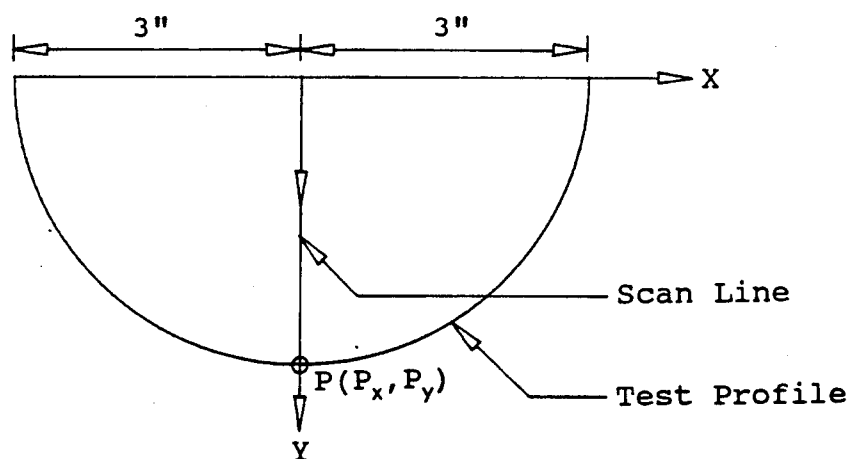
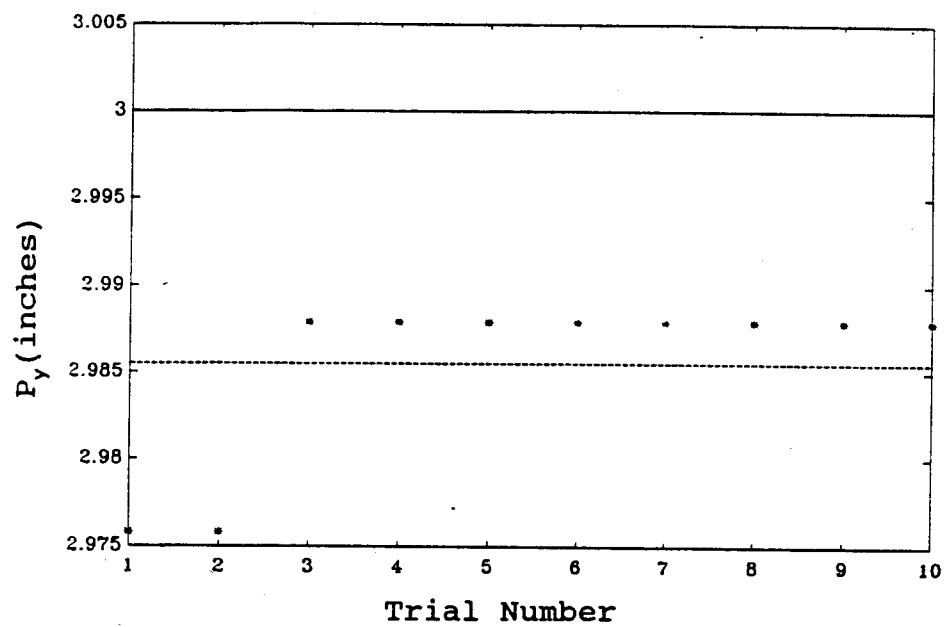


Figure 4.11. Test Profile for Statistical Evaluation of Vision System Performance

The robot arm moved the camera to the predetermined location for which the vision sensor had been calibrated. The first experiment evaluated the effect of the limited repeatability of the end effector pitch axis drive on vision system precision and accuracy. The end-effector pitch motion was driven by a DC servo motor under PID control. Since the camera had been calibrated with its optical axis normal to the viewed surface, the calibration parameters Δy and $grid_y$ were particularly sensitive to the positioning error of the DC servo of the pitch axis. The camera lens was approximately 16 inches from the viewed surface. A pitch axis positioning error of 0.1 degree would cause Δy to change by 0.3 inch because of the shift in the field of view and a change in calibration parameters.

A statistical test was conducted to estimate the precision and accuracy of the vision sensor. An absolute pitch angle of 0 degree positioned the camera axis horizontal and parallel to the viewed surface. An absolute pitch angle of 90 degrees brought the camera into viewing position, with its axis vertical and normal to the viewed surface. The end effector was first moved for a pitch angle of 0 degree. The camera was then brought into viewing position by setting the pitch angle at 90 degrees. Using the algorithm described in Figure 4.5, the test pattern was scanned along $x = 0$, to determine P_y , the Y coordinate of the point P on the test profile. From Equation 4.5, the true coordinates of the point P, (P_x, P_y) were determined to be (0.0, 3.0). Figure 4.12 is



Sample Mean = 2.99 inches
Sample Standard Deviation = 0.005 inch

Figure 4.12. Effect of End-Effector Pitch Repeatability on Vision Sensor Performance

a scatter diagram which plots the values of P_y , as computed by the vision system for a total of 10 trials. The precision was estimated by computing the standard deviation of the P_y values as determined by the vision system, and was found to be 0.005 inch. The sample mean of the distribution was 2.99 inches. The system accuracy, estimated by calculating the difference between the true value of the input variable and distribution mean of the measured values, was found to be 0.02 inches. The accuracy of the vision system, otherwise referred to as the bias error, was attributed to

1. positioning error during alignment of the test profile,
2. resolution of the pixel array, which was 0.01 inch, and
3. error in determination of calibration parameters.

The robot arm which was used to position the end-effector carrying the camera, was a 4-degree of freedom DC servo driven SCARA manipulator. Following the transfer of a turned collar from the end-effector to the creaser blade mechanism, the camera was moved into the calibrated location. In addition to the limitations of the pitch axis repeatability, the backlash and repeatability of the four DC servos of the robot arm affected the calibration parameters, and thereby the accuracy and precision of the vision system.

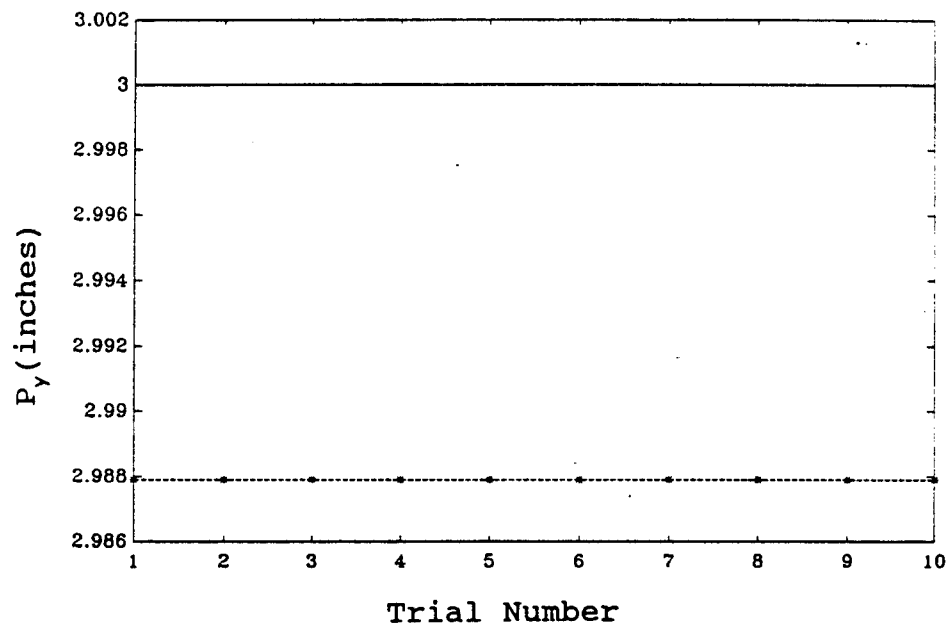
Another statistical test was conducted to evaluate the effect of limited repeatability of the servos of the robot arm on the vision sensor accuracy and precision. The same test profile that was used for the pitch repeatability evaluation

was used for this experiment. The Y coordinate P_y of the point P as computed by the vision system was recorded. The true value of P_y is 3.0 inches. Figure 4.13 is a scatter diagram which plots the values of P_y , as determined by the vision system, for 10 trials. The vision system precision was estimated by computing the standard deviation of P_y , the Y coordinate of point P, as determined by the vision system, and was found to be 0 inch. The mean of the distribution was 2.99 inches. The system accuracy, estimated by calculating the difference between the true value of the measured variable and its distribution mean was 0.01 inch. The factors affecting the accuracy of the vision system were

1. positioning error during alignment of the test profile,
2. resolution of the pixel array, which was 0.01 inch, and
3. error in determination of calibration parameters.

Collar Acquisition Repeatability

Collar acquisition repeatability refers to the capability of the creaser blades to position themselves inside the collar in the same location, every time they acquire a turned collar from the vacuum table. The concept of "double-point pressing" was based on the feasibility of transfer of a turned collar from a vacuum suction surface onto an expanding creaser blade mechanism. Variation in the configuration of a turned collar after acquisition by the creaser blades results in shifting of the free edge of the lower ply from collar to collar. Factors which cause variance include non-conformance of collar ply



Sample Mean = 2.99 inches
Sample Standard Deviation = 0 inch

Figure 4.13. Effect of Robot Arm Repeatability on Vision Sensor Precision and Accuracy

dimensions to pre-set values and variance in the initial positioning of the turned collar on the suction surface.

An experimental evaluation of the shift in the free edge of the lower ply was done. The edge was located by using the vision sensor to scan the binary image shown in Figure 4.4, at $x = -a$ and $x = a$ to locate two edge points, $(-a, y_1)$, and (a, y_2) on the lower ply edge. The average of y_1 and y_2 , y' , was a measure of the Y shift in the position of the lower ply edge from collar to collar. Figure 4.14 is a scatter diagram for y' , the location of the lower ply free edge, with repetitive trials on a set of 20 collars. The precision error, computed as the standard deviation of the distribution, was 0.04 inch.

Uncertainty Analysis

The statistics for the precision of the vision sensor and the shift in the position of the lower ply free edge were obtained from finite data sets. The means and standard deviations of the data sets were sample means and standard deviations. The sample sizes were finite and introduced a degree of uncertainty in the estimates of the true distribution means. The uncertainty in the mean can be estimated using the t estimator [15].

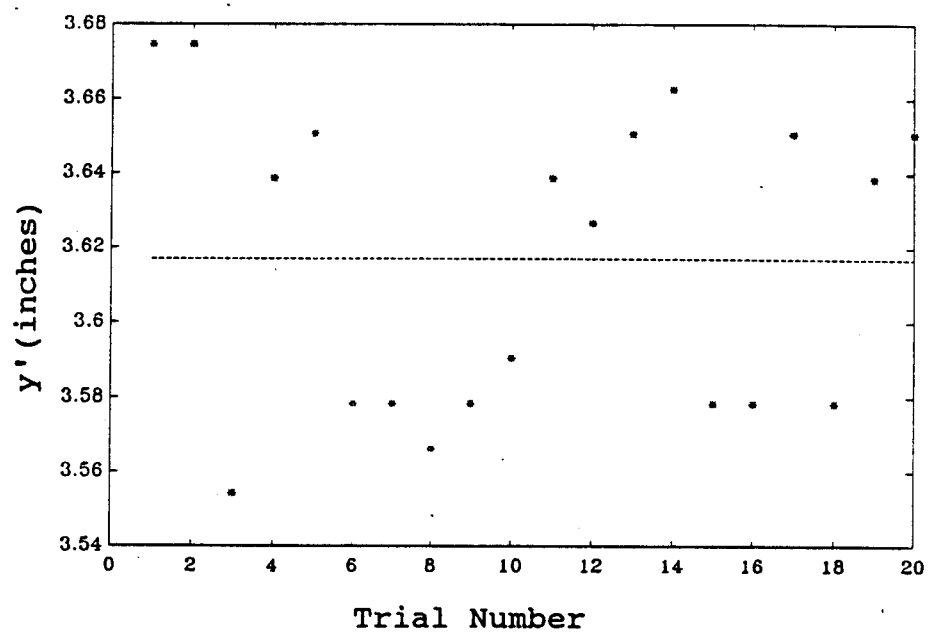
If x' and S_x are the sample mean and standard deviation of a normal distribution for a finite data set of size N, then

$$x'' = x' \pm t_{v,p} S_x (P\%), \quad (4.6)$$

where

x'' = true distribution mean,

x' = sample mean with finite sample size,



$$y' = (y_1 + y_2)/2$$

Sample Mean = 3.62 inches

Sample Standard Deviation = 0.04 inch

Figure 4.14. Statistical Evaluation of Collar Acquisition Process

$t_{v,P}$ = t-estimator,

S_x = sample standard deviation,

P = confidence level.

Equation 4.6 utilizes the t distribution, and can be used to estimate a confidence level P for a given confidence interval $t_{v,P}S_x$ and vice-versa, for finite sample sizes.

Uncertainty estimates for the sample means for the statistical experiments conducted with a finite number of trials are presented in Table I. The number of trials required for a 95% confidence level was also estimated and is presented in Table II.

Table I. Confidence Levels and Intervals for Statistical Experiments

Statistical Test	N	\bar{x} (inches)	S_x (inches)	Confidence Interval (inches)			
				50%	90%	95%	99%
Vision Sensor	10	2.99	0.01	± 0.003	± 0.009	± 0.01	± 0.02
Collar Acquisition	20	3.62	0.04	± 0.03	± 0.07	± 0.08	± 0.12

Table II. Number of Trials Required for a 95% Confidence Level

Statistical Test	N	\bar{x} (inches)	S_x (inches)	Confidence Interval (inches)	N_t for 95% Confidence Level
Vision Sensor	10	2.99	0.01	± 0.001	128
Collar Acquisition	20	3.62	0.04	± 0.01	70

CHAPTER V

CONCLUSIONS AND RECOMMENDATIONS

Conclusions

A study of the visual sensing and control issues for automated fabric edge alignment in automating the pressing of two dimensional apparel components has been made. An automation scheme using an indirect seam alignment method was developed for the automated pressing of shirt collars.

An analysis of manipulation primitives for manual shirt collar pressing led to the design conceptualization for automated collar acquisition and seam alignment. A proof-of-concept machine was designed and built to prove the feasibility of automated collar acquisition and seam alignment by indirect edge alignment. The concept of "double-point pressing of shirt collars", which has evolved from this thesis, represents an original machine automation concept.

Machine vision was employed as a feedback sensor to provide data on location of fabric ply edges. Edges were located by scanning a binary image for edge points, which were detected by looking for pixel value transitions from high to low. The performance of the proof-of-concept machine was evaluated by conducting a series of experiments.

The Double-Point Pressing Concept for Shirt Collars

The feasibility of "double-point pressing" of shirt collars has been shown. The capability of the creaser blade mechanism to reliably acquire a turned collar in a single stroke was evaluated by conducting repeated trials. The precision error was determined to be 0.04 inch, which indicated that the creaser blade mechanism could reliably acquire a collar.

The proposed edge alignment technique for indirect seam position control was successful. The vision system used to detect points on the free edges of fabric plies located edge points with an accuracy of 0.014 inch and a precision of 0.005 inch, which is better than apparel industry tolerances, that are of the order of 0.03 inch. Shirt collars pressed manually with a hand-held steam iron after using the automated indirect method for seam alignment were visually compared with those pressed manually on the Lunapress, and matched in quality and appearance of the seam. The difference in the sharpness of the collar points was attributed to the absence of heated dies in the case of collars from the proof-of-concept pressing machine.

The automated double point pressing method has many advantages over the conventional manual single-point collar pressing method. It ensures consistent quality of the pressed collar by eliminating the dependence on operator skill and dexterity for the seam alignment task. Collars can be pressed with a single loading operation, as compared to a two stage

skilled operation used in single-point pressing. The concept of automated double-point pressing of shirt collars has good potential for direct application in the apparel industry, because of process improvement and consistency of quality by automation.

The proof-of-concept machine was integrated with a robotic apparel assembly workcell (AAW), and successfully used as a "double-point collar pressing station". The successful integration with the AAW demonstrated the feasibility of robot assisted apparel manufacturing.

Automated Pressing of Two-Dimensional Apparel Components

The design, sensing and control principles developed for the automated pressing of shirt collars can be extended to a family of similar two dimensional apparel components. Examples of such apparel components include shirt cuffs, epaulets and pockets. These components are constructed from a pair of plies which are run-stitched and then turned inside out to conceal the stitch. The turning operation is followed by a block pressing operation involving the use of a metal creaser blade to generate a sharp crease. Workpiece setting and alignment for these components involves extensive hand-eye coordination as in the case of a shirt collar. The operation sequence and manipulation primitives for pressing these components are similar to those for shirt collars.

Recommendations

Design Improvements

1. The creaser blade mechanism was designed to accommodate a single collar size. The creaser blades were machined to match the run-stitch profile of a particular collar size which was used for experimentation. The run stitch profile changes with a change in collar size. The flexibility of the mechanism can be increased by modifying the design to accommodate a range of collar sizes without the need for a different set of creaser blades for each collar size. One solution is to split the creaser blade mechanism into two symmetric modules. The modules can be moved apart by connecting them to a ball screw and nut drive mounted underneath, with left handed and right handed ball nuts used to move the left and right modules respectively. The middle creaser blade is split into two parts. The ball screw can be driven by a stepper motor to move the left and right modules closer or further apart by commanding the motor in the clockwise or counter-clockwise direction. This design modification will permit the distance between the blade tips to be adjusted for a range of collar sizes.
2. The proof-of-concept pressing machine was designed with a two stage pneumatic drive for the slideway. The first stage is used to move the slideway over the vacuum table to transfer a collar from the vacuum table to the creaser blades. The second stage was provided to move the loaded collar over the vacuum table into a die press. Due to time constraints, a die press could not be installed. Installation of a die press as an additional module to the proof-of-concept machine will allow a complete collar pressing cycle to be executed.

Analysis of Fabric Edge Distortion

The spacing between the lines of action of the three linear drives affects the residual edge alignment error between the upper and lower ply free edges. This thesis discussed the distortion of the free edge of a fabric ply due to tensile and shear loads generated when an apparel workpiece is folded over a blade edge. Increasing the number of control

points progressively decreases fabric edge distortion and reduces edge alignment error. A mathematical analysis was beyond the scope of this thesis. A quantitative analysis by modeling and simulation of the distortion of a fabric free edge under tensile and shear loads needs to be done in order to establish analytical relationships between the number of control points, spacing between control points, and the profile of the distorted fabric edge. The edge alignment error could then be predicted as a function of the number of control points and the spacing between them. An optimal spacing between linear drives to minimize residual edge alignment error could be determined.

APPENDICES

Appendix AHardware Specifications

Controller Hardware

Motion Controller Board

Manufacturer : Precision Micro Control Corporation
3555 Aero Court
San Diego, CA 92123
(619) 565-1500

Vendor : Acquired directly from manufacturer

Part Number : DCX

Description : Eight-Axis Motion Controller Board

Stepper Motor Module

Manufacturer : Precision Micro Control Corporation
3555 Aero Court
San Diego, CA 92123
(619) 565-1500

Vendor : Acquired directly from manufacturer

Part Number : DCX-MC150

Description : Plug-in module for open loop stepper motor control

Data Acquisition Board

Manufacturer : Data Translation Inc.
100 Locke Drive
Marlboro, MA 01752-1192
(617) 481-3700

Vendor : Acquired directly from manufacturer

Part Number : DT-2821

Description : 8 channel differential or 16 channel single ended 12-bit A/D converters, 2 12-bit D/A converters and 2 8-bit digital I/O ports.

Arithmetic Frame Grabber

Manufacturer : Data Translation Inc.
100 Locke Drive
Marlboro, MA 01752-1192
(617) 481-3700

Vendor : Acquired directly from manufacturer

Part Number : DT-2861

Description : 512 x 512 x 8-bit frame grabber board with capabilities to capture images, perform arithmetic operations and real-time display at 30 frames per second

Electrical and Electronic Hardware

Stepper Motor and Driver Unit

Manufacturer : Oriental Motor U.S.A., Corp.
Head Office
2701 Plaza Del Amo, Suite 702
Torrance, CA 90503
(213) 515 2264

Vendor : EMCO, Inc.
P.O. Box 5618
Greenville, SC 29606
(803) 232-7616

Part Number : UMD 245-AA

Description : Super Vexta Mini Stepper Motor/Driver Package

CCD Camera

Manufacturer : Panasonic Industrial Company
1854 Shackleford Court, Suite 115
Norcross, GA 30093
(404) 925-6835

Vendor : Cartwright & Bean, Inc.
Eastland Executive Park
3557 N. Sharon Amity Rd., Suite 102
Charlotte NC 28205

Part Number : WV-CD50

Description : Compact CCD Camera for Closed Circuit TV.

Solenoid Valves

Manufacturer : Clippard Instrument Laboratory, Inc.
7390 Colerain Road
Cincinnati, OH 45239
(513) 521-4261

Vendor : Barker Air & Hydraulics, Inc.
211 Eisenhower Drive
Greenville, SC 29606
(803) 271-4910

Part Number : EMC-12-24-40

Description : Electronic Manifold Card with 12 3-way solenoid
valves operating on 24 V

Proximity Sensors

Manufacturer : EFFECTOR, Inc.
805 Springdale Drive
Whiteland Buisiness Park
Exton, PA 19341
1-800-441-8246

Vendor : Brown and Morrison
P.O. Box 240827
Charlotte, NC 28224
(704) 554-8570

Part Number : IS-3002-BPOG

Description : Positive Switching Inductive Proximity Sensor

Mechanical Hardware

Air Cylinders

Manufacturer : Compact Air Products, Inc.
P.O. Box 499
Westminister, SC 29693-0499
(803) 647-9521

Vendor : Acquired directly from manufacturer

Description : Double Acting Air Cylinders

Ball Bearings

Manufacturer : Fafnir Bearings
Div. The Torrington Company
New Britain, CT 06050

Vendor : Dixie Bearings, Inc.
215 McGee Road
Anderson, SC 29621
(803) 225-3791

Description : Inch Series Radial Bearings 1/4" S1K

Linear Anti Friction Bearings

Manufacturer : Thomson Industries, Inc.
Port Washington, NY 11050
(516) 883-8000

Vendor : Dixie Bearings, Inc.
215 McGee Road
Anderson, SC 29621
(803) 225-3791

Part Number : SUPER-4 (20 off)

Description : Self Aligning Anti Friction Ball Bushings 1/4"

Part Number : TWN-8-OPN (2 off)

Description : Twin Pillow Block Open Type

Part Number : TWN-4 (4 off)

Description : Twin Pillow Block

Part Number : SR-8-PD (2 X 24")

Description : Shaft Support Rails

Ball Screws

Manufacturer : Saginaw Steering Gear Division
General Motors Corporation

Vendor : Dixie Bearings, Inc.
215 McGee Road
Anderson, SC 29621
(803) 225-3791

Part Number : 0375-0125 (B1)

Description : 0.375 nominal diameter, 0.125 pitch RH ball nut

Part Number : 0375-0125

Description : 0.375 nominal diameter, 0.125 pitch RH ball
screw

Appendix BElectrical Wiring Diagrams

This appendix contains circuit diagrams for the stepper motor to controller and solenoid valves to controller interfaces.

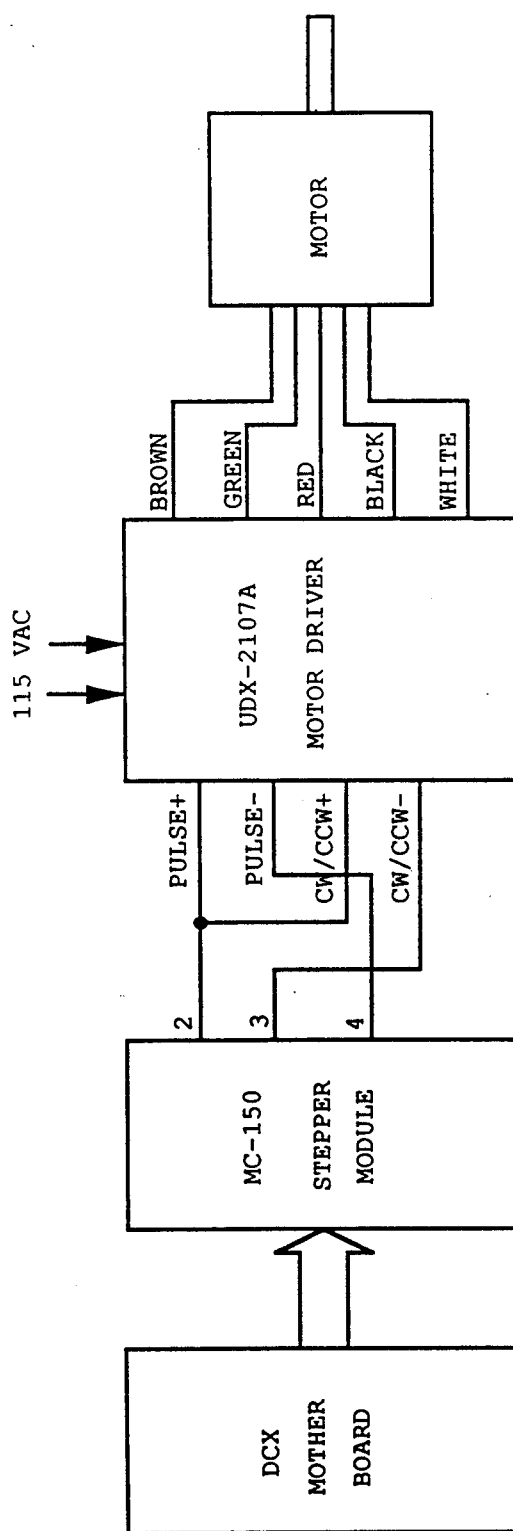


Figure B-1. Wiring Diagram for the Stepper Motors

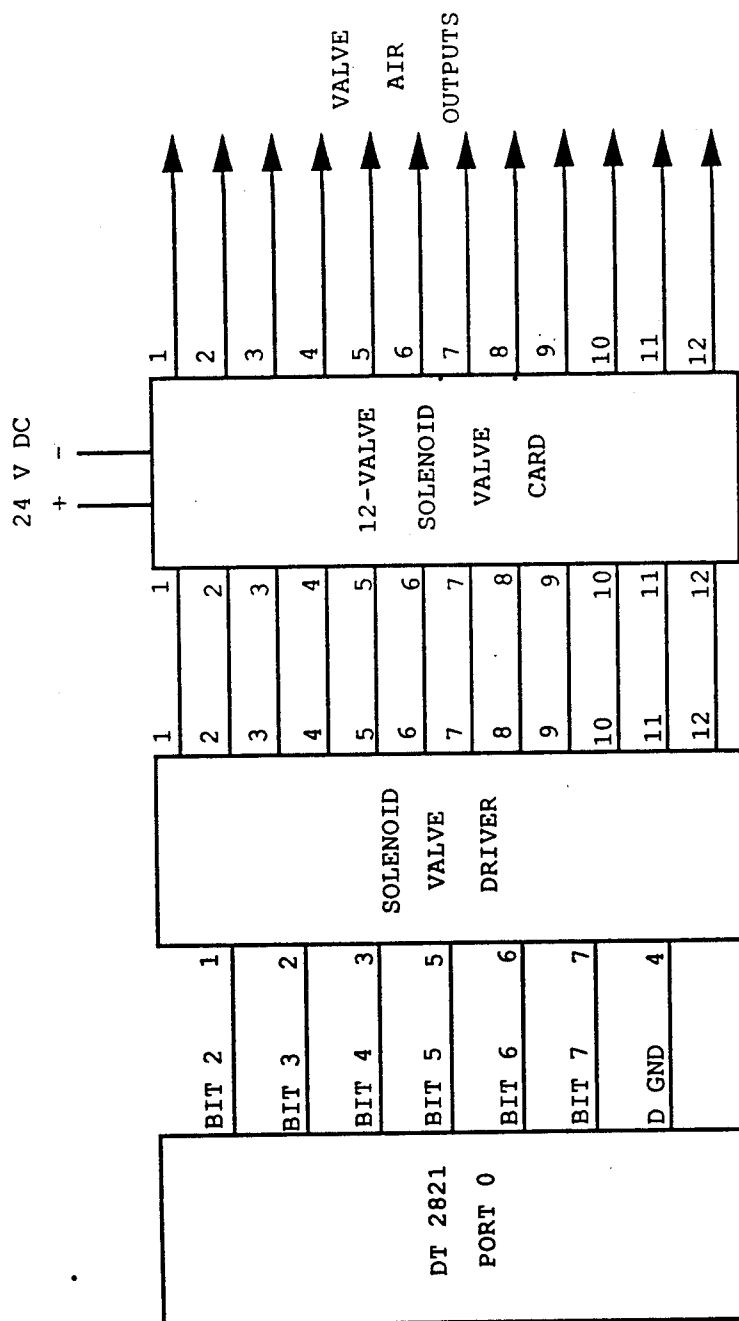


Figure B-2. Wiring Diagram for the Solenoid Valve Card

Appendix CProgram Listing

This appendix contains the source code listing for the software developed to run the proof-of-concept double-point collar pressing machine. Programs were written to demonstrate automated collar acquisition and automated indirect seam alignment. Test programs to verify vision sensor calibration were also written. Since the control hardware structure involved two microcomputers and a mobile camera, compilation and execution instructions are also included with the program listings.

Program	Computer
CAL-CHECK.C	Vision Controller
PR-VC2.C	Vision Controller
PR-SS2.C	System Supervisor

Vision Sensor Calibration Check

Compilation and Execution Procedure:

- 1) Load and Compile CAL-CHECK.C on the Vision Controller.
Ensure that all required header files are also loaded.
- 2) Move robot arm to camera viewing location.
Wrist Coordinates (mm):

X = -60.655
Y = 551.500
Z = 761.878

y = 0.0
p = 180.0 degrees
r = 180.0 degrees
- 3) Pitch End Effector to -90 degrees absolute.
- 4) Place test pattern on creaser blades.
- 5) Execute CAL-CHECK.C on the Vision Controller.

Demonstration of Automated Collar Acquisition
and Seam Alignment

Compilation and Execution Procedure :

- 1) Load and compile PR-VC1.C on the Vision Controller.
- 2) Load and compile PR-SS1.C on the System Supervisor.
- 3) Ensure that all required header files are loaded.
- 4) Move robot arm to camera viewing location.
Wrist Coordinates (mm) :

X = -60.655

Y = 551.500

Z = 761.878

y = 0.0

p = 180.0 degrees

r = 180.0 degrees

- 5) Pitch End-Effector to -90 degrees absolute.
- 6) Execute PR-VC1 on the Vision Controller and then PR-SS1 on the System Supervisor. Follow the prompts on the monitors of the System Supervisor and Vision Controller.

```

/*                                CAL-CHECK.C                                */

#include <dos.h>
#include <stdlib.h>
#include <stdio.h>
#include <math.h>
#include <iserrs.h>
#include <isdefs.h>
#include <vision2.h>

#define EXT_SYNC 1
#define INT_SYNC 0
#define X_GRID 0.015385
#define Y_GRID 0.012048
#define DEL_X 3.938
#define DEL_Y 0.0
#define NUM_POINTS 11
#define OFFSET 0.25
#define WINDOW_LENGTH 5.75
#define WINDOW_WIDTH 3.0

int thresh_value, j_1, j_2, j_3, i;
int axis_1[4] = {10,10,80,10};
int axis_2[4] = {10,255,80,255};
int text_1[1] = { 'X' };
int text_2[1] = { 'Y' };
int text_3[1] = { 'n' };
int text_4[1] = { 'm' };
double ref_contour[NUM_POINTS][2], profile[NUM_POINTS][2];
double move_1, move_2, move_3;
double scan_line();
void get_edge();
void inch_to_pixel();
void pixel_to_inch();

main()
{
    double x_1, y_1, x_2, y_2;
    int point_array[10];

    is_initialize();
    clear();
    is_init_luts();
    ilut(230, 6);
    is_select_font(0);
    is_select_ilut(0);
    is_select_olut(0);
    is_set_foreground(0);
    is_set_sync_source(EXT_SYNC);
    is_passthru();

    x_1 = -WINDOW_LENGTH/2.0;
    y_1 = OFFSET;
    x_2 = WINDOW_LENGTH/2.0;

```



```

y_2 = OFFSET + WINDOW_WIDTH;

is_set_sync_source(EXT_SYNC);
is_select_channel(0);
is_display(1);

is_freeze_frame();
is_select_ilut(6);
is_acquire(1,1);
is_set_active_region(330, 0, 182, 512);
is_and_constant(0,1,1);

is_set_sync_source(INT_SYNC);
is_select_output_frame(1);
is_display(1);

get_edge(profile);

is_save(1, 0, 1, 0, "c:\msc\image\calplot");

is_set_graphic_position(10, 325);
is_draw_lines(1, 2, axis_2);

is_set_graphic_position(20, 335);
is_draw_text(1, 1, text_1);
is_set_graphic_position(70, 265);
is_draw_text(1, 1, text_2);

inch_to_pixel(x_1, y_1, &point_array[1],
&point_array[0]);
inch_to_pixel(x_1, y_2, &point_array[3],
&point_array[2]);
inch_to_pixel(x_2, y_2, &point_array[5],
&point_array[4]);
inch_to_pixel(x_2, y_1, &point_array[7],
&point_array[6]);
inch_to_pixel(x_1, y_1, &point_array[9],
&point_array[8]);
is_set_graphic_position(point_array[0],
point_array[1]);

is_select_output_frame(1);
is_display(1);
printf("done\n");

is_end();
}

```

```

/*                      FUNCTION DEFINITIONS                      */

void inch_to_pixel(x, y, px, py)
int *px, *py;
double x, y;
{
    *px = (int)((x + DEL_X)/X_GRID);
    *py = (int)((y + DEL_Y)/Y_GRID);
}

void pixel_to_inch(px, py, x, y)
int px, py;
double *x, *y;
{
    *x = (float)(px * X_GRID - DEL_X);
    *y = (float)(py * Y_GRID - DEL_Y);
}

void get_edge(edge)
double *edge[NUM_POINTS][2];
{
    double x, y, w_l, yth, error;
    int i = 0;
    int pix_row, pix_col;

    while(i < NUM_POINTS)
    {
        w_l = WINDOW_LENGTH/2.0;
        x = ((double)(i)/(NUM_POINTS - 1)) * 2.0 * w_l
            - w_l;
        y = scan_line(x);
        yth = sqrt(9.0 - x*x) ;
        error = yth - y;
        printf("%10.4f %10.4f %10.4f %10.4f\n", x, y,
            yth, error);
        *edge[i][0] = x;
        *edge[i][1] = y;
        i = i+1;
    }
}

double scan_line(x)
double x;
{
    int start_pixel_row, start_pixel_col, end_pixel_row,
    end_pixel_col;
    int edge_pixel, pixel_count, dummy;
    int value_1[1], value_2[1];
    double y, y_start, y_end;
    int pline[2];
    y_start = OFFSET;
    y_end = OFFSET + WINDOW_WIDTH;

    inch_to_pixel(x, y_start, &start_pixel_col,

```

```

    &start_pixel_row);
    inch_to_pixel(x, y_end, &end_pixel_col,
    &end_pixel_row);

    pixel_count = start_pixel_row;

    while(pixel_count < end_pixel_row )
    {
        is_get_pixel(1, pixel_count, start_pixel_col, 1,
        value_1);
        is_get_pixel(1, (pixel_count + 1),
        start_pixel_col, 1, value_2);

        if(value_1[0] != value_2[0])
        {
            pline[0] = pixel_count + 1;
            pline[1] = start_pixel_col;

            pixel_to_inch(start_pixel_col,
            pixel_count, &dummy, &y);
            if(x == -WINDOW_LENGTH/2.0)
            {
                is_set_graphic_position(pline[0],
                pline[1]+1);
                is_draw_arc(1, pline[0], pline[1]-1,
                360);
                is_set_graphic_position(pline[0],
                pline[1]);
                return(y);
            }
            is_draw_lines(1,1,pline);
            is_set_graphic_position(pline[0],
            pline[1]+1);
            is_draw_arc(1, pline[0], pline[1]-1,
            360);
            is_set_graphic_position(pline[0],
            pline[1]);
            return(y);
        }
        pixel_count = pixel_count + 1;
    }
}

/*      End of CAL-CHECK.C      */

```

```

/*                                PR-VC2.C                                */

#include <dos.h>
#include <stdio.h>
#include <stdlib.h>
#include <strstuff.h>
#include <vccom2.h>
#include <vision.h>
#include <moses.h>
#include <kishore.h>

ts_main()
{
    struct char_pkt    ch_msg[NUMPCKTS];
    struct packet      msg[NUMPCKTS];
    struct packet_data p_data[NUMPCKTS];
    int                numpckts, charpos;
    int                point_array[10];
    double             x_1, y_1, x_2, y_2, motor_1, motor_2,
motor_3;
    double             y_ref_1, y_ref_2, y_ref_3, length;
    double             ref_1, ref_2, ref_3, ply_1, ply_2,
del_y;

    system("cls");
    xmitp_ss = fopen("xmitss.fil", "w+");
    recvp_ss = fopen("recvss.fil", "w+");

    com_setup_vc(port_ss, BUFFSIZE,
                  BAUD19200, EVENPAR, DATA8, STOP1,
CTSREQD);

    msgptr = spawn("Mssge_Handler_VC", 0x1200,
                  mssge_handler_vc);

    signal_ss();

    recv_ss(ch_msg);

/*****
*
*   START OF PLAN.
*
*****/

    is_initialize();

    is_set_sync_source(EXT_SYNC);

    clear();

    is_select_channel(0);

```

```

select(0);

is_select_font(0);

is_passthru();

thresh_value = 125;

ilut(thresh_value, 6);

is_set_foreground(0);

x_1 = -WINDOW_LENGTH/2.0;
y_1 = OFFSET;
x_2 = WINDOW_LENGTH/2.0;
y_2 = OFFSET + WINDOW_WIDTH;

BEF_PRT
printf("Starting edge detection.\n");
AFT_PRT

is_select_ilut(6);

signal_ss();      /* vc 100 */

is_freeze_frame();
is_set_sync_source(EXT_SYNC);
is_acquire(0,1);

is_set_active_region(0, 0, 48, 512);
is_or_constant(0, 255, 0);

is_set_active_region(330, 0, 182, 512);
is_and_constant(0, 0, 0);

is_set_sync_source(INT_SYNC);
is_select_output_frame(0);
is_display(1);

ply_1 = scan_line( -3.0 );
ply_2 = scan_line( 3.0 );

del_y = (ply_1 + ply_2)/2.0 - (key_point(-3.0) +
                               key_point(3.0))/2.0;

ref_1 = key_point(MX_1) + del_y ;
ref_2 = key_point(MX_2) + del_y ;
ref_3 = key_point(MX_3) + del_y ;

motor_1 = scan_line(MX_1);
motor_2 = scan_line(MX_2);
motor_3 = scan_line(MX_3);

```

```

BEF_PRT
printf("Edge Points:  %10.4lf  %10.4lf  %10.4lf\n",
      motor_1, motor_2, motor_3);
printf("Reference points: %10.4lf  %10.4lf  %10.4lf\n",
      ref_1, ref_2, ref_3);
printf("delta_y = %10.4lf\n", del_y);
AFT_PRT

signal_ss();      /* ss 110*/

numpckts = 0;
charpos = 0;
numpckts = asm_double_data(motor_1, p_data, &charpos,
                          numpckts, 1);
xmit_mssge_ss(numpckts, "VECTR", p_data);

numpckts = 0;
charpos = 0;
numpckts = asm_double_data(motor_2, p_data, &charpos,
                          numpckts, 1);
xmit_mssge_ss(numpckts, "VECTR", p_data);

numpckts = 0;
charpos = 0;
numpckts = asm_double_data(motor_3, p_data, &charpos,
                          numpckts, 1);
xmit_mssge_ss(numpckts, "VECTR", p_data);

numpckts = 0;
charpos = 0;
numpckts = asm_double_data(ref_1, p_data, &charpos,
                          numpckts, 1);
xmit_mssge_ss(numpckts, "VECTR", p_data);

numpckts = 0;
charpos = 0;
numpckts = asm_double_data(ref_2, p_data, &charpos,
                          numpckts, 1);
xmit_mssge_ss(numpckts, "VECTR", p_data);

numpckts = 0;
charpos = 0;
numpckts = asm_double_data(ref_3, p_data, &charpos,
                          numpckts, 1);
xmit_mssge_ss(numpckts, "VECTR", p_data);

is_set_foreground(0);
is_set_graphic_position(0, 80);
is_draw_lines(0, 2, axis_1);
is_set_graphic_position(0, 335);
is_draw_lines(0, 2, axis_2);
is_set_graphic_position(10, 80);
is_draw_text(0, 2, text_3);
is_set_graphic_position(60, 10);

```

```

is_draw_text(0, 2, text_4);
is_set_graphic_position( 10, 335);
is_draw_text(0, 1, text_1);
is_set_graphic_position(60, 275);
is_draw_text(0, 1, text_2);

```

```

inch_to_pixel(x_1, y_1, &point_array[1], &point_array[0]);
inch_to_pixel(x_1, y_2, &point_array[3], &point_array[2]);
inch_to_pixel(x_2, y_2, &point_array[5], &point_array[4]);
inch_to_pixel(x_2, y_1, &point_array[7], &point_array[6]);
inch_to_pixel(x_1, y_1, &point_array[9], &point_array[8]);
is_set_graphic_position(point_array[0], point_array[1]);
is_draw_lines(0, 5, point_array);

```

```

is_end();
/*****
*
*   END OF PLAN.
*
*****/

```

```

BEF_PRT
printf("Program Completed!\n");
AFT_PRT

```

```

while(1)
;
}

```

```

/*   End of PR-VC2.C   */

```

```

/*                                PR-SS1.C                                */

#include <dos.h>
#include <stdio.h>
#include <stdlib.h>
#include <strstuff.h>
#include <handetc2.h>
#include <sscom2.h>
#include <kishore.h>

ts_main()
{
    char                resp[80], type[6];
    struct char_pkt     ch_msg[NUMPCKTS];
    struct packet       msg[NUMPCKTS];
    struct packet_data  p_data[NUMPCKTS];
    int                 numpckts, charpos;
    double              fing_dist[3], ref[3];

    system("cls");
    xmitp_vc = fopen("xmitvc.fil", "w+");
    recvp_vc = fopen("recvvc.fil", "w+");
    xmitp_rc = fopen("xmitrc.fil", "w+");
    recvp_rc = fopen("recvrc.fil", "w+");

    com_setup_ss(port_vc, BUFFSIZE,
                  BAUD19200, EVENPAR, DATA8, STOP1,
                  CTSREQD);
    com_setup_ss(port_rc, BUFFSIZE,
                  BAUD19200, EVENPAR, DATA8, STOP1,
                  NOCTS);

    al_initialize();
    al_select_board(1);
    al_reset();
    al_enable_for_output(0);
    al_enable_for_input(1);
    al_output_digital_value(0, 0x01, 0x00); /* setting for
    RS-232 */

    kbdint = intatt(0x9, 0x100, kbd_isr, REPLACE, kbdptr);
    kbdptr = spawn("Kbd_Tsk", 0x400, kbd_tsk);
    msgptr = spawn("Mssge_Handler_SS", 0x1500, mssge_handler_
    ss);

    signal_vc();

    BEF_PRT
    printf("\nPress <ENTER> to begin! ");
    fget_sline(stdin, resp);
    system("cls");
    AFT_PRT

```



```

ssleep();
msg[0].id_no = xmit_count_vc + 1;
swake();
guc();
msg[0].packet_id = 01;
msg[0].packet_no = 01;
strcpy(msg[0].type, "INISV");
strcpy(msg[0].data, "*****");
asm_mssge(msg, ch_msg);
xmit_vc(ch_msg);

```

```

ssleep();
msg[0].id_no = xmit_count_rc + 1;
swake();
guc();
msg[0].packet_id = 01;
msg[0].packet_no = 01;
strcpy(msg[0].type, "INISR");
strcpy(msg[0].data, "*****");
asm_mssge(msg, ch_msg);
xmit_rc(ch_msg);

```

```

/*****
*
*   START OF PLAN.
*
*****/

```

```

ssleep();
init_aaw();
swake();

slideway(0);
clamps(0);
blades(0);
vacuum_table_elevation(0);

```

```

ssleep();
trans_fingers(1, 0.0);
trans_fingers(2, 0.0);
trans_fingers(3, 0.0);
swake();

```

```

vacuum_table_elevation(1);

```

```

BEF_PRT
while(!is_vacuum_table_up())
    printf("Waiting for vacuum table to go up.\n");
AFT_PRT

```

```

BEF_PRT
system("cls");
printf("Press ENTER after positioning collar on vacuum
table.\n");

```

```
fget_sline(stdin, resp);
AFT_PRT

vacuum(1);

wait_1s();
wait_1s();
wait_1s();
wait_1s();
wait_1s();

slideway(1);

wait_1s();
wait_1s();
wait_1s();
wait_1s();

blades(1);

wait_1s();
wait_1s();
wait_1s();
wait_1s();
wait_1s();

signal_vc();          /* vc 100 */

signal_vc();          /* vc 110 */

recv_mssge_vc(type, p_data);
numpckts = 0;
charpos = 0;
numpckts = dis_double_data(&fing_dist[0], p_data,
&charpos, numpckts);

recv_mssge_vc(type, p_data);
numpckts = 0;
charpos = 0;
numpckts = dis_double_data(&fing_dist[1], p_data,
&charpos, numpckts);

recv_mssge_vc(type, p_data);
numpckts = 0;
charpos = 0;
numpckts = dis_double_data(&fing_dist[2], p_data,
&charpos, numpckts);

recv_mssge_vc(type, p_data);
numpckts = 0;
charpos = 0;
numpckts = dis_double_data(&ref[0], p_data, &charpos,
numpckts);
```

```

recv_mssge_vc(type, p_data);
numpckts = 0;
charpos = 0;
numpckts = dis_double_data(&ref[1], p_data, &charpos,
numpckts);

```

```

recv_mssge_vc(type, p_data);
numpckts = 0;
charpos = 0;
numpckts = dis_double_data(&ref[2], p_data, &charpos,
numpckts);

```

```

BEF_PRT
system("cls");
printf("Edge Points: %10.4lf %10.4lf %10.4lf\n",
      fing_dist[0], fing_dist[1], fing_dist[2]);
printf("Reference Points: %10.4lf %10.4lf %10.4lf\n",
      ref[0], ref[1], ref[2]);
printf("Press ENTER to start edge alignment.\n");
fget_sline(stdin, resp);
AFT_PRT

```

```

BEF_PRT
trans_fingers(1, DELTA - fing_dist[0]);
trans_fingers(2, DELTA - fing_dist[1]);
trans_fingers(3, DELTA - fing_dist[2]);
AFT_PRT

```

```

clamps(1);

```

```

BEF_PRT
trans_fingers(1, DELTA - ref[0]);
trans_fingers(2, DELTA - ref[1]);
trans_fingers(3, DELTA - ref[2]);
AFT_PRT

```

```

vacuum(0);

```

```

slideway(0);

```

```

wait_1s();
wait_1s();

```

```

vacuum_table_elevation(0);

```

```

BEF_PRT
printf("Waiting for vacuum table to go down.\n");
while(is_vacuum_table_up())
    printf("Waiting for vacuum table to go down.\n");
AFT_PRT

```

```

slideway(2);

```

```

BEF_PRT

```

```
printf("Press ENTER after pressing collar.\n");
fget_sline(stdin, resp);
AFT_PRT

clamps(0);

blades(0);

slideway(0);

BEF_PRT
trans_fingers(1, 0.0);
trans_fingers(2, 0.0);
trans_fingers(3, 0.0);
AFT_PRT

/*****
*
*   END OF PLAN.
*
*****/

BEF_PRT
printf("\nProgram Completed!\n");
AFT_PRT

while(1)
    ;
}

/* End of PR-SS2.C */
```

REFERENCES

1. Gaetan, M., "Robots: Their Potential in the Apparel Industry", Bobbin, August 1981, pp. 83-92.
2. Hodge, G. L. and J. R. Canada, "Evaluating Advanced Apparel Sewing Equipment/Workstations", Apparel Manufacturer, August 1989, pp. 55-57.
3. Parker, J. K., R. Dubey, F. W. Paul and J. K. Becker, "Robotic Fabric Handling for Automated Garment Manufacturing", Transactions of the ASME Journal of Engineering for Industry, October 1982, pp. 1-6.
4. Torgerson, E. and F. W. Paul, "Vision Guided Robotic Fabric Manipulation for Apparel Manufacturing", Proceedings of the IEEE International Conference on Robotics and Automation, 1987, pp. 1196-1202.
5. Taylor, P. M. and S. G. Koudis, "The Robotic Assembly of Garments with Concealed Seams", Proceedings of the IEEE International Conference on Robotics and Automation, April 1988, pp. 1836-1838.
6. Bernadon, E. and T. S. Kondoleon, "Real-Time Robotic Control for Apparel Manufacturing", Conference Proceedings, Robots 9, Detroit, 1985, pp. 4-46 to 4-66.
7. Gershon D. and I. Porat, "Vision Servo Control of a Robotic Sewing System", Proceedings of the IEEE International Conference on Robotics and Automation, 1988, pp. 1830-1835.
8. Gershon D., The Application of Robotics to the Assembly of Flexible Parts by Sewing, Ph.D. Thesis, Department of Textile Industries, University of Leeds, Leeds, U.K., March 1987.
9. Torgerson, E. J., Robotic Fabric Acquisition and Manipulation with Machine Vision Assistance, M.S. Thesis, Mechanical Engineering Department, Clemson University, Clemson, SC, December 1986.
10. Gopalswamy, A. M., Design and Control of a Robot End-Effector for Three Dimensional Manipulation of Multiple-Ply Apparel Workpieces, M.S. Thesis, Department of Mechanical Engineering, Clemson University, Clemson, SC, December 1990.

11. Solinger, J., Apparel Manufacturing Handbook - Analysis, Principles and Practice, Van Nostrand Reinhold Company, New York, NY, 1980, pp. 293 - 321.
12. Hearle, J. W. S., P. Grosberg and S. Backer, Structural Mechanics of Fibers, Yarns and Fabrics, Volume 1, John Wiley and Sons, New York, NY, 1969, pp. 339 - 369.
13. Zuech, N., Applying Machine Vision, John Wiley and Sons, New York, NY, 1988, pp. 125 - 135.
14. Fu, K. S., R. C. Gonzalez and C. S. G. Lee, Robotics-Control, Sensing, Vision and Intelligence, McGraw Hill Book Company, Singapore, 1988, pp. 296 - 339.
15. Figliola, R. S. and D. E. Beasley, Theory and Design for Mechanical Measurements, John Wiley and Sons, New York, NY, 1991, pp. 105 - 135, 141 - 146.
16. Data Translation, User Manual for DT2821 Series, Marlboro, MA, 1986.
17. Data Translation, IRIS Tutor User Manual, Marlboro, MA, 1987.
18. Precision Micro Control Corporation, DCX Programmable Multi-Function Controller Operator's Manual, San Diego, CA, 1989.